FUSION TECHNOLOGY

Annual Report of the Association EURATOM/CEA

1998

Compiled by : P. MAGAUD and F. LE VAGUERES

ASSOCIATION CEA/EURATOM
DSM/DRFC
CEA/CADARACHE
13108 Saint-Paul-Lez-Durance (France)

FUSION TECHNOLOGY

Annual Report of the Association CEA/EURATOM

1998

Compiled by : P. MAGAUD and F. LE VAGUERES

ASSOCIATION CEA/EURATOM
DSM/DRFC
CEA CADARACHE
13108 Saint-Paul-Lez-Durance (France)

Tél. : 33 - 4 42 25 46 59
Fax : 33 - 4 42 25 64 21

Cover : DIADEMO experimental device for double-wall tube validation

The consequences of these new findings are discussed in the light of recent publications which suggest that:

1. the previously assumed limits for tritium permeation into the coolant (1 g/d to maintain a maximum tritium activity in the coolant of 1 Ci/kg) were much too severe even from a safety point of view and

2. the uncertainty concerning tritium permeation from ion impingement on the first wall calculated with the accepted Pick's model is much lower than previously assumed.

As a consequence, the required end-of-life performance of permeation barriers and tritium extraction from Pb-17Li could be further reduced. The conditions under which this blanket could even operate without permeation barriers are outlined and appear feasible.

CONCLUSIONS

The results for the reference boundary conditions were confirmed and claim that a tritium permeation of 1 g/d limited by the extraction capacity from the water, can be respected. Several combinations of parameters are possible, e.g. PRF = 75, η = 83% and n = 10.

Additionally, it was shown that when assuming a permeation barrier on one cooling circuit, an equally efficient one is required on the other to obtain a reduction of tritium losses into the coolant. As expected, this "bypass" effect is the more pronounced the better the permeation barrier (high PRF). This detrimental effect is less significant when only coating the double-walled tubes.

The influence of Pb-17Li recycle rate onto permeation was demonstrated to be significant.

This study provided a strong incentive to modify the tritium management for this blanket. A detailed feasibility and cost analysis for tritium extraction from water was launched for 1999 and will decide if permeation barriers will be required.

PUBLICATIONS

[1] P. Magaud, F. Le Vaguères (eds.), Fusion Technology, Annual Report of the Association CEA/Euratom 1997, Task WP-A-1.2, CEA DSM/DRFC, May 1998.

[2] M. A. Fütterer, O. Ogorodnikova, S. Thareau, L. Marié, Tritium migration in the European water-cooled Pb-17Li blanket for DEMO, CEA report DRN/DMT SERMA/LCA/RT/98-2371/A, September 1998.

[3] M. A. Fütterer, O. Ogorodnikova, L. Marie, S. Thareau, L. Giancarli, Management of tritiated coolant in the European water-cooled Pb-17Li blanket for DEMO, Proc. SOFT-20, Marseille, France, September 7-11, 1998.

TASK LEADER

Michael A. FÜTTERER

DRN/DMT/SERMA/LCA
CEA Saclay
91191 Gif-sur-Yvette Cedex

Tél. : 33 1 69 08 36 36
Fax : 33 1 69 08 99 35

E-mail : michael.futterer@cea.fr

WP-A2-1.1

Task Title : TEST BLANKET MODULE FEASIBILITY AND DESIGN, DESIGN AND ANALYSIS

TBM design, analysis and manufacturing sequence

INTRODUCTION

Since 1996 a water-cooled Pb-17Li test blanket module (WCLL-TBM) for ITER was developed in the EU [1]. With this module, representative for the corresponding blanket designed for DEMO, tests were envisaged in ITER to take benefit from the unique possibility to operate and qualify a blanket system in a combination of strong magnetic field, high surface heat flux and neutron wall loading, the values of which are close to what is expected for a DEMO blanket.

1998 ACTIVITIES

In 1998, the TBM design was finalized for the boundary conditions given in the ITER Final Design Report. The WCLL-TBM is basically a modified and shrunk straight DEMO inboard blanket module dimensioned to fit the test port geometry [1]. It is characterized by four functional elements: a water-cooled steel box including the first wall reinforced with stiffeners, a tube plate with the lithium-lead (Pb-17Li) and coolant headers, a poloidally oriented cooling tube bundle and a bottom cap. Work in 1998 focused on an improved design of the bottom cap of the TBM. This component is of particular interest because it has to resist the full coolant pressure in accidental situation and has to conform with temperature and stress limits. A 3D-thermomechanical analysis of an improved design of this bottom cap was performed. The objective was to obtain a bottom cap thin enough to minimize heat deposition and thermal stress, but thick enough to resist a pressurization of the box in case one of the cooling tubes fails. The routing of the cooling tubes in the bottom was optimized to avoid separate cooling in this area.

The bottom cap was modeled like a plane plate welded at all sides to the SB. The thickness of the bottom plate was estimated, preliminarily, by means of a static mechanical calculation. Subsequently, the plate thickness and the connection radius were modified to minimize the plate thickness while keeping the thermal and mechanical stresses below the acceptable limits. The principal results are a thickness of the bottom cap of 4 cm with a corner radius of 2 cm.

The maximum temperature value was, obviously, obtained on the FW (Fig. 1). As regards the bottom cap, the maximum temperature was obtained on the lower surface near the FW.

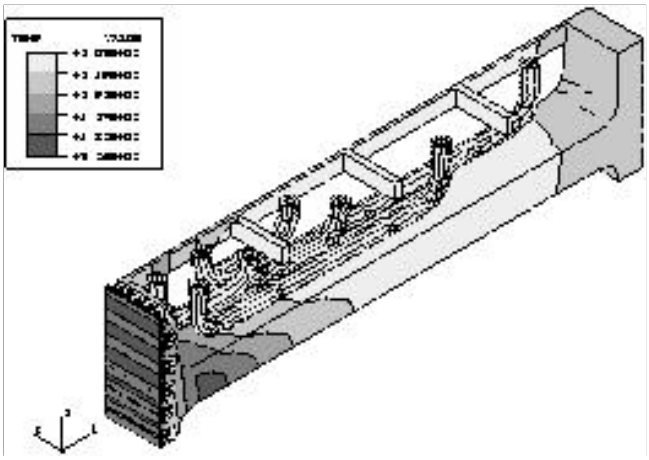

Figure 1 : Temperature distribution in the WCLL-TBM during normal operation

This value (495 °C) is lower than the accepted limit for the steel. The temperature at the interface between the Pb-17Li and the steel is 474 °C, thus being uncritical for corrosion. This result is due also to the optimized routing of the cooling tubes in the bottom region of the BZ.

Concerning the mechanical results, Fig. 2 shows the elastically calculated Von Mises stress distribution related to the nominal load condition (i.e. nominal temperature field and pressure in the tube of the FW). These results show that the adopted configuration of the bottom cap is satisfactory, because the thermal Von Mises stresses are everywhere lower than the acceptable limit given by the RCC-MR code.

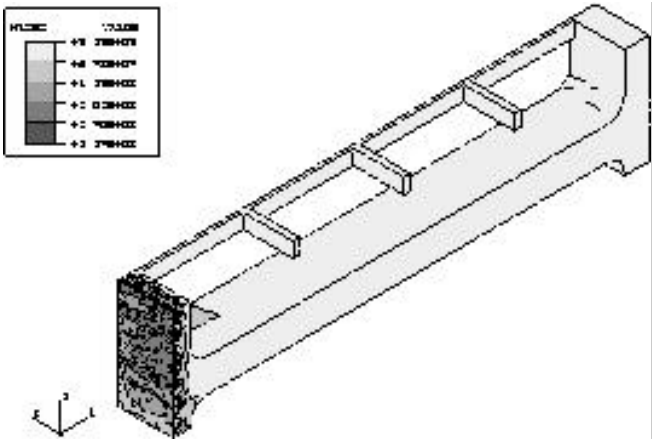

Figure 2 : Equivalent thermal von Mises stress [Pa] distribution in the bottom cap during normal operation

The mechanical results obtained in the case of pressurization to coolant pressure, are equally acceptable. The maximum displacement of 1.35 mm in the poloidal direction is localized in the center of the plate.

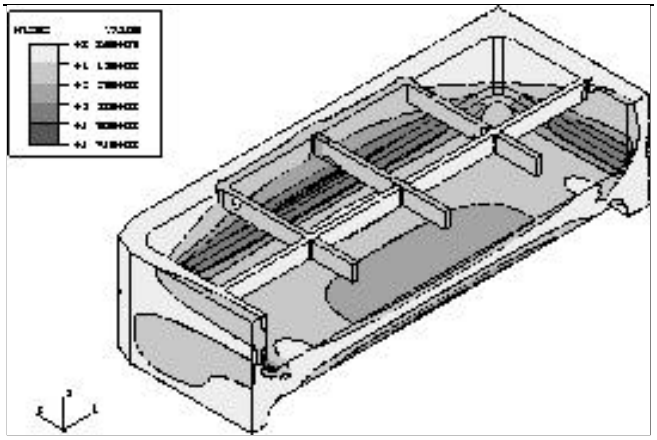

Figure 3 : Equivalent primary von Mises stress [Pa] distribution in the bottom cap during pressurization

CONCLUSIONS

The new bottom cap design respects the imposed temperature limits, the maximum temperature at the interface between the Pb-17Li and the steel is 474 °C, thus being uncritical for corrosion.

With regard to the mechanical results, the proposed design of the component is satisfactory.

PUBLICATIONS

[1] P. Magaud, F. Le Vaguères (eds.), Fusion Technology, Annual Report of the Association CEA/Euratom 1997, Task WP-A-2.1, CEA DSM/DRFC, May 1998.

[2] M. A. Fütterer, J. Szczepanski, J.-F. Salavy, L. Giancarli, B. Bielak, Y. Poitevin, Progress on the WCLL-Test Blanket Module Design, CEA report DRN/DMT SERMA/LCA/99-2399/A, December 1998.

[3] G. Vella, M. A. Fütterer, L. Giancarli, A. Li Puma: "Structural design optimization of the European water-cooled Pb-17Li Test Blanket Module", Proc. SOFT-20, Marseille, France, September 7-11, 1998.

TASK LEADER

Michael A. FÜTTERER

DRN/DMT/SERMA/LCA
CEA Saclay
91191 Gif-sur-Yvette Cedex

Tél. : 33 1 69 08 36 36
Fax : 33 1 69 08 99 35

E-mail : michael.futterer@cea.fr

WP-A2-2.1

Task Title : TEST BLANKET MODULE FEASIBILITY AND DESIGN, TBM SUBSYSTEMS

TBM ancillary equipment design

INTRODUCTION

The water-cooled Pb-17Li test blanket module (WCLL-TBM) in ITER [1] required the lay-out, dimensioning and integration of ancillary equipment into the allocated space. This ancillary equipment comprises two primary cooling circuits using pressurized water and one Pb-17Li circuit for the ex-situ extraction and measurement of the generated tritium. Additionally, the circuits required for the occasional demonstration of electricity production from the TBM power were to be considered.

1998 ACTIVITIES

The design of the ancillary circuits for the water-cooled Pb-17Li test blanket module for ITER was further refined to reach full consistency with the requirements in the ITER-FDR. The operating conditions, lay-out and size of the coolant loops were specified in detail. With optimized equipment, the thermal efficiency at PWR conditions would attain > 34.5%.

This additional requirement aggravated the already stringent space problem in the pit. For space reasons it was impossible to install all equipment for a steam cycle (e.g. steam generator, turbine, alternator, condenser) in the pit area. Moreover, it would be problematic to operate rotating metallic machines (turbine, alternator) in a relatively strong magnetic field as long as no space for sufficient magnetic shielding is available. The power conversion equipment had therefore to be installed in the Tokamak Services Building (East). With the ITER duty cycle of 45% and a realistic thermal conversion efficiency of 20% for non-optimized equipment, the produced electric power (averaged over a back-to-back cycle) would become 57 kWe from the BZ cooling circuit and 79 kWe from the SB cooling circuit (if assuming a surface heat flux of 0.5 MW/m^2).

Several circuit arrangements are feasible and differ in terms of complexity (lay-out and operation), power output, required heater power and space. Due to the uncertainties related to the surface heat flux, and consequently the SB power, the SB power is only to be used if maximizing the electricity production would be the main objective. A definite choice between the various options was not made yet because ITER did not clarify the question whether or not an intermediate cooling circuit would be required.

Table 1: Various configurations for power production

Configuration	A	B	C	D	E	F	G
intermediate cooling circuit	yes (2)	no	no	no	no	yes	yes
origin of power	BZ +SB	BZ + SB	BZ + SB	BZ	BZ	BZ	BZ
number of steam generators	1	2	1	1	1	1	1
primary cooling circuit slip-stream	no	no	no	no	yes	no	yes
Criteria and Evaluation							
complexity (lay-out and operation)	2	2	3	3	3	3	3
electricity output	4	5	5	4	3	3	2
ancillary heater requirements	1	1	1	2	3	2	4
space requirements	1	1	2	2	4	3	4
safety	4	2	2	2	2	4	4

marks from 1 (poor) to 5 (good)

Configuration A has used the objective to produce a maximum of power while keeping the safety and operational advantages of the intermediate cooling circuits. The space requirements for the secondary system were minimized by using one single steam generator. The ancillary heater requirements are high.

Configuration B would maximize the achievable electricity production by avoiding an intermediate cooling circuit and by using both the SB and BZ power. The use of two steam generators would simplify the SG design but, in return, require more space. The complexity of the circuit is considerable and so is the heater power required to avoid thermal cycling of the circuits between pulses.

Configuration C is the same as A, however without the intermediate cooling circuits. This would enhance the power output, and reduce space requirements and complexity.

Configuration D would reduce the complexity and space requirements, but produce less power. The required heater power to compensate thermal cycling is still considerable.

Configuration E would respond to the objective to reduce the space requirements for power production and the required heater power by using only a fraction of the flow-rate of the BZ cooling circuit.

Configuration F would use an intermediate cooling circuit. This can be considered advantageous or even required by avoiding the routing of activated primary cooling across the seismic gap into the Tokamak Services Building. The risk of contaminating ancillary equipment would thus be minimized. Even though the intermediate cooling circuit is somewhat detrimental for the complexity and thermal efficiency, the produced power is still relatively elevated, but the required heater power as well.

Configuration G is the same as F but uses only a fraction of the BZ power which would minimize the space and heater requirements for the equipment. However, the achievable electricity production is only small. This configuration is shown in Fig. 1.

Alternative power conversion methods (e.g. thermoelectric conversion) were not investigated yet in detail. Thermoelectric generators for a heat source at PWR conditions and a heat sink at 300 K could attain conversion efficiencies of approx 14% which would be equivalent to averages of 40 kWe from the BZ circuit and 55 kWe from the SB circuit when taking into account the 45% duty cycle. The advantages would be to reduce the auxiliary heating requirements between pulses, considerably less components, no moving parts, lower space requirements, probably reduced costs, relative ease to produce power from both cooling circuits and no additional safety or contamination risks.

Finally, a test rig containing all components for a WCLL-TBM mock-up was designed [2] to enable the out-of-pile qualification of the system.

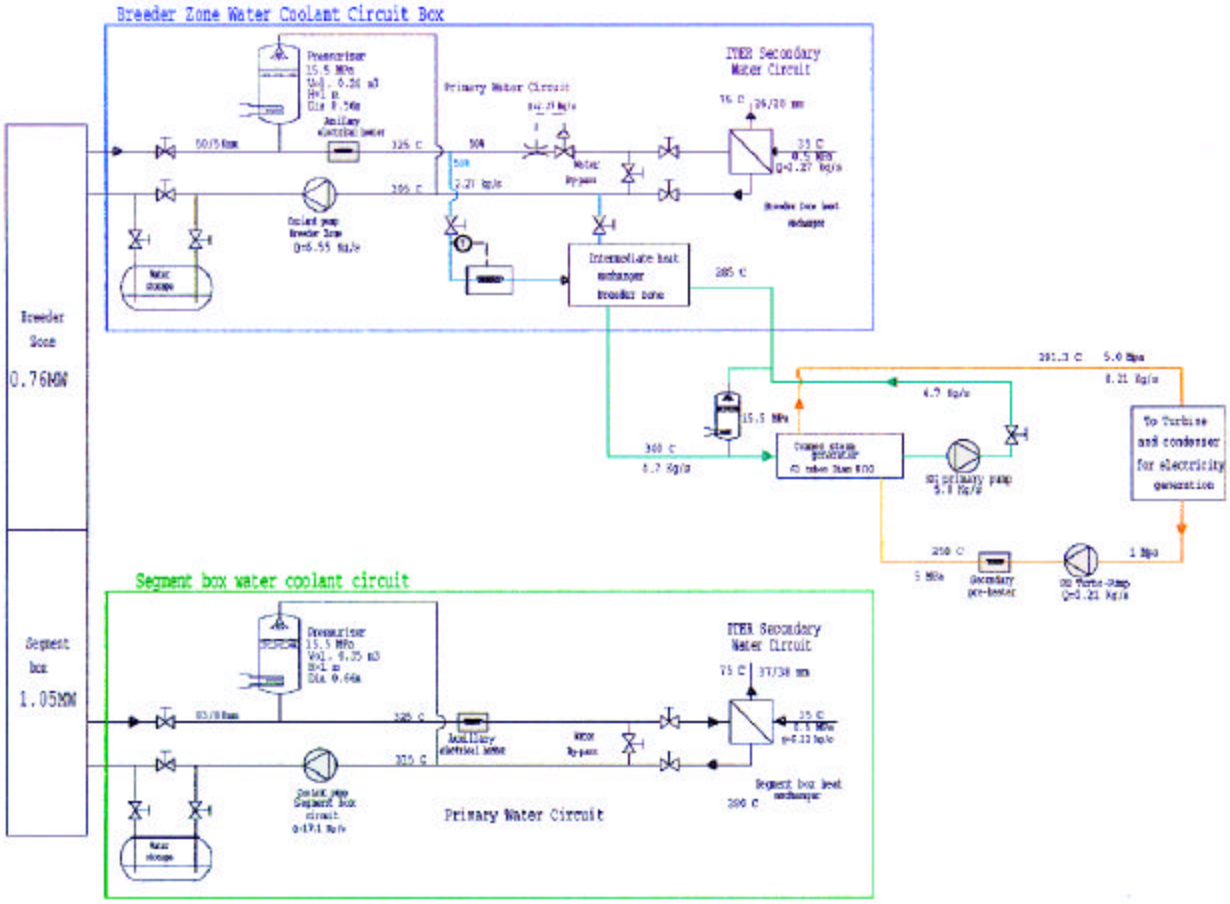

Figure 1 : Ancillary circuit lay-out for WCLL-TBM including IHX and power conversion

CONCLUSIONS

A refined lay-out of the primary and secondary cooling circuits for the WCLL-TBM was performed. The possibility for electricity generation was considered and led to a selection of several configurations. A test system for a WCLL-TBM mock-up and its cooling circuits was also conceived. Such an experiment will be required to qualify the TBM system as a whole or any other water-cooled component in representative operating conditions before installation in a test reactor.

PUBLICATIONS

[1] P. Magaud, F. Le Vaguères (eds.), Fusion Technology, Annual Report of the Association CEA/Euratom 1997, Task WP-A-2.2.1, CEA DSM/DRFC, May 1998.

[2] Y. Severi, ITER Test Blanket Module - Out-of-pile blanket system mock-up proposal, CEA report DRN/DER STML/LCFI-98-043, October 1998.

TASK LEADER

Michael A. FÜTTERER

DRN/DMT/SERMA/LCA
CEA Saclay
91191 Gif-sur-Yvette Cedex

Tél. : 33 1 69 08 36 36
Fax : 33 1 69 08 99 35

E-mail : michael.futterer@cea.fr

WP-A2-3.1

Task Title : TEST BLANKET MODULE FEASIBILITY AND DESIGN, INTERFACE WITH ITER AND TEST PROGRAM

ITER interface and TBM test program

INTRODUCTION

The WCLL-TBM shall be tested in ITER. The main objectives of these tests are:

1. to verify and demonstrate the general functionality and the performances of the system, including Tritium production, extraction, and recovery;

2. to verify and demonstrate the general functionality and the performances of specific fabrication technologies, such as those concerning Tritium permeation barriers, double-wall tubes, and HIPped structures;

3. to validate and calibrate calculation codes and models used for the different design analyses;

4. to verify and demonstrate the performance of high-grade heat production and removal system by establishing a complete power balance.

1998 ACTIVITIES

A feasibility assessment for achieving these objectives was performed and a preliminary test plan was outlined. It foresees the installation of the TBM already in the BPP which can be used to test the functionality of certain systems. All performance tests will then be performed during the D-T stage.

The WCLL-TBM test strategy is based on the following points:

1. all technologies required for the corresponding DEMO blanket are to be used (i.e. same structural material, double-wall tubes, permeation barriers);

2. functional tests should start before the TBM will be activated, preferably with the first H-H plasma;

3. the TBM should remain in place as long as possible to obtain reliability estimates for components; no TBM exchange is foreseen unless dictated by failures and/or by the decision of using new technologies;

4. the WCLL-TBM tests should be independent from the tests of other TBMs, i.e., no sharing of components.

The TBM geometry is similar to the corresponding DEMO blanket. Despite the lower heat flux and neutron wall loading, temperature and stress levels relevant to those of DEMO can be obtained by properly choosing wall thickness and coolant parameters. Electromagnetic loads and thermal cycling will be even much more severe than those expected in DEMO. The neutron fluence is insufficient to evaluate high-dose irradiation effects on materials and components.

MINIMUM OPERATING REQUIREMENTS

The most important operating parameters for the TBM are the heat flux on the FW, the neutron wall loading, the pulse length and corresponding duty cycle, and the number of back-to-back pulses. It is essential to evaluate reasonable minimum requirements for such parameters in order to achieve the fixed testing objectives. Such requirements are related to the time needed for the TBM to reach relevant temperatures and Tritium concentration conditions.

THERMO-MECHANICAL TIME CONSTANT

The thermal transient calculations, performed with CASTEM 2000, have shown that the front part of the TBM achieves temperature steady state after about 60 seconds while the rear part never does. However, the thermo-mechanical analyses have shown that thermal stresses in TBM structures after 60 seconds are comparable to those of DEMO. From a thermo-mechanical point of view the test objectives are already satisfied after this short time.

TRITIUM TIME CONSTANT

The time-dependence of tritium concentration in water and in Pb-17Li can be measured on-line to evaluate the tritium permeation rate into the coolant and to provide data for establishing the Permeation Reduction Factor (PRF) of the permeation barrier by the comparison of the experimental and the calculated results during a given transient.

In general, the higher the PRF, the faster a certain tritium concentration in the Pb-17Li will be achieved. As an example, for reference pulse conditions with 1000 s burn time and 1200 s dwell, the time required to reach an average tritium partial pressure of 100 Pa in the Pb-17Li in contact with the cooling tubes would be approx. 4 pulses without permeation barriers and only 3 pulses for PRF=100 (see Fig. 1), supposed the Pb-17Li is kept stagnant (no pumping). With PRF=100, 1000 Pa (maximum in DEMO) would be reached after 10 pulses (no pumping).

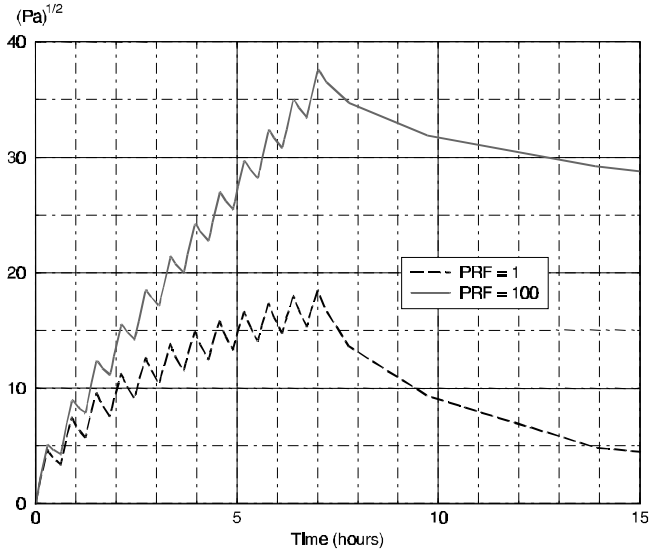

Figure 1 : Average tritium partial pressure transient in Pb-17Li during the reference pulses with/without permeation barriers (no Pb-17Li Pumping)

Yet, it is expected that if Pb-17Li circulation and detritiation are taken into account, a much larger number of pulses will be required.

Best results and most reliable data interpretation can in fact be obtained from irradiating the TBM without Pb-17Li circulation for a number of pulses and only then start Pb-17Li pumping with or without tritium extraction. The tritium related kinetics of the Pb-17Li circuit can be measured in an out-of-pile experiment and confirmed during the D-D phase. They are expected to be comparable to the TBM kinetics.

DISCUSSION

As it is shown in Table I, the reference ITER operating parameters, such as heat flux on FW and neutron wall loading, permit to reach a TBM design point representative of DEMO. The performed transient analyses have shown that representative thermal and thermo-mechanical conditions can be reached after less than 100 seconds. It is expected that representative conditions can be achieved also with significantly reduced wall loading (i.e. 50%), provided that the TBM design is performed for these conditions.

On the other hand, a single pulse is not sufficient for reaching relevant Tritium parameters. In view of the requirements presented above in terms of tritium balance, experimental repetitivity, number of data points to generate and time needed for one measurement, it can be estimated that the required number of uninterrupted back-to-back cycles is of the order of 100.

PROPOSED TEST PROGRAM

A test program for the WCLL TBM has been defined for both the BPP and the EPP of ITER taking into account the testing strategy, the TBM responses and the ITER operating scenario. The test program in ITER is based on the assumption that the whole TBM system was previously tested in an out-of-pile experiment before the installation in ITER.

ENVISAGED ITER OPERATING SCENARIO

The ITER BPP is expected to last about 10 calendar years. In the first 2 ½ years, the machine will not be activated (H-H plasma), then after a 6-month period of D-D operation, tritium will be used for D-T operation. The reference pulse is expected to last 1000 s, with 1200 s of downtime leading to a 45% duty cycle. In case of back-to-back pulses this would mean about 40 pulses per day. Maximum expected values for heat flux and neutron wall loading on ITER FW (and assumed for the TBM analyses described above) are respectively 0.5 MW/m^2 and 1.2 MW/m^2.

During the last four calendar years of the BPP, 2 - 4 periods with an extended burn time could be expected, e.g., two 6-week periods or four 3-week periods of back-to-back pulses. Long pulses of up to 10,000 s length might be available also. The expected total neutron fluence during the BPP is about 0.3 MWa/m^2.

The ITER EPP is also expected to last about 10 calendar years with an expected total neutron fluence of about 1.0 MWa/m^2 and a large number of back-to-back reference pulses.

TESTS TO BE PERFORMED DURING THE H-H AND D-D PLASMA PULSES

Significant information can be obtained during the H-H phase, especially concerning the system functionality. The advantages of testing the TBM during this phase is the possibility of hands-on intervention in case of problems.

Major tests to be performed are:

1. overall functionality of the TBM system (e.g., thermo-couples, sensors, pumps, heat exchanger, flow-meters);

2. verification of safety-relevant functions (e.g., Pb-17Li draining) implemented in the TBM system;

3. MHD pressure drop as a function of Pb-17Li flow-rate;

4. H/D permeation from Pb-17Li to coolant and vice-versa by introducing H/D in the Pb-17Li circuit for different DEMO-relevant H/D-partial pressures such as 100 Pa, 500 Pa, and 1000 Pa.

The D-D phase is assumed to last a short period (approx. 6 months), three years after the first plasma. Significant information can be obtained from the comparison with results obtained in the H-H phase, especially concerning the system functionality, in particular temperature transient monitoring. An important measurement, which can only be performed during this short D-D phase is the permeation to the FW-cooling water of D coming from the plasma. Impinging ion-permeation is expected but its estimation is very uncertain.

TESTS TO BE PERFORMED DURING THE BPP D-T PLASMA PULSES

This part of the tests is characterized by the deposition of nuclear volumetric heat in the TBM. Significant information can be obtained from the comparison with results obtained in the H-H and D-D phase, especially concerning the system functionality.

Major items to be measured for comparison with the theoretical estimates are:

1. TBM temperature distribution;

2. neutron and gamma fluxes distribution;

3. maximum stress level in the structure;

4. tritium production rate and integral tritium production;

5. Tritium permeation rate into the cooling water and establishment of the Permeation Reduction Factor (PRF) of the used permeation barriers.

Tritium inventory and permeation will be evaluated in three different scenarios leading to different T-partial pressures in the Pb-17Li:

1. the Pb-17Li is maintained static (short time constant);

2. the Pb-17Li flows but no T-extraction is performed;

3. the Pb-17Li flows and the T-extractor located in the pit is operating (corresponding to the larger time constant).

TESTS TO BE PERFORMED DURING THE ITER EPP

The same tests performed in the previous phase will be repeated for confirmation. The remaining operating time is devoted to reliability growth and to the verification of higher-fluence induced irradiation effects (such as a possible shift of the ductile-to-brittle temperature transition in the structural material and performance of joints). Demonstration of electricity production could be envisaged.

FEASIBILITY ASSESSMENT

In order to achieve the test objectives, sensitive and reliable measurement techniques and powerful theoretical interpretation tools have to be used. In particular, the effective TBM operating conditions have to measured with appropriate detectors installed in the TBM.

MEASUREMENT INTERPRETATION

The most complex measurements are those concerning the Tritium parameters during the D-T pulses, in particular because of the pulsed operation and of the fact that Tritium can be measured only outside the vacuum vessel.

One main uncertainty is the Tritium production itself. The idea is to perform on-line thermal measurement for calibrating the Tritium sources. Thermal and thermal-hydraulics calculations and associated codes are assumed to be already validated. Thus, thermal measurements will be used to estimate the actual heat flux received from the first wall and the nuclear heat deposition, and then derive the actual neutron wall loading. This information will be used to calculate the tritium production so as to validate the Monte Carlo code and neutron cross-sections from neutron detector signals.

The T-permeation rate to the water and the corresponding barrier PRF can be estimated as follows. In the last experiment the Pb-17Li is flowing (the flow-rate is adjusted so as to obtain a DEMO-relevant T-partial pressure) and the tritium is extracted by the T-extractor located in the pit. The time constant is relatively large (approx. 100 back-to-back pulses are required). Information on T-inventory in the external circuit and components will become available. The T-concentration in the Pb-17Li as a function of time and flow rate will be measured in the pit, both before and after the T-extractor. The T-concentration in the water-coolant, due to the permeated tritium to the water-coolant within the TBM, will be measured in the pit as a function of time. A full T-balance evaluation can then be performed. The tritium production will therefore be evaluated and compared to the results of the neutronic calculations. With the help of the previous experiments (Pb-17Li stagnant and/or no T-extraction, which are less affected by the pulse length) the PRF of the T-permeation barriers can be evaluated.

Uncertainties of measurements and of theoretical predictions have to be investigated.

CONCLUSIONS

The present EU R&D program for the water-cooled Pb-17Li DEMO blanket foresees to test a representative test blanket module in ITER from its initial phase. The performed work shows that a WCLL-TBM can be manufactured and safely operated in the ITER environment. Its DEMO relevancy depends on the outcome of ongoing R&D, in particular concerning the development of a suitable structural material, permeation barriers and double-walled tubes. It has also been shown that the proposed test program is able to give essential information for the development of relevant technology to be used in a DEMO reactor.

The possibility of achieving the WCLL-TBM testing objectives have been discussed from the point of view of the presently defined ITER operation conditions and of the availability and installation of appropriate instrumentation. No major difficulties are expected although further R&D is required for ensuring a complete interpretation of the expected experimental data, especially on both instrumentation technology and numerical on-line analysis.

PUBLICATIONS

[1] L. Giancarli, M. A. Fütterer, B. Bielak, Y. Poitevin, J.-F. Salavy, J. Szczepanski, WCLL-TBM test strategy during ITER-BPP, CEA report DRN/DMT SERMA/LCA/98-2400/A, December 1998.

[2] L. Giancarli, B. Bielak, M. A. Fütterer, O. Ogorodnikova, Y. Poitevin, J.-F. Salavy, J. Szczepanski, Y. Severi, G. Marbach, G. Benamati, C. Nardi, J. Reimann, Objectives feasibility assessment of the WCLL mock-up testing in ITER, Proc. SOFT-20, Marseille, France, September 7-11, 1998.

TASK LEADER

Michael A. FÜTTERER

DRN/DMT/SERMA/LCA
CEA Saclay
91191 Gif-sur-Yvette Cedex

Tél. : 33 1 69 08 36 36
Fax : 33 1 69 08 99 35

E-mail : michael.futterer@cea.fr

WP-A2-4.1

Task Title: TEST BLANKET MODULE FEASIBILITY AND DESIGN, MAINTENANCE, SUPPORT, REMOTE HANDLING, WASTE DISPOSAL

TBM support system and maintenance procedure

INTRODUCTION

The drain system to purge the Pb17Li from the TBM and the instrumentation both require penetrations through the backplate of the TBM. In both cases it had to be ensured that these penetrations will not challenge the structural integrity of the TBM during accidental pressurization. For hydraulic reasons, the Pb17Li draining would be incomplete and slow if no additional gas injection into the TBM is performed.

Additionally, the instrumentation needs identified in WP A2.3.1 were integrated in the TBM design. This concerns in particular the measurement of temperature and deformation. The locations of thermocouples and strain gauges were selected and design solutions were found to install this instrumentation in the TBM.

1998 ACTIVITIES

The objective of this work was to integrate auxiliary functions in the design of the water-cooled Pb17Li Test Blanket Module (WCLL-TBM). Such auxiliary functions are :

- a Pb17Li drain system to remove the liquid Pb17Li from the TBM during extended shut-down periods and before removal; this system is required to avoid the freezing and consecutive re-melting of Pb17Li inside the TBM which is a complex operation and may challenge the integrity of the TBM;

- the acquisition of different kinds of measurement data for determining the operating conditions and for safety surveillance, e. g. temperatures and deformations;

Pb17Li DRAIN SYSTEM

Because melting of solidified Pb17Li in the TBM itself may provoke structural damage of the TBM box, the Pb17Li shall be removed from the TBM during extended shut-down phases. Most of the Pb17Li can be removed when inserting a drain pipe from low on the back plate. For remote handling reasons the pipe dimensions are identical to the other pipes, i. e. $\varnothing 50 \times 3$ mm. This drain pipe leads to the Pb17Li storage tank located on a lower level than the TBM to facilitate gravity draining.

The drain pipe is equipped with a valve and is constantly trace heated to speed up draining. Temperature gradients between TBM and valve should be minimized to avoid segregation of the alloy. Inert gas injection is foreseen in both the Pb17Li inlet and outlet pipes to further accelerate the process and to compensate the drained Pb17Li volume.

INSTRUMENTATION

In the Design Description Document for the WCLL-TBM, several types of instrumentation for installation within the TBM were proposed to meet the test objectives. These included thermocouples for mapping the temperatures in various areas, electrical potential probes to determine currents, stress transducers or strain gauges to monitor deformation during operation, neutron detectors and gamma scan wires to measure flux and fluence and to calibrate neutronic calculations.

More recently, additional electrodes for the determination of a local Pb17Li velocity were proposed to investigate MHD phenomena, which can be done even without plasma operation. With thermocouples and strain gauges as examples for performing the thermomechanical measurements, it was demonstrated that the instrumentation is feasible and that it is adapted to the TBM environment.

INSTALLATION OF INSTRUMENTATION

All instrumentation was installed respecting the following requirements:

- no connectors between sensor and pit area as connectors are a source of malfunction and almost inaccessible without TBM removal;

- electrical insulation between sensor wires and TBM/interface frame to protect the measurement signal from leak currents;

- attachment of wires to the TBM by spot welded clamps so as to maintain their position;

TEMPERATURE

The following provides examples for the installation of thermocouples in various places of the TBM. If desired, the TBM could be more amply equipped to improve temperature mapping.

Pb17Li TEMPERATURE

2 × 7 thermocouples are foreseen for this purpose. Their tentative position is shown in Figs. 1 and 2.

Located in the lower section of the TBM, two sets of 7 thermocouples each read the Pb17Li temperatures in two parallel radial directions, one in the central channels, one in the lateral channels. These thermocouples will be installed on two fingers that will be inserted in the TBM from behind.

These fingers consist essentially of an open tube connected to a flange that ensures the sealing with the backplate. This flange can be either bolted or welded to the backplate. The passage of the thermocouple wires is sealed with Swagelock type connectors. The tube is open to freely allow the Pb17Li to penetrate and thus to minimize tritium trapping. Behind the First Wall, the tube is positioned by a support. The passage of the tube across the stiffener plates is ensured by drilling holes from the backplate. Play between tube and holes should be minimized to avoid Pb17Li shortcircuits.

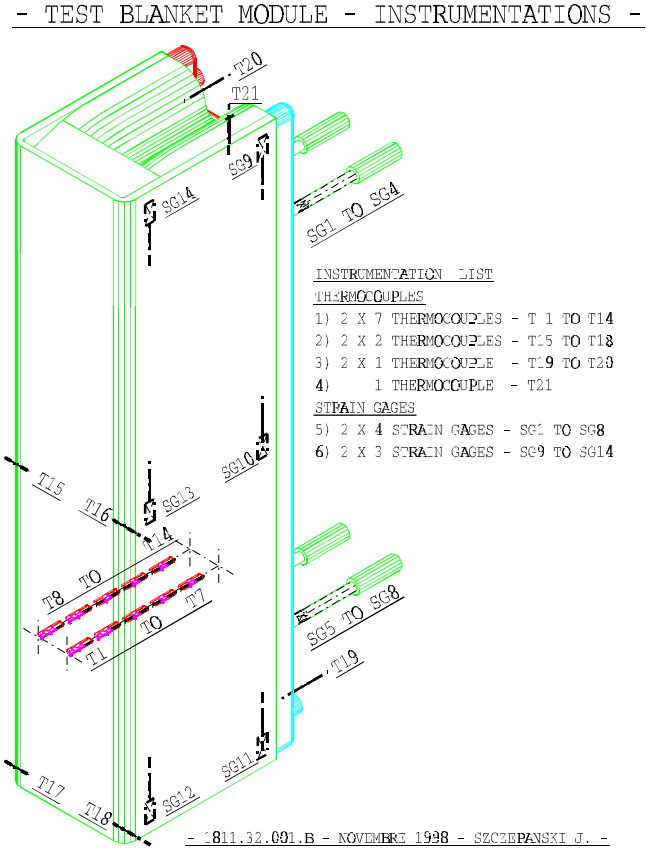

Figure 1 : Location of thermocouples and strain gauges

FIRST WALL TEMPERATURE

2 × 2 thermocouples are foreseen for this purpose. Their position is shown in Fig. 2.

These thermocouples will be installed in the middle of the first wall thickness, one pair on the lower part, the other in the middle of the TBM height.

This requires holes to be drilled in the middle of the first wall thickness and between two first wall cooling tubes. A small groove will accommodate the thermocouple around the corner before the installation of the Be armor. On the TBM side walls the thermocouples will be attached with small spot welded clamps.

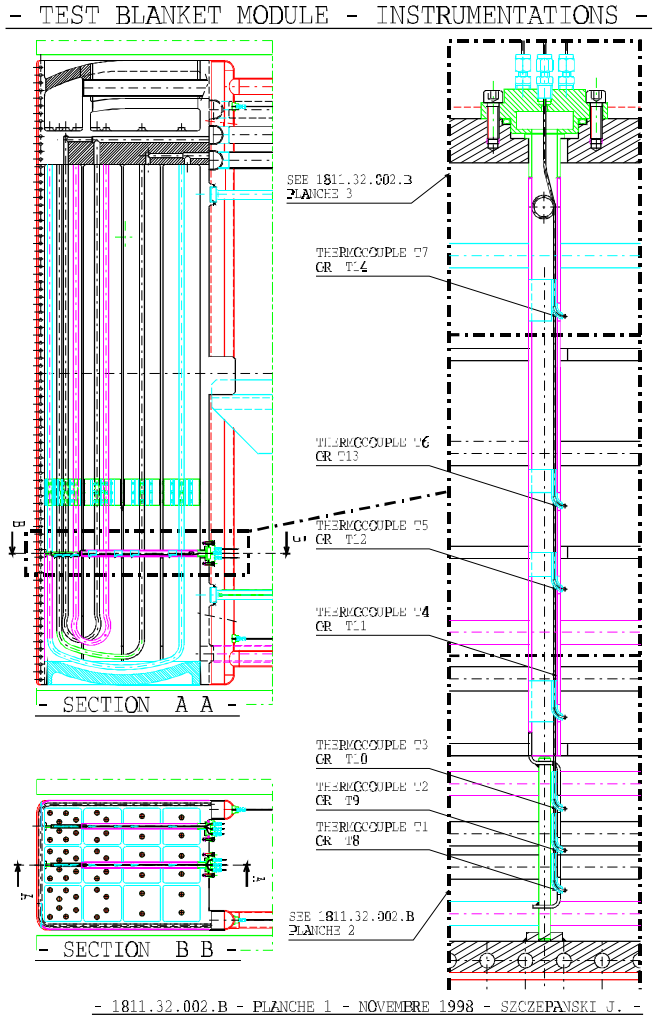

Figure 2 : Thermocouple holders (general view)

FIRST WALL COOLANT TEMPERATURE

2 × 1 thermocouple are foreseen for this purpose. Each First Wall coolant manifold is equipped with one thermocouple on the inlet and another on the outlet. Swagelock type connectors are foreseen to seal the thermocouple against coolant pressure and vacuum. Alternatively, simple welded penetrations could be used to improve leak tightness if required.

BREEDER ZONE COOLANT TEMPERATURE

1 thermocouple (T21) is foreseen for this purpose. Its position is shown in Fig. 2.

This thermocouple will be located inside the coolant outlet collector chamber to read the average Breeder Zone coolant outlet temperature. It is attached to the inside of the coolant outlet chamber by spot welded clamps.

Swagelock type connectors are foreseen to seal the thermocouple against coolant pressure and vacuum. Alternatively, simple welded penetrations could be used to improve leak tightness if required.

DEFORMATION

Tie rod elongation and deflection

2 × 4 strain gauges are foreseen for this purpose. Their position is shown in Fig. 1.

Two of the four tie rods for the mechanical TBM attachment to the interface frame will be instrumented with 4 strain gauges each. This double instrumentation has been chosen for different reasons:

- confirmation of the tie rod deformation calculated for the attachment analysis
- confirmation of symmetric deformation of TBM
- functional redundancy (relatively short lifetime of strain gauges is expected)

TBM deformation

3 × 2 strain are foreseen for this purpose. Their position is shown in Fig. 1.

Three pairs of strain gauges will be installed on the TBM side walls, on pair on the top, the second in the middle and the third on the bottom. One strain gauge out of each pair is close to the plasma facing front corner, the other close to the back plate.

This distribution was chosen to measure the global TBM deformation and to confirm the information from the tie rod deformation.

CONCLUSIONS

The auxiliary functions Pb17Li draining and the thermomechanical instrumentation of the WCLL-TBM were successfully integrated in the overall design. A degree of detail was reached that allows to confirm the feasibility on the one hand, but that leaves enough flexibility for future modifications on the other.

PUBLICATIONS

[1] M. A. Fütterer, B. Bielak, J. Szczepanski, L. Giancarli, Drain system and instrumentation of a water-cooled Pb17Li test blanket module, CEA report DRN/DMT SERMA/LCA/98-2460/A, December 1998.

TASK LEADER

Michael A. FÜTTERER

DRN/DMT/SERMA/LCA
CEA Saclay
91191 Gif-sur-Yvette Cedex

Tél. : 33 1 69 08 36 36
Fax : 33 1 69 08 99 35

E-mail : michael.futterer@cea.fr

WP-A3-1.1

Task Title : ITER TEST MODULE FABRICATION : DOUBLE WALL TUBE DEVELOPMENT AND FABRICATION

Double Wall Tube HIP Fabrication

INTRODUCTION

In the DEMO Water Cooled Lithium Lead blanket, cooling of the LiPb breeder alloy is made thanks to bent martensitic steel (MS) tubes. Each module is equipped with a bundle of 24 tubes.

For safety reasons, it is necessary to use two concentric tubes (each of them designed to withstand the full load by itself) separated by a compliant layer. The role of the compliant layer is to stop or to deviate cracks that could potentially develop through one of the tubes. Furthermore, this layer shall provide a good thermal contact between the tubes.

A fabrication sequence based on Hot Isostatic Pressure Diffusion Bonding has been developed. HIP-DB allows to eliminate the gap between the two tubes while at the same time insuring a full contact between the compliant layer and the steel.

1998 ACTIVITIES

MECHANICAL PROPERTIES OF THE JOINTS

The mechanical properties of the MS/interlayer/MS joints have been assessed using several testing methods. Tensile specimens, Charpy impact specimens and Compact Tension specimens have been fabricated using F82H martensitic steel and 0.1mm foils. Decohesion tests using double wall rings made of T91 steel have been also used.

Three cases have been studied : a pure Fe or a pure Cu interlayer HIPed at 1050°C and a titanium interlayer HIPed at 750°C. In the case of high temperature diffusion bonding, the samples were quenched and tempered at 750°C. In the case of low temperature diffusion bonding, no further heat treatment was necessary.

The results are as follows : rupture occurs within the Fe and the Cu compliant layer, while interface decohesion is observed in the case of Ti. The force to rupture is higher with Fe than with Cu due to the higher strength to rupture of Fe itself. Detailed results for double-ring decohesion testing are given in table 1.

Table 1 : Results of double ring decohesion test (T91 steel)

interlayer	*Copper*	*Iron*	*Titanium*
force to rupture	650±40 daN/mm	1430±60 daN/mm	710±320 daN/mm
comments	ductile rupture in Cu	ductile rupture in Fe	interface decohesion

Despite the better behaviour of iron, it has been decided to choose copper as a compliant material because copper coating is easily achievable by electroplating, whereas iron coatings are not available on an industrial scale.

Tensile and impact results for Cu are given in table 2 :

Table 2 : tensile and impact results for F82/Cu/F82H joints

	0.2% yield strength	strength to rupture	total elongation	impact resistance (KCU)
F82H/Cu/F82H joint	520 MPa	605 MPa	2.5%	48±21 J/cm²
F82H	550 MPa	650 MPa	20%	~190 J/cm²

The yield strength of the F82H/Cu/F82H joint is 30MPa lower than that of as received F82H due to a slight softening of F82H steel during the HIP cycle. The rupture of the joint occurs after a limited elongation of the sample due to the "weakness" of copper, but the strength to rupture far exceeds the strength to rupture of pure copper due to constraining effects. The impact resistance of the joint is about 25% of those of the base F82H, which is not surprising considering the much lower strength of copper. Examination of the rupture surface of impact specimens revealed that the rupture path oscillates between the two Cu/F82H interfaces but keeping within Cu. Dimples of about 1µm diameter are observed.

MOCK UPS FABRICATION

During 1997, small length mock ups were fabricated using T91 tubes and 0.1mm foils. For longer DWT it was necessary to coat the inner MS tube in order to insure the continuity of the compliant layer all around the tubes. During 1998, three mock ups about 450mm long were fabricated. A description of the fabrication sequence follows.

Coating

The Cu coating technique is electrodeposition. First, chemical cleaning of the 11x13.5mm T91 tube using a nitric acid based solution is made. Then, it is necessary to deposit a nickel underlayer to get a fair adherence of the copper coating. The thickness of this underlayer is about 0.1µm. Copper deposition is made using an electrolytic bath typically used for electroforming. The choice of this bath is justified by the relatively high thickness of the coating compared to the thickness of decorative coatings.

For the three tubes, the coating thickness lied between 0.15 and 0.2mm. The excess of copper was carefully machined until the coated tube could fit in the outer 14x17mm tube.

The microstructure of the as deposited coating is characterised by the presence of rather numerous inclusions at the steel / copper interface. This is typical of the electrodeposition process (figure 1).

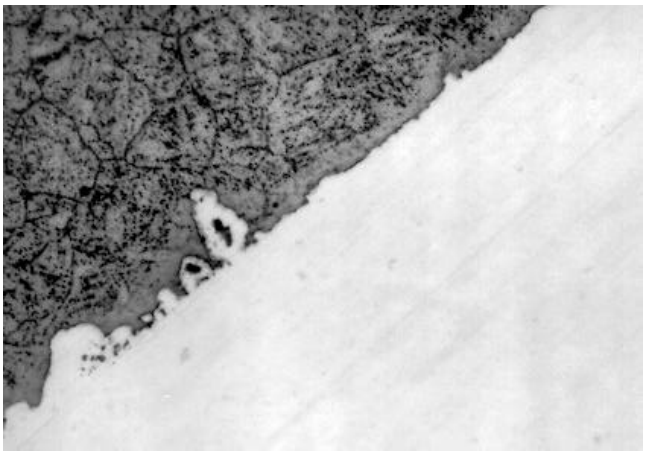

Figure 1 : As-deposited copper coating (right) on T91 tube (left), x1000

HIP DW

The electroplated tubes were degreased and heat treated at 750°C for 1h30 under vacuum for outgassing. Electroplated coatings usually contain great amounts of absorbed gases.

Then, inner and outer tubes couples were prepared by means of degreasing and acid pickling. The tubes were fitted one in each other, both ends TIG welded and the interface was outgassed.

The HIP cycle is as shown on figure 2. To avoid damage of the tubes, heating is made under low pressure. Then a 1h step at 850°C and a 1h increase to 1040°C are applied during which the pressure is increased to 140MPa. Normalising conditions are applied for the joining (1040°C, 40min for T91). The maximum cooling rate of the HIP equipment used for this fabrication was only about 4.5°C/min, so further normalising at 1040°C for 40min, gas quench and tempering for 1h at 750°C were applied after HIP.

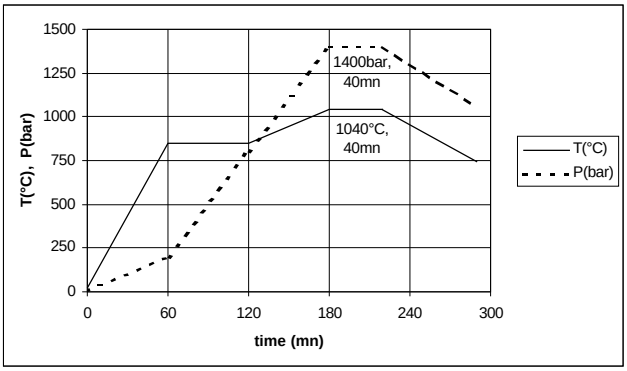

Figure 2 : HIP cycle used for DWT fabrication.

Microstructure and properties

The microstructure of the joint after HIP and post treatments is characterised by :

- a diffusion affected zone in steel on the inner tube side (figure 2). Martensite platelets morphology differs from that of base T91 steel due to nickel enrichment. The microhardness of this zone is about 300Hv0.015 against 240Hv0.1 for the base T91 steel.

- a very fine precipitation of chromium and iron in the copper layer. This is due to the rapid decrease of the solubility of these elements in copper, on cooling.

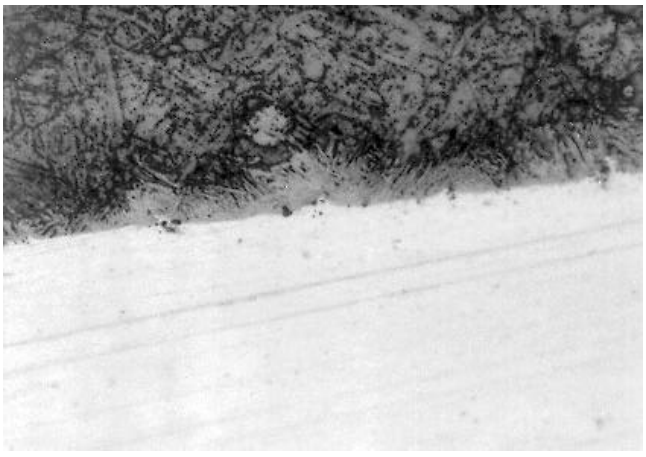

Figure 3 : T91(top) / copper(bottom) interface after DWT fabrication, x1000

Samples were cut for double-ring decohesion test. The force to rupture was about 800daN/mm for 1.5mm thick rings compared to 640daN/mm for samples fabricated with a foil. The difference is probably due to the longer exposure of the DWT mock ups at high temperature : no further normalisation heat treatment was necessary in the first case because the HIP cooling rate was high enough to insure the martensitic transformation.

Bending

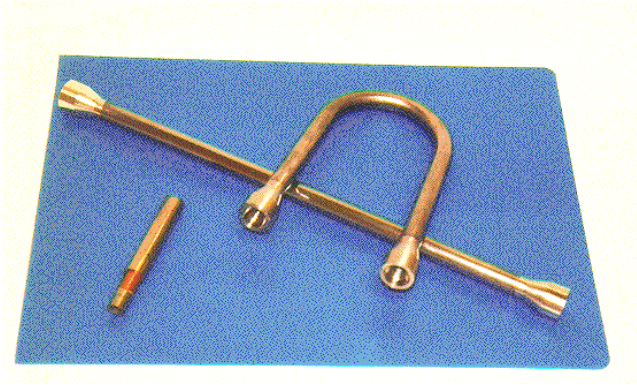

Figure 4 : Straight and bent 440mm long mock ups

The allowable cold deformation during bending is 15% for T91. The minimum distance between axes in U shape DWT for DEMO TBM is 103mm, which corresponds to a deformation of 16.3%. However, experiments showed that cold bending with a distance between axes equal to 100mm does not lead to cracking on the outer fiber.

One mock up has been bent, heat treated at 750°C for 1h for stress relieving and characterised (figure 4). The section reduction has been evaluated to 6%.

CONCLUSIONS

Copper has been chosen as compliant material. Good results were obtained with iron too, but iron is technologically less relevant in terms of coating deposition and behaviour under irradiation. Iron can be considered as a back up solution.

The mechanical properties of the joints have been measured by classical mechanical testing (tensile and impact) on F82H/Cu foil/F82H samples. The tensile strength is slightly higher than the F82H yield strength. The impact resistance is much lower than that of both pure annealed copper and F82H. Stress triaxiality in the joint area is responsible for this behaviour. Die-and-plug testing allowed to measure the decohesion force of the two concentric tubes. About 800daN/mm is obtained for 1.5mm high rings.

A straight and a bent mock up have been fabricated using T91 tubes copper coated by electroplating. Due to the poor quality of the pipes used to manufacture the tubes, the DWT has defects on the inner surface. This mock up will be tested in the DIADEMO loop.

The microstructure of the interfaces are characterised by only little reaction between copper and steel. However, a transformed zone in T91 was observed due to the diffusion of the nickel underlayer. A microhardness increase is noticed in a 10µm thick zone.

PUBLICATIONS

[1] E. Rigal "Double wall tube fabrication by hot isostatic pressing. Task WPA3.1.1, final report (1998)". NT DEM n° 68/99.

[2] "HIP diffusion bonding and forming of martensitic steel for ITER test blanket modules", E. Rigal, L. Briottet, Ch. Dellis, G. Le Marois, Proc. 20th Symposium on Fusion Technology, Marseille, France 7-11 sept. 1998

TASK LEADER

Emmanuel RIGAL

DTA/DEM/SGM
CEA Grenoble
17, rue des Martyrs
38054 Grenoble Cedex 9

Tél. : 33 4 76 88 97 22
Fax : 33 4 76 88 95 38

E-mail : rigal@chartreuse.cea.fr

WP-A3-2.1

Task Title : DOUBLE-WALL TUBE OUT-OF-PILE TESTING - DIADEMO EXPERIMENTAL PROGRAMME

INTRODUCTION

Within the framework of the study on Water-Cooled Lithium-Lead tritigenous Blankets for a fusion reactor, technological choices on cooling tubes must be validated. Within this context, tests on Double-Wall Tubes (DWT's) through which reactor power will be transferred must be carried out.

The state of the art technology of these tubes is of utmost importance as it conditions the concept and must be validated from both mechanical and thermal point of view. Before considering industrial manufacturing, samples have to be tested under fusion reactor nominal.

The main objective of DIADEMO experimental device is to validate, in close collaboration with the task WP-A3-1 (Double-Wall tube fabrication), the choice of the double-walled tube for the future Fusion reactor.

1998 ACTIVITIES

This task (WP A3-2.1) has been launched in 1996. Following that :

- A preliminary feasibility study, concerning an experimental device in order to test DWTs, has been performed by mid of 1996.
- A pre-design study has been, then, performed during the second half of 1996 in order to launch, beginning of 1997.
- A call for tender for the fabrication study.
- Following this fabrication study, a call for tender has been launched for the manufacturing of the mechanical part of the experimental device.
- In the mean time (summer 1997), a call for tender has been launched in order to perform the study and the manufacturing concerning the 'Instrumentation and Control' of the experimental device.
- The end of the year 97 and the year 98 have been devoted to the fabrication of the experimental device (mechanical part, instrumentation and control, thermal isolation).

This task is performed in close collaboration with task WP-A3-1, driven by CEA/ CEREM, responsible of the fabrication of the DWTs (choice of the DWT fabrication procedure, DWT manufacturing). It is forecasted as a first step, the fabrication of small size test samples (straight and bent), and in a second step the fabrication of large size bent DWTs (~2. meters developed length).

The first straight sample (length 500 mm, heated on 200 mm) has been manufactured by CEA/ CEREM during the first half of the year 98. It has been delivered to Cadarache during the SOFT period (11th, September). It has been hydraulically tested (up to 25 Mpa).

The straight DWT sample has been fitted and prepared during the rest of September. It is now installed on the DIADEMO test loop.

Concerning DIADEMO experimental device, the year 1998 has been devoted as follows :

- January - end of July 98, ***Manufacturing of the Mechanical Part***.
- January - end of November 98, ***study, fabrication and acceptance tests of the Instrumentation and Control part***.

THE EXPERIMENTAL DEVICE.

The experimental device "DIADEMO" has to satisfy to fusion reactor operating conditions. So the circuit has been designed for pulsed conditions (in order to perform thermal fatigue tests on the DWTs. 3000 thermal cycles are foreseen for the first mock-up) and for long time thermal steady-state operating conditions (in order to perform endurance tests).

The final experimental device is as follow :

Two test stations :

i) the first one called "**Air Test Station**", using only the pressurized water cooling circuit. The test samples are electrically heated (not use of Pb-17Li loop),
ii) the second one called "**Pb-17Li Test Station**", using the entire circuit; the Pb-17Li being also electrically heated.

The "Air Test Station" will be used for the small size tests samples. The "Pb-17Li Test Station" will be available for the final qualification of the DWT in presence of the eutectic.

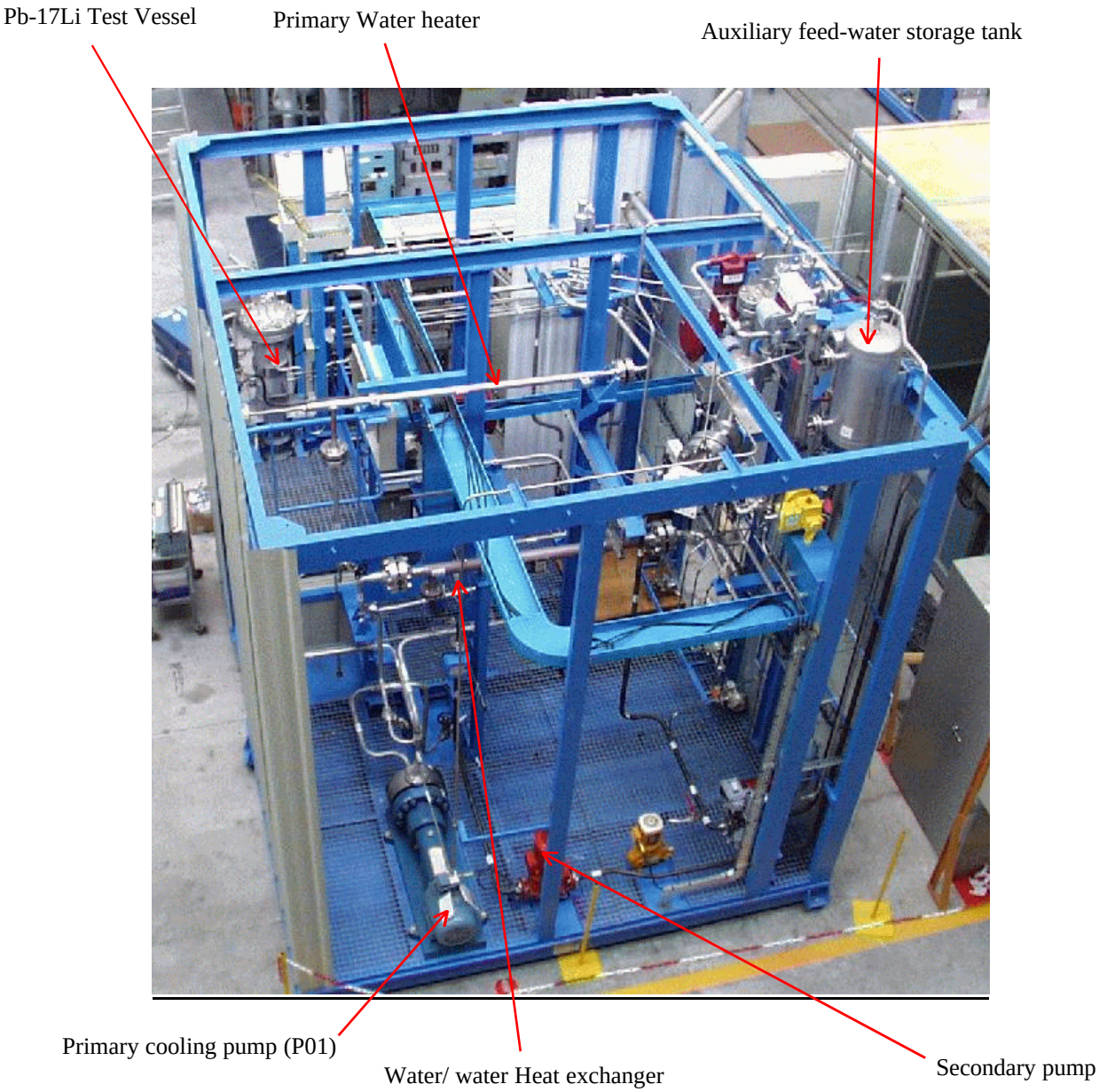

DIADEMO test loop (up) - Air Test Section inside DIADEMO Loop (down)

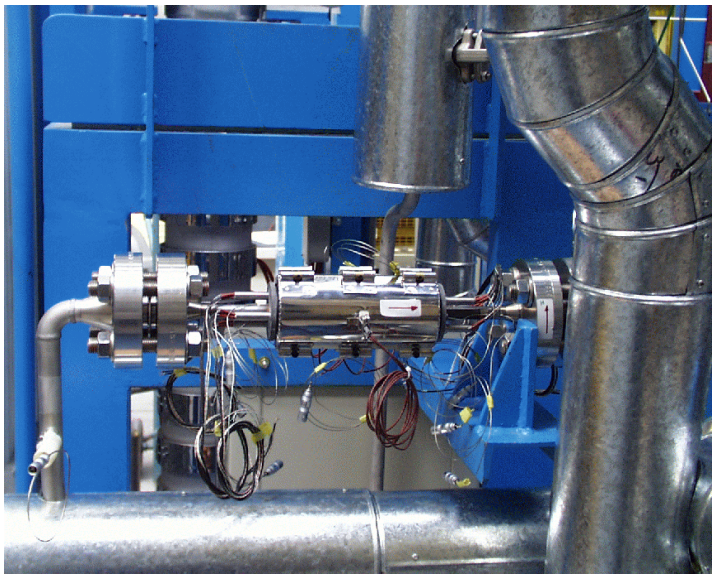

AIR TEST SECTION

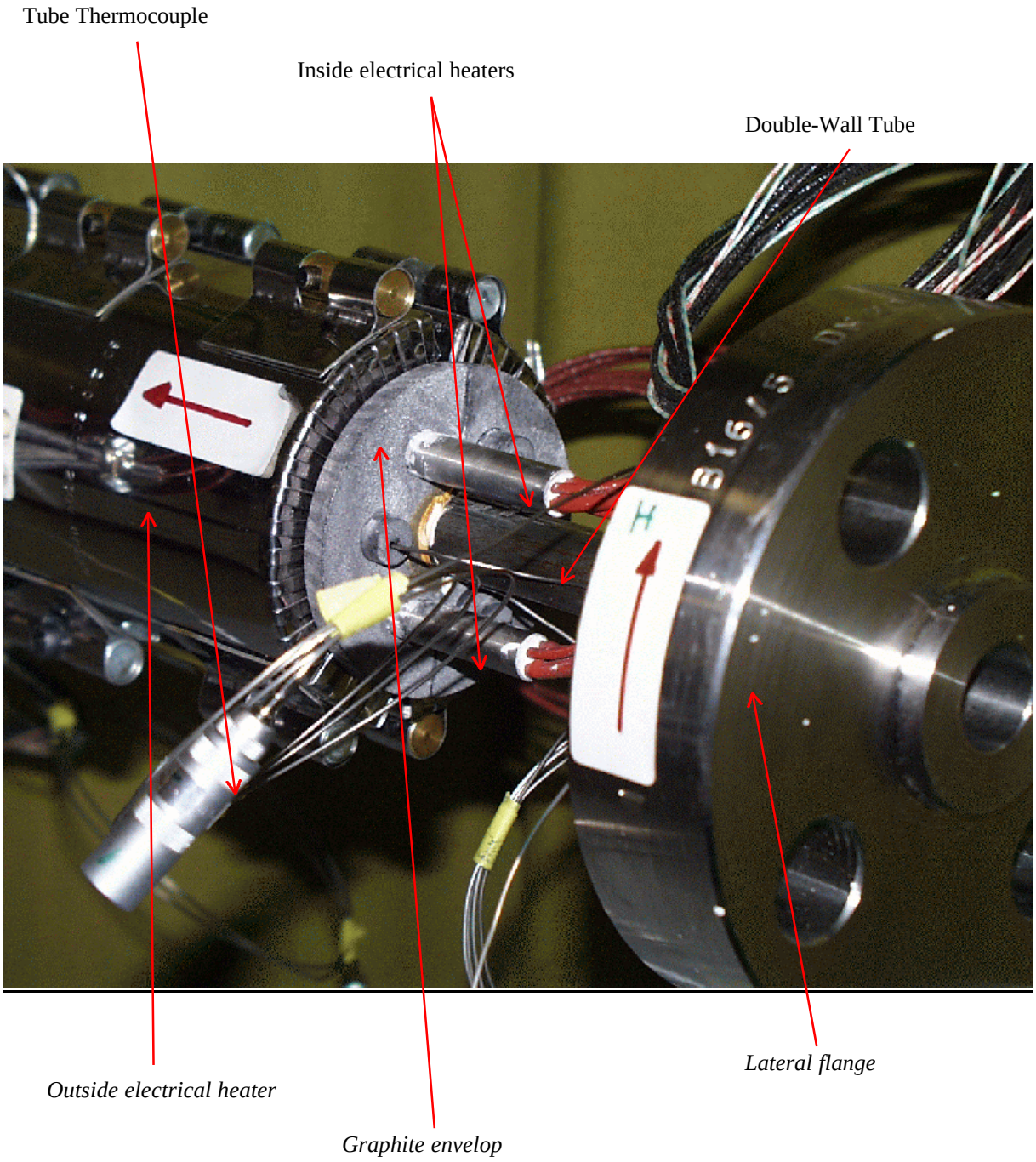

View of the Straight Double-Wall Tube Sample (200 mm)

Lithium-Lead Loop

The maximum operating temperature in the Pb-17Li is 550°C (Reactor operating condition in the blanket). Nevertheless it will be possible to perform thermal transients in the liquid metal for Reactor pulsed operating conditions. The operating temperatures in this case will be between 300 and 390°C.

Primary Water Cooling Loop

The operating conditions of the primary water cooling circuit will simulate reactor conditions :

- Maximum water temperature : 325°C,
- Minimum water temperature : 265°C,
- Water pressure : 15.5 MPa,
- Water tube flow rate : 0.37 kg/s.

The "Air Test Station" is in fact a derivation on the main water loop. The test samples will be connected to the water cooling loop with flanges and externally electrically heated. It is forecasted to test on this station small size samples (straight and bent).

Secondary Water Cooling Loop

The operating conditions of the secondary water cooling circuit are the following :

- Mean water temperature : 55°C,
- Water pressure : 1.5 MPa,
- Water tube flow rate : 1.5 kg/s.

The secondary water loop is connected to an external air cooler, in order to remove the final thermal power.

THE INSTRUMENTATION AND CONTROL - DATA- ACQUISITION

During the year 1998 (up to the end of November), the detailed study, the fabrication and the acceptance tests of ***"the Instrumentation and Control -Data Acquisition"*** has been performed.

In the mean time, in order to get the authorization to start the loop, a safety study has been performed [1].

TIME SCHEDULE

As it has been explained previously, the Instrumentation and Control-Data Acquisition with acceptance tests have to be completed by the end of November.

The first acceptance tests of the complete loop (in temperature) have started by mid of December 98.

REFERENCES

[1] NT. DER/ STML/ LCFI - 98-017. (20/ 05/ 1998). "Installation d'essais DIADEMO - Dossier se Sécurité "

[2] 20th SOFT - September 7-11, 1998. MARSEILLE - FRANCE. "Water-Cooled Pb-17Li Blanket - Diademo Experimental Programme for Double-Wall Tube Qualification"

[3] NT. DER/ STML/ LCFI - 98-046. J.P. DIEPPOIS - Y. SEVERI « WATER-COOLED LITHIUM-LEAD BLANKET - Task Sheet TS A 3.2 - Progress Report (1998) - DIADEMO EXPERIMENTAL PROGRAMME »

TASK LEADER

Yves SEVERI

DRN/ DER/ STPI/ LCFI
CEA Cadarache
13108 St Paul Lez Durance Cedex

Tél. : 33 4 42 25 64 01
Fax : 33 4 42 25 66 38

E-mail : severi@macadam.cea.fr

WP-A3-4.1

Task Title : ITER TEST MODULE FABRICATION ITM BOX FABRICATION USING POWDER HIP TECHNIQUE

INTRODUCTION

Hot Isostatic Pressing (HIP) is foreseen to produce components of fusion reactors blanket. This technology can be used to manufacture net shape components from powder. Due to large deformations (up to 30% in volume), an helpfull tool is finite element calculation. Modelling the densification of the powder in a container allows to predict the kinetic of consolidation of the component and so to improve the HIP cycle. The final shape, the residual stresses and strains state are also predicted.

Numerical simulation required a finite element code with the adapted constitutive equations implemented, and the material data base.

The finite element code which is used for this study is called PRECAD. Developed by CEA/CEREM, it is devoted to thermomechanical calculations of multimaterials. Classical plastic and viscoplastic models are available. The parameters of the laws may depend on temperature. The specific viscoplastic law for porous materials has been implemented for 2D-axisymmetric configuration and for 3D geometries.

In 1997 a small-scale mock-up had been manufactured in view to validate the material data base for a simple shape part.

In 1998, a more relevant size mock-up for the primary wall of the WCLL ITER Test Module (ITM) has been designed, simulated and manufactured, in order to validate:

- the material data and the finite element calculation,
- the capabilities of the powder metallurgy route to manufacture complex parts such as a test blancket module.

The manufacturing route for the fabrication of the test blancket module (TBM) according to the Water Cooled Lithium Lead (WCLL) concept has been described.

1998 ACTIVITIES

DESCRIPTION OF THE MANUFACTURING ROUTE FOR THE FABRICATION OF THE TEST BLANCKET MODULE

An advanced manufacturing route ihas been proposed for the fabrication of the test blanket module (TBM) according to the Water Cooled Lithium Lead (WCLL) concept developped by CEA/Saclay. Both reference fabrication Method and alternative fabrication method (using powder metallurgy) have been detailed. This manufacture route is the conclusion of a work performed by the CEREM and the DMT. The route using the powder metallurgy displays some simplifications if compared with the reference route. Those simplications ensure a highest quality of the final part.

RELEVANT SIZE MOCK-UP MANUFACTURING

This component is 390 mm in height and 175mm in diameter at initial. It is made of a coiled stainless steel tube (fig 1) (8-10 mm inner and outer diameters) representing the first wall cooling channels. A 200 µm thick copper compliant layer is deposited on the coiled tube.

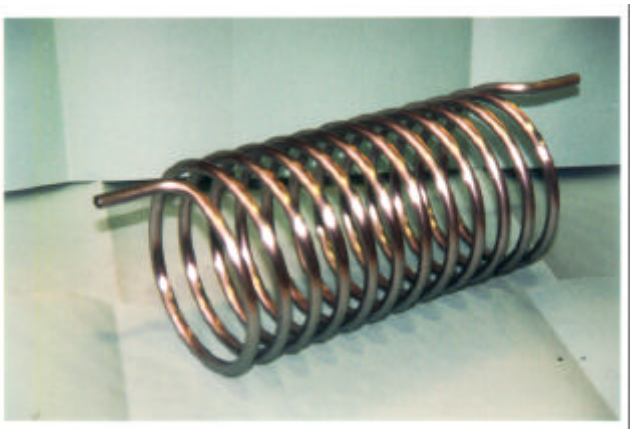

Figure 1 : Coiled tube made of 304L before coating

4 tubes of T91 (fig 2) (representative of the LiPb tubes) are inserted within the inner diameter with the T91LiPb tank plate (fig 3). Preliminarly, tubes of T91 are closed at the top by welding small plates (fig 4).

Figure 2 : Drilled tubes and plate tube before hipping

Figure 3 : Drilled tubes and plate tube before hipping

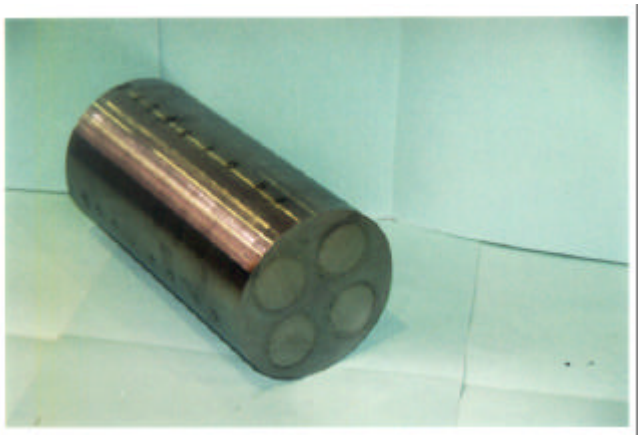

Figure 4 : Drilled tubes and plate tube and welded before hipping

Initial geometry is measured before HIP'ing to validate simulation.

For consolidation, the powder is encapsulated in the cylindrical canister made of 304LN steel. This canister is filled with the powder, degassed for several hours at medium temperature (200°C), and closed. Filling is done under vibration to obtain a uniform distribution of the particles. The tap density obtained is 64 %. The canister is put into the HIP vessel. Gas pressure and temperature are raised simultaneously, then maintained for some hours at the specified values, and finally decreased. In the case of F82H martensitic steel, temperature and pressure are increased in one hour to 800°C and 100 MPa, then increased in 30 minutes to 1050°C and 140 Mpa.

During the single HIP step, both powder compacts and parts made of T91 diffusion-bonded.

Figures 5 displays details of the mock-up and more particularly the Cu-coating on the coiled tube. Figure 6 display the insertion of the mock-up within the canister before the powder filling.

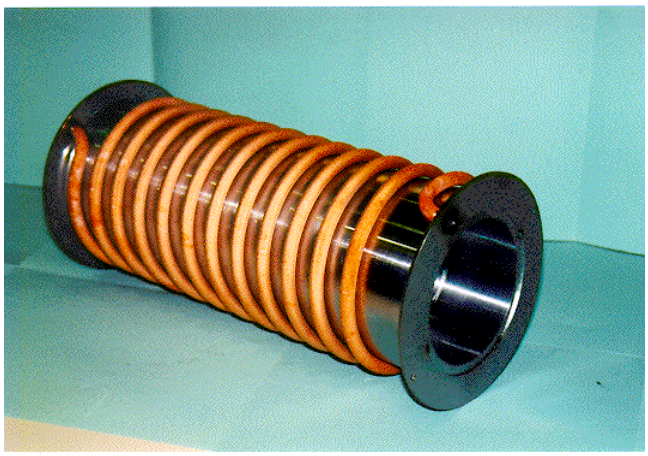

Figure 5 : Welded components before hipping

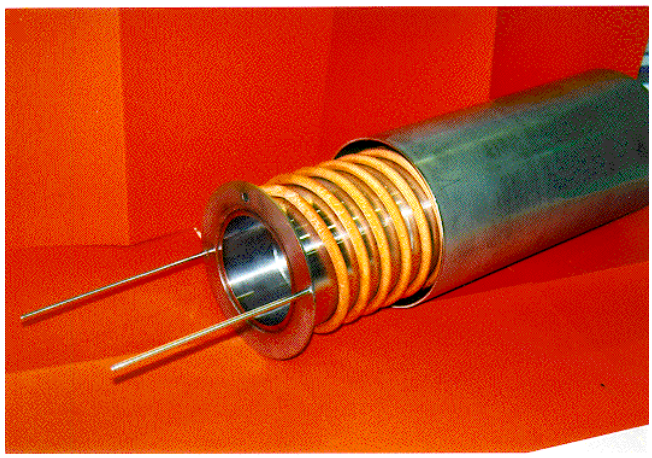

Figure 6 : Welded components before hipping with the canister before hipping

SIMULATION THE MOCK-UP

A data base has been identified on F82H material. This data base is used in PRECAD® software developped by CEA/CEREM to simulate the consolidation of the powder during hipping. This modelling is shown on figure 7.

CONCLUSIONS

A relevant size mock-up has been manufactured. It confirms the possibility to manufacture a complex part by powder metallurgy.

The modelling of HIP forming of F82H powder has been developped and used on this relevant size mock-up relevant of ITM first wall.

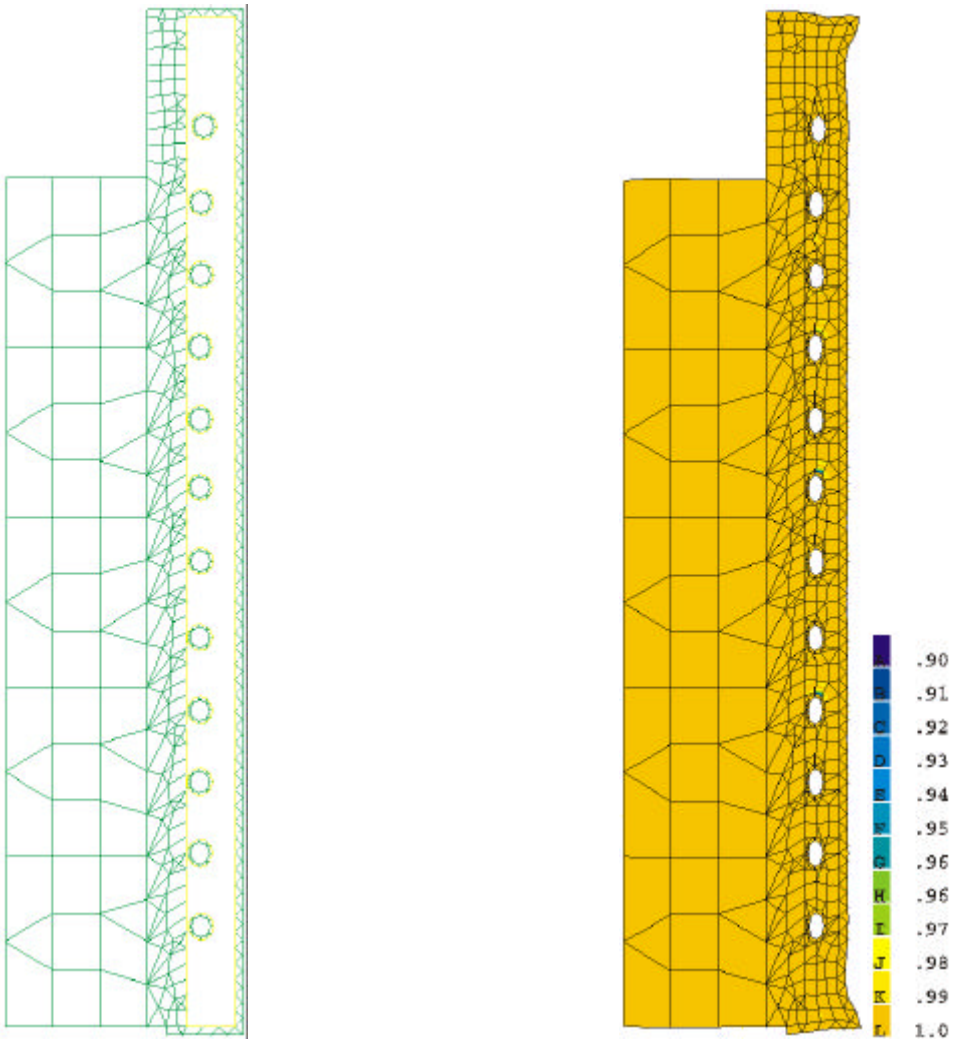

before consolidation

after consolidation (density distribution)

Figure 7 : Modelling with PRECAD

PUBLICATION

[1] Ch. Dellis, L. Federzoni, R. Baccino, G. Le Marois. Powder HIP manufacturing fusion reactor blancket. Proceeding of SOFT-1998, vol 2, p.1231-1234.

TASK LEADER

L. FEDERZONI

DTA/DEM/SGM
CEA Grenoble
17, rue des Martyrs
38054 Grenoble Cedex 9

Tél. : 33 4 76 88 57 26
Fax : 33 4 76 88 54 79

E-mail : federzoni@chartreuse.cea.fr

WP-A3-9.1

Task Title : TBM FABRICATION : DEVELOPMENT OF MINOR COMPONENTS AND INSTRUMENTATION
PABLITO : A NEW LITHIUM-LEAD TEST FACILITY FOR INSTRUMENTATION TEST

HISTORY

The PABLITO test facility was initially built (in 1996) in order to permit physico-chemical studies on the eutectic Li17 Pb83. It has been adapted for a study and development program on the instrumentation of lithium-lead circuits associated to the development program of representative test modules in ITER. The goal of this program of study is, on one side to determine the capacity of adaptation of instruments used on the fast breeders' sodium circuits to the lithium-lead circuits of fusion reactors, on the other side to study the modifications which would be necessary for a more specific adaptation, and finally to develop, if necessary, new instruments.

1998 ACTIVITIES

PROGRAM OF STUDY ON THE INSTRUMENTATION OF LITHIUM-LEAD CIRCUITS

Instrumentation of lithium-lead circuits can be classified in two categories :

- measure instrumentation (flowmeters, pressure collectors, level probes, temperature measures...),
- functionning instrumentation (pumps, valves, heaters...).

Among the first problems which were identified at the level of instrumentation, those can be mentionned :

- pumping of lithium-lead and up-raising,
- flow measure and flowmeters gauging,
- the study of quick valves permiting the closure of lithium-lead circuits in case of incident,
- consequences of the closure of quick valves on the pressure inside circuits.

Lithium-lead pumping

The case of electromagnetic pumps

Many sodium test facilities are equiped with electromagnetic pumps. In that sort of pump, the liquid metal is moved thanks to the Laplace powers. The liquid metal located in a magnetic field is traversed by an electric current (inducted or not). Then Laplace powers appear inside the liquid, which provoque its movement.

The powers are proportional to the intensity of the currents circulating inside the liquid metal. If electrical resistivity of the lead-lithium ($56.3 . 10^8 . \Omega . m$) is compared to that of the sodium ($24.58 . 10^8 . \Omega . m$) at 450°C it can be seen that lithium-lead is much less conductor than sodium. Electromagnetic pumps which efficiency with sodium was already low see their capacity strongly reduced with lead-lithium (minimum factor 4 on pressure and flows). Thus they cannot be envisaged for lead lithium circuits. They can be used in the case of small test facilities to obtain, at best, low flows of some hundreds of liters per hour.

The case of mechanical pumps

Even with sodium, when high flows and efficiencies are required, mechanical pumps are used. Actual technology permits to pump lead and raise it back at any height if the power of the engine (mainly electrical) is correctly adapted. The LEET (Laboratoire d'Exploitation et d'Essais Technologiques) has ordered a wheel pump in order to set it on the PABLITO test facility. This pump will permit to raise the lithium lead back from the emptying tank (low), on which it will be set, up to the loading tank (high), which makes a height of some three meters (height of the facility).

Calculated characteristics of the lithium-lead pump are the following :

Flow	:	0,144 to 0,72 m^3/h
Pump speed	:	1 050 à 1 100 t/mn
Absorbed power	:	1,5 à 2 kW
Engine power	:	4 kW
Wheel diameter	:	180 mm
Maximum pressing back height	:	5,2 à 5,5 m

This pump will be usable by mid-august, 1998. An other "circulation" pump, totally water-tight and that may be set on a pipe in order to ensure a circulation, is under study and may be achieved in 1999. Some details on the thermic reaction of reels are still to be resolved.

Flowmeter for lithium-lead on a magnetically perturbated context

The main measure instrument used on sodium circuits is the electromagnetic flowmeter. That sort of instrument uses a permanent magnet. The presence of strong interfering magnetic fields can alter the measures. An other system based on an alternative, relatively high frequency magnetic field, is thus envisaged: the "flow distorsion flowmeter", or FDF.

It uses Foucault currents. It is made of three coaxial reels: one central emiting reel traversed by an alternative current, and two receiving (passive) side reels connected in opposition.

When there is no circulation of lithium-lead in the pipe the magnetic field is symetric on both sides of the emiting reel and the sum of tensions of the two secondary reels is zero. When there is a flow, the Foucault currents inducted in the liquid are draged by it. The fields perceived by the secondary reels are different, and the difference of tension between the secondary reels is no more zero. This tension is proportionnal to the speed of the liquid, and thus to the flow.

Our tests aim to :

- verify the possibilities of applying the FDF to lead-lithium,
- study its utilisation limits according to the nature of the flow,
- verify the influence of an external magnetic field on the reaction of the instrument.

Two test pipes have been realised. Both are equipped with removable FDF which aim is to explore the different sorts of reaction along the piping after a singularity (knee, broadening, narrowing...).

Utilisation of valves on lithium-lead circuits

The high volumic mass of lithium lead, may in case of the quick closure of a valve generate phenomenons of the "battering ram effect" category, which consequences can be bad for the installations. A test pipe that may be set on Pablito has thus been designed. Its aim is to study from a qualitative point of view the apparition of "battering ram effects" according to the speeds of closure of a valve. It may be tested in 1999-2000.

Furthermore, test programs to study quick closure valves, that may answer safety problems, may be built (electropneumatic, membrane, electromagnetic... valves).

PABLITO TEST FACILITY

Work realised in 1996/1997 permitted to adapt this pipe for instrumentation tests (pumps, flowmeters, level gauges...). We thus chose a simple and quick installation permitting to change the models to be tested. We thus realised two removable parts which can each be replaced by a piping element carrying instrumentation.

The lower pipe can receive different sorts of "circulation pumps", whereas the higher pipe is more adapted to light instrumentation (flowmeters, valves...).

A weighing installation permitting flowmeters gauging has also been installed at the upper loading tank level.

Finally, the setting of a mechanical pump for raising back the liquid on a quick and simple way was necessary to make the installation totally operational.

The facility now has two pumps:

- a mechanical pump ensuring the raising back of lithium lead from the lower tank to the upper tank. This tank is equipped with a weighing system for flowmeters gauging.
- an electromagnetic pump located on the lower test pipe, ensuring circulation in the whole circuit. This CA 81-type pump has a relatively low flow (500 litters/hour).

CONCLUSION

The Pablito test facility thus allows an important flexibility for instrumentation tests.

Its 1997-1998 program includes :

- adaptation of the test facility and requalification,

- study, fabrication and test of a mechanical pump for lead-lithium,

- flow measure tests with a FDF under different outflow configurations and according to magnetic perturbations.

REFERENCE

[1] D. Piat « PABLITO : a new Lithium-Lead Test facility for Instrumentation Test » Proc. of the 20th Symposium on Fusion Technology, MARSEILLE, 7-11 September, 1998

TASK LEADER

Didier PIAT

DRN/DER/STPI
CEA Cadarache
13108 St Paul Lez Durance Cedex

Tél. : 33 4 42 25 35 16
Fax : 33 4 42 25 79 49

E-mail : piat@macadam.cea.fr

WP-A4-1.1

Task Title : PERMEATION BARRIERS FABRICATION AND CHARACTERISATION

Permeation Barriers Fabrication and Characterisation by CVD and HIP

INTRODUCTION

The objectives of this task are the fabrication and the characterization of tritium permeation barriers (TPB) for outside martensitic steel tubes. Two of the different methods studied for the fabrication of alumina as TPB material were :

- Chemical Vapour Deposition (CVD)
- Hot Isostatic Pressing (HIP).

In the second case, major technical problems have been met for the obtention of good quality of barriers made by the diffusion welding technique because of the high oxidability of the FeCrAl material chosen for the purpose. In addition, its availability as thin wall tubes seems to be a major issue.

So, during 1998, the effort has been focused on the CVD technique to develop TPB with the following items as main objectives :

- Coating qualification
- Technical evaluation of the CVD fabrication procedure.

1998 ACTIVITIES

COATING QUALIFICATION

The aim of this part has been :

- to describe precisely the operating procedures used for the different processes involved in the TPB fabrication,
- to perform a basic characterization of the CVD coatings,
- to provide specific specimens for standard qualification tests.

The CVD coating proposed for the TPB is consisted of two layers :

- a Fe-Al sub-layer performed by pack-cementation,
- an alumina top layer performed by MOCVD using a Pyrosol® method.

An optimization of the different processes used for this deposition has been carried out in order to perform a coating with good metallurgical properties with regards to the barrier function. In particular, the development has been focused on deposition techniques involving temperatures which do not exceed 750°C (steel tempering conditions) in order to avoid any further heat treatment necessary to restore the material properties. In addition, specific conditions have been optimized in order to avoid the formation of brittle intermetallic phases during pack-cementation.

In those conditions, the CVD procedure used to deposit the TPB is the following one :

1 - Fe-Al deposition by pack-cementation : the piece to be treated is put in a box in contact with a cement, which powder is composed of Al and Fe as donors, NH_4Cl as activator which allows the transport of the metallic species and Al_2O_3 as inert filler which role is to avoid the sintering of the cement. This cement is specifically prepared using a sray-drying process which provides a fine grained (50-100µm) and homogeneous powder. The treatment is performed during 1 or 2 hours at a temperature of 750°C : in fact, we take advantage of the Fe-Al deposition to performed simultaneously the tempering necessary to restore the steel properties after the HIP of the double-wall tubes. The formation of Al-rich intermetallic phases such as Fe_2Al_5 is avoided thanks to a work under reduced pressure (a few mbar) and thanks to the use of a (Fe,Al) donor which enables a codeposition of Fe and Al.

2 - Al_2O_3 deposition by Pyrosol® method : the principle of this method is based on the pyrolysis of an aerosol generated from a solution containing a metalorganic precursor (Al-i-propoxide) and a solvent . Air is used as carrier gas and alumina can be deposited in the range 450-500°C. The process is performed under atmospheric pressure which is a real advantage for industrial applications since long tubes can be coated in an air-air conveyor belt system.

The coating which is formed is consisted of a FeAl/Fe_3Al sub-layer and a covering alumina top layer. It has a total thickness of about 7 µm (Fig. 1). It is very uniform, dense and adhesive, without cracks or porosities.

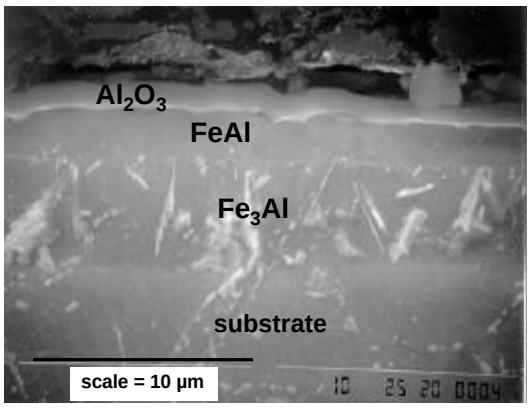

Figure 1 : Al_2O_3/FeAl/Fe_3Al coating performed by CVD (SEM cross-section)

Different specimens with specific geometries have been coated for standard qualification tests in order to qualify the coating behaviour during exposure to Li-Pb and to evaluate its barrier efficiency through permeation tests in gas or in Li-Pb. Fig. 2 gives some results of the Permeation Reduction Factors (PRF) obtained in gas at ENEA. These results are very promising.

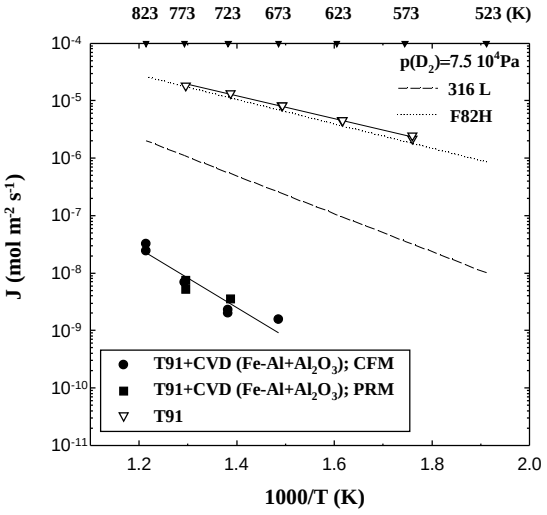

Figure 2 : Arrhenius plot of deuterium permeation rates for T91 and CVD coated T91 steel

TECHNICAL EVALUATION

The objective of this part is to gather some technical and economical data about the different processes involved in the TPB fabrication by CVD, e.g. pack-cementation, spray-drying, Pyrosol®, in order to study the industry assessment of permeation barriers. The pieces to be coated with TPB are the Double-Wall tubes (outer side) and the box itself (inner side). First considerations have shown that the CVD route seems to be compatible with the Double-Wall Tube and the Test Blanket Module fabrication procedures as defined today. Since both pack-cementation and Pyrosol® are performed at temperatures not exceeding 750°C, no additional heat treatment is necessary. In addition, the tempering necessary after the HIP step can be performed during the Fe-Al deposition itself. Some informations have been given about the R&D and industrial experiences existing for each process in different fields. An evaluation of the time and the cost of fabrication has been tried taking into account the number and the geometry of the pieces to be coated and the existence of adapted equipments. All these different items will be completed and precised in 1999.

CONCLUSIONS

A procedure of TPB fabrication by CVD involving a Fe-Al deposition by pack-cementation and an alumina deposition by Pyrosol® has been described. The metallurgical characterization of the coating has been performed and its qualification is still carried on through standard permeation and compatibility tests. Other coated specimens will be provided in 1999 for complementary tests. The preliminary technical evaluation of the different processes will be completed in 1999 in the frame of the industrial assessment of barrier fabrication. In addition, the scale-up demonstration necessary to develop all the processes at an industrial scale will be studied in the frame of the WPA3.1 task.

PUBLICATIONS

[1] C. Chabrol, F. Schuster « Tritium permeation barrier fabrication by chemical vapour deposition (CVD) - Coating Qualification Report » NT DEM n° 98/32.

[2] C. Chabrol, F. Schuster « Tritium permeation barrier fabrication by chemical vapour deposition (CVD) » NT DEM n° 98/67.

[3] C. Chabrol, F. Schuster, E. Serra, G. Le Marois « Development of Fe-Al CVD coatings as tritium permeation barrier » Fusion Technology 1998, Proceedings of the 20th SOFT, Marseille, France, 7-11 sept.1998, pp. 1227-1230

TASK LEADER

Emmanuel RIGAL

DTA/DEM/SGM
CEA Grenoble
17, rue des Martyrs
38054 Grenoble Cedex 9

Tél. : 33 4 76 88 97 22
Fax : 33 4 76 88 95 38

E-mail : rigal@chartreuse.cea.fr

WP-A4-2.1

Task Title : PERMEATION BARRIERS OUT-OF-PILE TESTING (PB PERFORMANCE)

PRF in Pb17Li & in water (and corrosion)

INTRODUCTION

The cooling of the water-cooled Pb17Li blanket developed in Europe, is insured by pressurized water flowing in tubes which are immersed in Pb17Li. For economical and safety reasons, the permeation through the tubes of the produced tritium in Pb17Li has to be minimized. To decrease this permeation, the use of coatings as tritium permeation barrier is considered. To validate such a solution, the permeation barrier efficiency has to be evaluated in experimental conditions taking into account the main features of the blanket operating conditions.

But, in a first step, the coatings have to be tested in simplified conditions to make a first selection between the potential candidates. After, the performances of the selected ones have to be evaluated in conditions as representative as possible of the running conditions of the blanket.

A device to test the performance of coatings as tritium permeation barrier in presence of gas and Pb17Li has been built. It has been used this year to test an aluminized coating supplied by CEA/CEREM Grenoble. Moreover, to take into account the presence of the water in the cooling tubes, a permeation device with water and Pb17Li has been designed.

1998 ACTIVITIES

PERMEATION TESTS WITH GAS AND Pb17Li

The device

The device [1] consists in a cylindrical external envelope made of aluminized 316L stainless steel in which are located the permeation chamber (length 150 mm, internal diameter 23 mm, thickness 1 mm), a finger for a thermocouple and a bubbling device as it is shown on Figure 1. The envelope is continuously swept by an argon or helium hydrogen mixture and the inside of the permeation chamber is swept by a continuous helium flow. The space between the envelope and the permeation chamber can also be filled with some Pb17Li. An iron membrane enables to measure the hydrogen concentration in the gas or in the Pb17Li. The gas is analyzed with a chromatograph.

The permeation chamber

Tests have been performed using two permeation membranes: one made of a 1.4914 martensitic steel and which was used for the tests carried out in this device in 1996 and 1997. In July 1998, it has been received from CEA/CEREM/DEM a 1.4914 steel membrane externally covered (except on the weld between the cylindrical part and the top cover of the membrane) with an aluminised coating obtained by CVD process.

Conditions of the tests

Two kinds of tests have been performed: one for which the medium inside the envelope was a gas flow and the other, for which the inside of the envelope was filled with Pb17Li in which a gas was bubbling.

All the tests have been performed in the following conditions:

- gas pressure in the permeation chamber or in the envelope: $1.13 \pm 0.01\ 10^5$Pa;
- gas flow rate in the permeation chamber or in the envelope: 100 $cm^3\ min^{-1}$;
- hydrogen content in the envelope sweeping gas (argon or helium): 2 vol%;
- sweeping gas in the permeation chamber: helium.

During the envelope filling with Pb17Li, some liquid metal went up in the envelope tubes dedicated to the gas admission and exit. Therefore, some Pb17Li has been lost and the precise Pb17Li level in the envelope, initially calculated to be 30 mm under the top of the iron membrane, was not precisely known. It is possible that the top part of the iron membrane was not immersed in Pb17Li. Moreover, as the Pb17Li liquid surface is very often covered by an oxide layer, the top part of the iron membrane might have been covered by these oxides.

Results

The hydrogen content and the hydrogen permeation flux towards the permeation membrane are measured at steady state and represent the mean values obtained during 2 to 4 tests.

During the tests with gas in the envelope, the hydrogen pressure in the iron membrane was 2260 ±10 Pa, corresponding to the hydrogen content in the gas. On the other hand, when some Pb17Li was in the envelope, although the hydrogen content in the bubbling gas was also 2 vol%H_2, the hydrogen pressure in the iron membrane after a 80 hour bubbling was only equal to 940 Pa. This difference between the hydrogen partial pressure in the bubbling gas and the pressure in the iron membrane can be explained in two ways. First, it could result from a malfunction of the iron membrane (especially if it has been covered by oxides as Pb17Li was introduced) and the hydrogen partial pressure in Pb17Li corresponds to that in equilibrium with the bubbling gas, that is to say 2260 Pa. Second, the hydrogen diffusion in Pb17Li is too slow to enable to the hydrogen partial pressure in Pb17Li to reach the value corresponding to the equilibrium with the bubbling gas and consequently the hydrogen partial pressure in Pb17Li is 940 Pa. Therefore, we have considered for the permeability calculations the two values, 940 and 2260 Pa for the partial pressure of the dissolved hydrogen in Pb17Li.

The permeability values, given in the Table 1 have been deduced from the permeation flux using the Richardson equation assuming that the permeation is controlled by the diffusion and using the Fick equation for an infinite hollow cylinder :

$$J = \Phi \left(P_H - P_{Ho} \right) / r_o \ln(r/r_o) \qquad (1)$$

with:

- J: hydrogen permeation flux per unit of surface area (mol m^{-2} s^{-1})
- P_H : hydrogen partial pressure in the envelope (Pa)
- P_{Ho} : hydrogen partial pressure in the permeation chamber (Pa)
- r: external radius of the permeation chamber (m)
- r_o: internal radius of the permeation chamber (m)
- Φ: permeability of the permeation chamber material (mol m^{-1} s^{-1} $Pa^{-1/2}$)

Discussion

The permeability values obtained with the 1.4914 steel permeation chamber are shown on the Figure 1 together with the values obtained in 1996 [2] and 1997 [3]. We can notice that the values obtained in 1997 [3] and 1998 are lower than those obtained in 1996 [2].

This difference could be due to an oxidation of the membrane. These values are also lower than those given by other authors by a factor between 10 and 20. From 1998 data, we have deduced an activation energy of 50 kJ mol^{-1} which is higher than the values from the literature (between 35 and 46 kJ mol^{-1}).

The permeability values obtained with the coated permeation membrane are shown on Figure 1. The difference between the values obtained when the envelope is swept by a gas and those when the envelope contains Pb17Li is of the same order of the uncertainties on the values obtained when the envelope contains some Pb17Li. Therefore, it cannot be put in evidence a difference in the permeability of the membrane when it is swept by gas or when it is immersed in Pb17Li.

From Figure 1, we can also see that, in the tested conditions, this coating enables to achieve a maximum permeation reduction factor of 10 if we compare the permeation fluxes of the coated membrane with those obtained with the bare material in [2] but only a factor 2 if the comparison is made with the results obtained in 1997 [3] and in 1998. But this latter comparison is probably made with a 1.4914 oxidized membrane. In any case, it is less than what is reported in [4] with T91 material (up to 5000). However, these results would require to be validated and completed. Microscopic observations of the coating would be necessary to assess the quality and homogeneity of the coating. Moreover, the results shown in [4] were obtained with a different technique and only in the gas phase (disk technique).

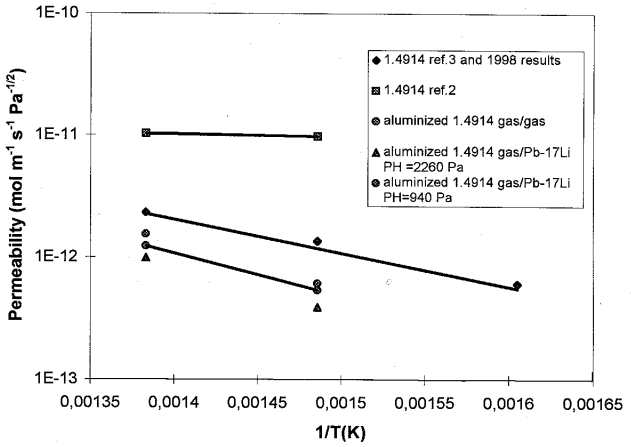

Figure 1 : Hydrogen permeability of 1.4914 steel with and without coating

PERMEATION DEVICE WITH WATER AND Pb17Li

In this device, the produced tritium in PB17LI will be simulated by deuterium which will be dissolved in PB17LI by bubbling. The water will have a chemistry representative of the blanket circuit water. This chemistry will be chosen to avoid large corrosion damage. Moreover, dissolved hydrogen will be added in the pressurized water as it will be done in the blanket water circuit to counteract radiolysis effects. This device will enable to determine the hydrogen and deuterium fluxes through a martensitic cylindrical membrane by measuring the partial pressures of hydrogen and deuterium in the water and PB17LI. The same measurements will be performed with a membrane covered by a coating in order to evaluate the efficiency of this latter to decrease the deuterium permeation.

Moreover corrosion studies of the martensitic steel with and without a coating by the pressurized water will also be performed .

The detailed design of the device has been done. The equipment has been chosen and is being supplied except for the gas compressor of the gas circuit. In fact, the compressors which have been proposed up to now either enable to fight again the gas pressure drop due to PB17LI height but the flow rates are too large or have a convenient gas flow rate range but a too low compression ratio. Other suppliers are being consulted.

The end of the construction of the device is planed in the second 1999 quarter.

CONCLUSION

Hydrogen permeation tests have been performed with a 1.4914 steel permeation membrane with an aluminized CVD coating on its external side. The coating was in contact either with a gas flow or with stagnant Pb17Li in which an helium/hydrogen gas mixture was bubbling. The hydrogen permeation fluxes in the two cases are similar and taking into account of the experimental uncertainties, it is not possible to put in evidence some difference in the permeabilities. If we compare these results with those obtained in the same device with the uncoated material, a maximum permeation reduction factor of ten can be deduced. These results would require to be confirmed and microscopic observations of the coated membrane would be necessary.

The detailed design of the permeation device with pressurized water and Pb17Li has been done and the equipment is being supplied. The complete construction is planed for the second 1999 quarter.

REFERENCES

[1] S. Berger, A. Terlain
Hydrogen permeation: experimental device and analysis technique
CEA Report, RT SCECF 371 (September 1995)

[2] T. Dufrenoy, M. Perrot, A. Terlain
Hydrogen permeation, First results with 1.4914 martensitic steel -Task WP-A-5-3-
CEA Report, RT SCECF 408 (December 1996)

[3] A. Terlain, T. Dufrenoy
Trittium permeation barrier testing devices
CEA Report, RT SCECF 448 (December 1997)

[4] C. Chabrol, F. Schuster
Tritium permeation barrier fabrication by chemical vapor deposition (CVD). Coating qualification report
CEA Report, NT DEM 98/32 (July 1998)

REPORT

[1] T. Dufrenoy, A. Terlain, Hydrogen permeation measurements with an aluminized martensitic steel, CEA Report, RT SCECF 487 (December 1998)

TASK LEADER

A. TERLAIN

CEREM/SCECF
CEA Saclay
91191 Gif-sur-Yvette Cedex

Tél. : 33 1 69 08 16 18
Fax : 33 1 69 08 15 86

E-mail : TERLAIN@ortolan.cea.fr

WP-A5-1

Task Title : TRITIUM EXTRACTION FROM Pb17Li

INTRODUCTION

The Melodie loop is an experimental facility dedicated to test gas-liquid contactors to extract the tritium produced in the water cooled liquid blanket of fusion reactors. This tritium extraction will allow not only to supply the plasma with tritium but also to decrease the tritium permeation in the coolant by lowering the inventory in the blanket.

In 1995, a 600 mm high packed column was settled in the loop where hydrogen is used to simulate tritium. The choice of this type of extractor was due to the expected beneficial impact of the liquid film flow involved in this type of contactor on the kinetic of the mass transfer. During 1996 and 1997 tests, a 22% maximum efficiency was reached at 673 K [1] but incoherence about the hydrogen mass balance was observed, for which no satisfactory explanation was found [2], in spite of the experimental work performed in that aim.

This year, a new contactor was settled and tested. It differs from the previous one by its height (800 mm), the absence of dead volume between the packing and the envelope and several internal devices allowing to study the contactor either in a bubble or in a film configuration. Moreover, a new acquisition data system has been installed.

1998 ACTIVITIES

NEW DEVICES SETTLED AND ELECTRO-MAGNETIC PUMP PERFORMANCES

A new liquid distributor, constituted by a plate perforated with 30 holes of 3 mm diameter and crossed by four pipes of 4 mm diameter allowing the gas to go out of the packing, was settled. As expected from the preliminary experiments in a glove box which has led to its design [2], a liquid retention occurs on the liquid distributor necessary to insure a good radial spreading on the first packing cylinder. Indeed, with the lowest liquid flow rate investigated during the extraction tests, the retention height estimated via level electrodes, was between 1 and 4 centimetres. Moreover, due to the new configuration of the gas evacuation from the packing (four pipes attached to the liquid distributor), a constant gas flow rate of 1000 N.T.P. cm^3 mn^{-1} of argon was maintained during the extraction tests in a bubble column configuration without electromagnetic pumps breakdowns.

The previous gas flow sparger, a perforated pipe, was changed to a sintered disk with an average porosity of 3 µm.

This device is well suited to the bubble column since in that case, the interfacial area is the area of the whole generated bubbles and is all larger since the bubbles are small. In the liquid column, the sparger gas flow has only to insure a radial distribution of the gas stream. The pore diameter has been chosen in order to maintain the head losses compatible with the extractor design. However, the high inlet pressure obtained experimentally (5 10^5 Pa) results from both the flow through the sintered disk and the likely partial plugging of the flow inlet way, may be by some oxide or by solid Pb17Li in cold zones.

The packed cold trap settled at the exit of the gas stream has not solved problems of the gas exit control valve plugging. Observations with an optical microscope showed that the particles trapped in this valve had an average dimension lower than 1 µm. Regarding to this size, the best way to trap them seem to be a process based on filters.

Regarding the previous high intensities delivered to the electromagnetic pump coils in 1996 and 1997 and past problems of coil overheating, an optimisation of the column gas pressures was done to share at best between each pump the supplementary rise of power required to increase the Pb17Li lifting height of 200 mm when the column is in film configuration. The resulting intensities, about 10 A each, led to a liquid flow rate between 35 and 100 10^{-3} m^3 h^{-1}. In this configuration, many break downs of the pumps occurred due to a high sensibility to any variation of the gas pressure in the extractor (likely related to a sudden modification of the retention height). Moreover, a significant instability of the liquid flow rate was observed, the larger variations being due to drops of tension in the supply network. However, most of the time, the liquid flow rate evolved by steps whose durations were sufficient to determine its incidence on the efficiency but not sufficient to quantify the extraction efficiencies at an established steady state.

CHECKING OF THE MEMBRANE RELIABILITY

An experiment was performed to check the reliability of the hydrogen pressure sensors of the membranes immersed in the Pb17Li at the extractor entrance and exit, which are used to calculate the extraction efficiency. In that aim, the whole loop was saturated with a 2% hydrogen gas which allowed to check that the resulting pressures were similar and around 2370 Pa.

EXTRACTION TESTS IN A BUBBLE COLUMN CONFIGURATION

The bubble column configuration corresponds to the whole immersion of the packing, the gas phase being a flow of bubbles.

From extracting tests in that hydraulic configuration, experiments were performed in order to :

- validate that, for an identical small gas flow rate, the extraction efficiency is lower than in a liquid film column,

- investigate the potential of a bubble packed column when increasing the gas flow rate to generate interfacial area. In a bubble packed column, it is expected that the packing would organise the flow of bubbles thus preventing or limiting their coalescence.

Therefore, two series of tests were performed respectively at 500 and 1000 N.T.P $cm^3\ mn^{-1}$. These tests which were carried out with inlet hydrogen pressures ranging from 1100 to 1300 Pa in Pb17Li entering the reactor, showed:

- a beneficial impact of a higher retention time of the liquid alloy on the extraction efficiency since a rise of its flow rate provoked reproducibly, a decrease of the efficiency. Quantitatively, as no steady state could be reached at high retention time, it can only be asserted that the efficiency increases from 10 to at least 13.5% when decreasing the liquid flow rate from 90 to 60 $10\text{-}^3\ m^3\ h^{-1}$.

- a negligible impact of an increase of the purge gas flow rate on the extraction efficiency since for an equivalent range of liquid flow rate tested (80 to 110 $10^{-3}\ m^3\ h^{-1}$), the efficiencies were quite the same, in a 10 to 12% range.

If we rely on the capability of the packing to prevent efficiently the bubble coalescence, these results would indicate that the efficiency which could be expected from a bubble column will be mostly function of the retention time of the liquid.

EXTRACTION TESTS IN A LIQUID FILM COLUMN CONFIGURATION

The decrease of the liquid flow rate injected on the packing always involved an increase of the extraction efficiency. The best result obtained is 33 % for the lower liquid load, about 31 $10^{-3}\ m^3\ h^{-1}$, which represents a superficial velocity of 2.8 $10^{-3}\ m^3m^{-2}\ s^{-1}$ for the 62.7 mm diameter packing. This value is in the range advised by the packing manufacturer for its petrochemical reference liquids (3 10^{-4} to 4 $10^{-3}\ m^3m^{-2}\ s^{-1}$).

The 1996 and 1997 investigations on the liquid flow rate had led to conclude to the non incidence of this latter in the 70 to 100 $10^{-3}\ m^3\ h^{-1}$ range. At this time, the calculations were based on average values because of the lack of real time data. It is clear that with the inaccuracy resulting from these averages, we were not able to detect a possible weaker impact of the liquid load in this range.

The beneficial influence of the liquid flow rate decrease, observed this year, could be due to a separated or a combined effect of :

- the increase of the retention time,

- a thinner liquid film on the packing favourable to the kinetics of transfer, if it is assumed that this film takes place.

There is no significant impact of the gas flow rate on the extraction efficiency, in the 100 to 500 N.T.P. $cm^3\ mn^{-1}$ range investigated. If an effect was further observed at a flow rate larger than 500 N.T.P. $cm^3\ mn^{-1}$, it should be compared on an economical point of view to the increase of the column height leading to similar performances.

COMPARISON BETWEEN THE PREVIOUS 600 mm EXTRACTOR AND THE PRESENT 800 mm ONE IN A LIQUID FILM FLOW CONFIGURATION

For an equivalent liquid flow rate, 80 $10^{-3}\ m^3\ h^{-1}$, the efficiency obtained is quite the same, about 21%, with the 800mm high packing and with the 600 mm one ([1] and [2]).

If the mass transfer model of NUT and HUT, comprehensibly described in [2] is used, the 800 mm high column efficiency should have been about 27%.

Regarding this result, the problem is to know if the absence of improvement of the efficiency signifies that no better performance has to be expected from an increase of the packing height or if it is just due to a not justified extrapolation and comparison between two systems which were not exactly the same in their design and which were not studied with the same tools (recording of the data in real time in 1998, dead volume).

In order to evaluate the impact of a packing height increase of the present extractor, a test was performed with the first half of the column in a film flow configuration and the second one in a bubble flow configuration.

The liquid flow rate was maintained at a 40 $10^{-3}\ m^3\ h^{-1}$ average value. The resulting efficiency varied in a 20 to 22% range for an inlet hydrogen pressure in Pb17Li between 1050 and 1100 Pa.

The real efficiency of the 400 mm packing used in a film flow configuration is in fact inferior to the 21% observed for the whole column because of the supplementary extraction occurring in the last 400 mm bubble flow. Therefore, the 400 mm packing efficiency is at least 10% inferior to the one reached with 800 mm of packing for the same liquid load, 33%, as reported before. It is consequently highly probable that further improvements of the efficiency have to be expected from an increase of the packing height settled.

COMPARISON BETWEEN THE BUBBLE FLOW AND THE LIQUID FILM FLOW CONFIGURATIONS IN A PACKED COLUMN

From the presented results, it can be concluded that for a similar liquid flow rate of 80 10^{-3} m^3 h^{-1}, the liquid film flow leads to higher efficiency than the bubble flow (21 against 10.5%). Since the retention time should be higher in the bubble flow than in the film flow, this difference can be attributed to:

- the suitability of the liquid film flow for the kinetics of mass transfer (diffusion of atomic hydrogen in the liquid as the limiting step),

- the difficulty to generate interfacial area via bubbles.

PROSPECTS

A device insuring a stabilisation of the liquid flow rate would be highly convenient. It should allow to reach established steady state and should be absolutely necessary for the resolution of the mass balance incoherence.

A new trap based on filters should be settled on the loop whatever the column flow configuration. These filters could avoid plugs to occur during long time running even at low gas flow rate.

An improvement of the average 30 % efficiency can be expected from:

- a decrease of the superficial velocity below the lowest value investigated, 2.8 10^{-3} $m^3s^{-1}m^{-2}$.

- an increase of the packing height .

CONCLUSIONS

An improvement of the extraction efficiency was obtained in 1998, up to about 30%, for 1000 Pa inlet hydrogen pressure in Pb17Li entering the extractor. The previous efficiency reached at the same temperature of 673 K was 22%. It was achieved thanks to a reduction of the liquid load injected, the lowest investigated (2.8 10^{-3} $m^3s^{-1}m^{-2}$) being still not the optimal one.

An experiment, performed with the 1998 extractor, showed that an increase of 400 mm of the packing height leads to at least 10% of supplementary efficiency (for an hydrogen pressure in the 400 to 1000 Pa range). However, by extrapolation of the results obtained with the previous column [1] and for the same conditions of liquid load, the prediction of the efficiency consecutive to the 200 mm increase of the packing height, was not reliable. It may be attributed to the lack of control of the previous extracting process (data record, dead volume).

The behaviour of the bubble packed column was investigated. It led to efficiencies lower than the ones obtained in a liquid film flow configuration. According to these experiments, the only way to improve the bubble packed efficiency column would be an augmentation of the retention time.

REFERENCES

[1] N.ALPY, T. DUFRENOY, A. TERLAIN
Hydrogen extraction tests in Melodie: 1996 results with a packed column
CEA report, RT-SCECF 407 (December 1996)

[2] N. ALPY, A. TERLAIN, M. PERROT, T. DUFRENOY
Hydrogen extraction from Pb17Li: 1997 results on the packed column running and 1998 views
CEA report, RT-SCECF 446 (December 1997)

1998 PUBLICATION

[1] N. ALPY, A. TERLAIN, V. LORENTZ
Hydrogen extraction from Pb17Li: 1998 results with a 800 mm high packed column
CEA report, RT-SCECF 485 (December 1998)

TASK LEADER

Anne TERLAIN

DTA/CEREM/DECM/SCECF
CEA Saclay
91191 Gif-sur-Yvette Cedex

Tél. : 33 1 69 08 16 18
Fax : 33 1 69 08 15 86

E-mail : TERLAIN@ortolan.cea.fr

WP-A6-1.1

Task Title : SAFETY ANALYSIS FOR DEMO POWER PLANT

INTRODUCTION

Technological analyses relative to the blankets of a DEMOnstration reactor based on the principle of a Tokamak associated with the DT reaction have been performed in Europe for several years now.

The European strategy foresees that the DEMO reactor will have its place between the next experimental machine, ITER, intended to demonstrate the feasibility of fusion power, and a series of fusion reactors.

In a fusion reactor, the blankets have several functions:

- they serve to produce the tritium needed for the D-T reaction (by neutronic reaction with lithium);
- they serve to remove heat in order to convert it into mechanical energy;
- and lastly, they help protect the components behind them, particularly the superconducting magnets at cryogenic temperature, from radiation.

Of the two concepts retained after selection in 1995, one option uses the eutectic alloy lithium-lead as breeder material and water as the coolant (WCLL: water-cooled, lithium-lead) [1].

The purpose of this task is to make a preliminary assessment of the safety of such a concept. Without detailed drawings of the other components of the reactor, preparing an actual safety analysis, however, is out of the question.

1998 ACTIVITIES

OVERVIEW OF THE SAFETY APPROACH

Introduction

The safety studies made in the framework of SEAFP and SEAFP2, and particularly the development of a safety assessment in the framework of ITER, permitted the development of a safety approach suited to fusion facilities.

As in any nuclear facility, the objective is to protect the general public, workers, and the environment from radioactive hazards. It is natural, therefore, that the same generic principles developed for other nuclear applications should similarly be applied, and, among these, particularly that of "Defence in Depth".

Generally speaking, this is an exhaustive and progressive approach that consists in setting up various levels of prevention, protection, and mitigation with the aim of limiting the risk and the environmental consequences of an accident.

Identification of Safety Functions

The main objective of safety is to protect the general public against any dispersal of radioactive material into the environment, and the way to prevent such an eventuality is to ensure the containment of this radioactive material by providing for robust and reliable containment barriers.

These containment barriers must be protected against possible aggression related to the presence of energy sources in the facility, which can be of three types: chemical, thermal, and magnetic.

Figure 1 gives a summary of these energy sources, the risks they induce, and the safety functions to be put in place to protect the containment barriers against these risks.

We shall rapidly review the identified safety functions and highlight the aspects linked to blanket design:

Plasma Energy Control

An undeniable advantage of fusion energy is that any failure (a coolant leak, for example) that occurs within the vacuum chamber inevitably leads to plasma shutdown. With respect to blanket design, this means taking into account the thermal and mechanical effects of such a disruption.

The automatic shutdown of the plasma within a reasonable lapse of time is particularly useful when the initial failure is located outside the vacuum chamber: it permits averting an internal LOCA in the event of an external break or a LOFA.

The presence of two cooling circuits on the blankets, however, permits avoiding a rapid temperature rise and should enable easily managing this type of incident without generating an internal break in the short term

Residual Power Removal

The studies conducted in the framework of SEAFP and SEAFP2 showed that, in the event of even complete cooling failure, the increase in temperature due only to residual power does not reach a temperature high enough to result in rapid structural collapse.

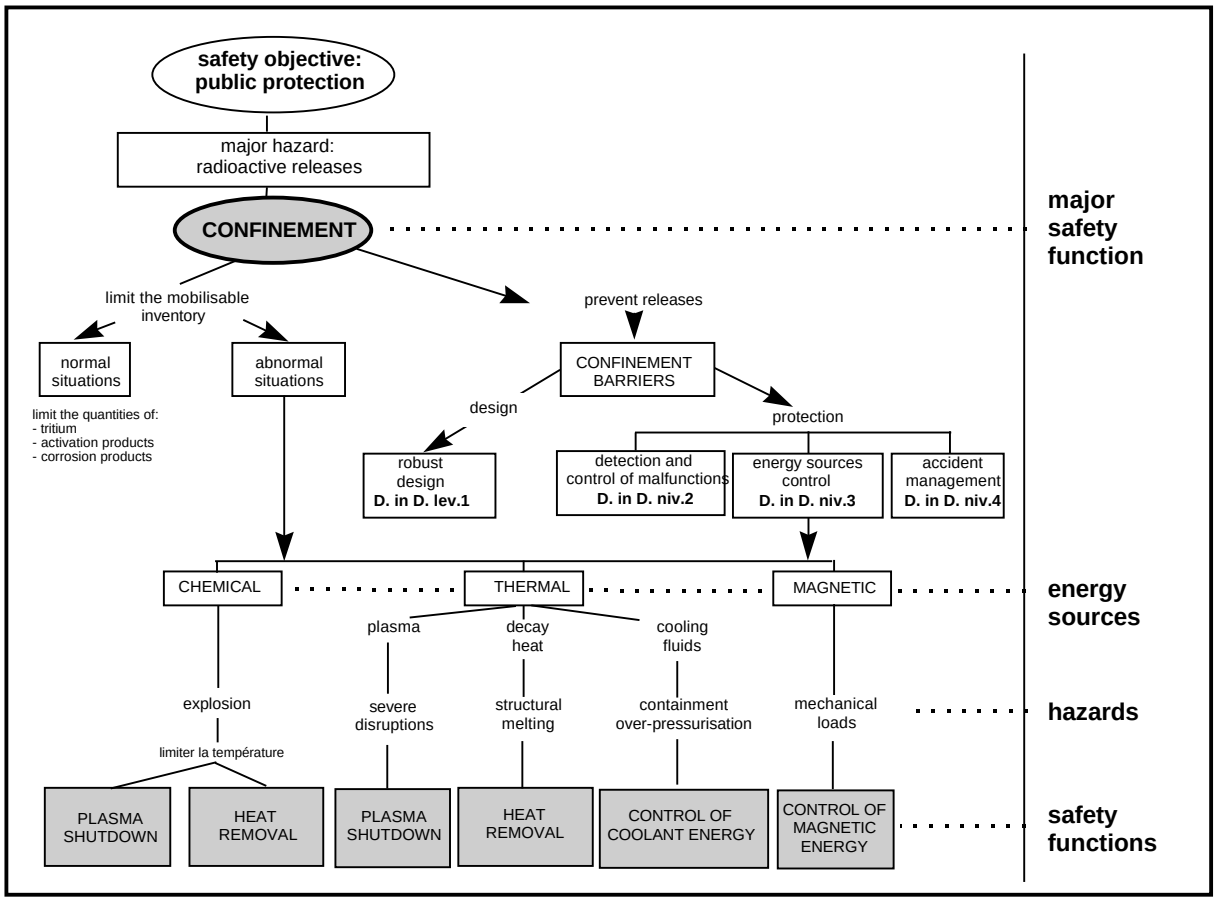

Figure 1 : Fusion Power Plant Safety Functions

However, the presence of a residual power removal system can greatly facilitate the management of such an accident and prevent further degradation.

Chemical Energy Control

A risk of chemical reaction exists as a result of the design of the WCLL blankets itself: this is the reaction between the lithium contained in the LiPb alloy and the water that serves as a coolant.

The control of this reaction is the subject of an extensive R&D programme, not only to estimate its consequences (the LIFUS experiment and modelling) but also to define detection methods [4].

The chemical reaction between water and the material of the first wall should also be considered, depending on the nature of the latter.

Coolant Energy Control

The consequences of failures should be taken into account in the design of the various containment barriers, as well as in the definition of systems permitting these barriers to be protected.

As regards the design of the blankets, a mechanical analysis of the structures should take into account the pressure linked to the coolant, considering, if need be, overpressure linked to thermal and/or chemical interaction due to water-LiPb interaction.

Magnetic Energy Control

The SEAFP studies showed that correct design of the magnets permitted averting the risk of missiles.

The possibility of an electric arc should, however, be considered, as it can lead to containment degradation.

IDENTIFICATION OF DESIGN BASIS ACCIDENT SEQUENCES

In the framework of the SEAFP programme, as in the framework of ITER/FDR, it was demonstrated that all the sequences resulting from a single failure, such as, for example, a LOCA or LOFA, result only in minimal releases provided the containment barriers have been correctly designed (with the possible presence of safety systems enabling these barriers to be protected even under the most severe conditions: pressure suppression systems, expansion volumes, etc.) [2].

The conclusion in this case is the same as for the more complex sequences considered in the framework of SEAFP2 [3].

This systematic study has permitted identifying the most severe design basis accident for the containment strategy: the loss of heat sink. The management of this accident sequence is not linked to the design of the blanket itself; it determines, however, containment strategy for the components within the torus building.

Analysis also shows that particular attention should be given to the management of other sequences, such as:

- those involving an electric arc around the magnets (with no direct relation with blanket design);

- those involving hydrogen release due to chemical reaction (once again, risk of a water-LiPb reaction and possible water-first wall material reaction).

Outside releases can be kept to a very low level that depends essentially on two factors, for a given containment strategy:

- the mobilisable radioactive inventory inside the vacuum chamber (mainly the tritium contained in first wall material and dusts),

- the radioactive inventory in the fluid circuits, particularly in the coolant.

The tritium content in the coolant can also have a direct effect on the level of releases and therefore should be carefully controlled.

CONCLUSION

Analysis has thus shown that the DEMO reactor safety assessment is covered by that made in the framework of the SEAFP and SEAFP2. In particular, the conclusions relative to the containment strategy defined in the SEAFP2 context are also applicable.

The review we have made has nevertheless permitted noting certain points that deserve clarification or examination.

The studies on the DEMO blankets do not take into account any first wall armour. The presence of the latter proves to have an effect on the analysis of accident sequences (possible reaction with water in the event of a LOCA).

An appropriate containment strategy permits keeping releases to a very limited level in the event of an accident of internal origin; this depends, however, on the radioactive material inventory inside the vessel (tritium and dusts), as well as on tritium and corrosion product activity in the coolant**.**

The studies performed on long-term safety programs and the ITER program have permitted identifying design basis accidents. Among these, the accident that concerns the blanket design of interest is related to the case of a water leak in the lithium lead: its analysis confirms that priority must be given to studies relative to this accident sequence (with respect to both the estimation of its consequences and its detection).

REFERENCES

[1] L. GIANCARLI, M. DALLE DONNE, W. DIETZ - « Status of the European Breeding Blanket Technology » Fusion Engineering and Design 36 (1997) 57-74

[2] J. RAEDER and all « Safety and Environment Assessment of the fusion Power (SEAFP) » EUFURBRU XII 217/95

[3] G. MARBACH, I. COOK « Safety and environment aspects of a Fusion Power Reactor »
Invited SOFT Communication to be published in FUSION TECHNOLOGY

[4] P. SARDAIN, G. BENAMATI, I. RICAPITO, G. MARBACH « Consequences of Pb-17Li/water Interaction within a Blanket Module » Proc. of the 20th Symposium on Fusion Technology, MARSEILLE, 7-11 September, 1998

TASK LEADER

Gabriel MARBACH

DRN/DER/SERSI
CEA Cadarache
13108 St Paul Lez Durance Cedex

Tél. : 33 4 42 25 34 14
Fax : 33 4 42 25 48 68

E-mail : marbach@babaorum.cad.cea.fr

WP-A6-2.1

Task Title : SAFETY ANALYSIS OF ITER WCLL TEST MODULE DEFINITION OF SAFETY APPROACH

INTRODUCTION

ITER is an experimental D-T fusion reactor.

One of the objectives of this facility is to include and irradiate experimental test blanket modules.

These ITER test-blanket modules (TBM) will help qualify a tritium breeding blankets for a future fusion power reactor [1].

The main objectives of this experimental programme are to :

- Verify and demonstrate the functionality of the integrated system, subsystems and individual components in the fusion environment,
- Verify and demonstrate the performance of tritium production, extraction and recovery by establishing a complete tritium balance of the system which has to correctly simulate future reactor conditions,
- Verify and demonstrate high-grade heat production and removal by establishing a complete power balance of the system with a concept representative of reactor conditions,
- Calibrate and validate the analysis, including the calculations and modelling used.

The WCLL concept has the following main characteristics [2] :

The coolant is water at a pressure of 15.5 MPa and the outlet temperature is 325°C.

The breeder is the liquid eutectic alloy Pb-17Li. (This alloy whose melting point is 235°C has the following composition : 17 at % Li with up to 90 % ^{6}Li enrichment for breeding and 83 at % Pb for neutron multiplication).

The structural material is a martensitic steel (EUROFER - 97 which is being developed for reduced activation and good irradiation characteristics.

The WCLL blanket concept is based on a type of box which is cooled separately and can withstand disruption and pressure loading. This box confines a pool of the liquid alloy Pb-17 Li which is slowly pumped through the blanket for tritium extraction and Pb-17 Li replenishment in dedicated equipment.

The heat generated in the pool is extracted by bundles of double-walled U-tubes and through conduction to the cooled walls of the segment box.

The test module will be surrounded by a frame made of stainless steel and cooled by water. The first wall is covered with a 5 mm beryllium layer and is cooled, like the side walls, by toroidal-radial cooling tubes.

1998 ACTIVITIES

THE WCLL-TBM - GENERAL SAFETY APPROACH

TheTBM safety approach has to follow the guidelines and recommendations issued for ITER's global installation.

The implementation of these safety principles has to take into account the experimental aspects of the TBM. The main issues are as follows:

The safety analysis has to take in account TBM failures and induced potential hazards from the defence in depth point of view (prevention, detection, protection and mitigation of consequences),

TBMs are designed in such a way that an operation or accidental sequence does not lead to unacceptable consequences with respect to the safety of the ITER facility, workers and the public in the vicinity of the facility,

The analysis of TBM roles, as far as the main safety functions of ITER are concerned, has to demonstrate that :

- Either that the safety functions planned for the reactor itself are not degraded by any potential risks generated by the implementation of TBMs,
- Or that the safety functions planned for TBM design cover these risks,

RADIOLOGICAL AND ENERGY SOURCE TERMS

Tritium Production

Tritium production is a function of ^{6}Li enrichment.

Even with naturally abundant ^{6}Li, daily tritium production is still almost half as high as with the 90 % enrichment foreseen for the DEMO blanket.

Most of the test objectives could be attained with natural abundance so that high enrichment is not a priority requirement for a WCLL-TBM.

Nevertheless, assuming a 45 % duty the cycle, the highest value of tritium production is rather low : 67 mg/d (with 90 at % ^{6}Li enrichment)

Energy Sources

The inventory of energy sources is summarised in the table below :

The figures for the coolant and Pb-17Li are quite similar, and together represent ¾ of the total inventory. The contribution of the steel is quite small, however, the small amount of Be armour already has a relatively high potential.

Table 1 : Estimate for the energy inventory in the WCLL-TBM (excluding afterheat).

	Mass [kg]	**T [°C]**	**p [MPa]**	**C_p (average) [kJ kg^{-1}K^{-1}]**	**ΔH [kJ kg^{-1}]**	**ΔH_f [kJ kg^{-1}]**	**Energy [MJ]**	**[%]**
Steel	950	500	-	0.7			**319**	**8.74**
Pb-17Li	3955	500	-					
liquid				0.19			199	5.45
latent heat		235				33.9	134	3.67
solid				0.17			145	3.97
reaction with water		527			214.88		850	23.29
Pb-17Li							**1328**	**36.39**
Be	8.75	500	-					
thermal				2.8			12	0.33
reaction								
with-water					40000		(350)	
with-air					67400		590	16.17
Max. (Be)							**602**	**16.50**
Coolant	1000	350	15.5		1400		**1400**	**38.37**
Max. TBM							**3649**	**100.00**

EFFLUENTS AND EMISSIONS UNDER NORMAL OPERATING CONDITIONS

Effluents and emissions result from diffusion and leaks from the piping.

Considering the amount of tritium and other activation products generated in the TBM, this part is negligible in comparison with the ITER facility as a whole.

WASTE MANAGEMENT AND DECOMMISSIONING

After irradiation, the inventory in the TBM and the ancillary circuits is composed of Be (≈ 8.75 kg), steel (≈ 950 kg + TBD kg in the circuits), water with additives (FW 11.1 kg, BZ 8.7 kg, headers ≈ 40 kg + 1000 kg in the circuits + TBD g corrosion products, max. tritium concentration 1 Ci/kg), Pb-17Li (≈ 3955 kg + ≈ 4000 kg in the circuit). Some of the materials (in particular the steel) are activated and contain a total of up to 1 g of tritium. A permeation barrier (aluminization oxidised to Al_2O_3 on the surface) and joining or filler materials are equally present.

The activity of the reduced activation martensitic steel is on the same level as, or lower than, the structural material of ITER.

Therefore management of the structural material waste could follow the same operations as for ITER waste.

Pb-17Li management has yet to be defined, taking into account a low activation value after temporary storage.

ANALYSIS OF REFERENCE EVENTS

Identification of Events and Postulated Initiating Events

A Failure Mode and Effects Analysis has been performed on the WCLL-TBM.

A set of possible failures has been taken into account for each component. Each failure has been classified where applicable as a Postulated Initiating Event (PIE) for which the expected frequency has been determined.

A first analysis and grouping of these events has shown that the consequences are covered by a set of a limited number of sequences :

- In-vessel LOCA,
- In-TBM LOCA,
- Ex-vessel LOCA,
- Loss of on-site power (decay heat removal).

In addition, accidental sequences affecting the in-vessel part are covered by the ITER standard case (like in vessel LOCA).

Consequences of Accidental Events

Calculations of the consequences of the main sequences were performed.

The results of two representative cases are reported below :

Case A : In-vessel LOCA

An in-vessel LOCA is a Class IV event. The consequences are identical to an in-vessel LOCA from the ITER shielding blanket. The ingress of water into the vacuum vessel extinguishes the plasma immediately, but no leak due disruption is assumed. Surface and nuclear heating disappear instantaneously, only decay heat remains. Both cooling circuits are assumed to be non-operational.

Postulating a blow-down of the complete water inventory of both cooling circuits (1 m^3 at 300°C, 15.5 MPa) into the vacuum vessel (3800 m^3), this would first lead to the release of a two-phase mixture with approx. x = 0.45 (evaporation at constant enthalpy). The remaining water would then gradually evaporate on the hot first wall (evaporation at constant density) and would reach saturated steam conditions (0.03 MPa at 69°C). In the long term, and if no countermeasures are taken, this steam would superheat to the shielding blanket coolant inlet temperature of 140°C (superheating at constant density), corresponding to 0.036 MPa. This is much lower than the design guideline, 0.5 MPa, for the ITER vacuum vessel with respect to an in-vessel LOCA event of ITER in-vessel components.

Case B : In-TBM LOCA

This event is classified as Class IV. A LOCA inside the TBM causes the interaction of the cooling water with the Pb-17Li. The determination of the subsequent generation of heat and hydrogen is being investigated within the ongoing EU R&D program [3]. Previous experiments seem to indicate a self-limiting reaction. Nevertheless, due to the remaining uncertainties, the maximum values for reaction enthalpy and hydrogen production are calculated. The hydrogen is assumed to remain confined in the TBM (no release into the vacuum vessel).

Pb-17Li inventory in the TBM : 3955 kg (excluding ancillary circuits),

thereof Li (0.68 wt %) : 26.89 kg = 3898 mol Li.

Assuming the worst possible reaction for enthalpy and hydrogen production in Pb-17Li.

$2\ Li + H_2O \rightarrow Li_2O + H_2$ - 31.6 kJ/g Li, T = 800 K

the required water mass would amount to 1949 mol (35.1 kg) to react the entire Li inventory in the TBM (excluding ancillary circuits). This is of course a very theoretical assumption as the injected water would displace much of the Pb-17Li. Also, the pressurization of the TBM box would limit the amount of injected water, so that the reaction would remain incomplete.

A hypothetical complete reaction would release an enthalpy of 850 MJ and 3.9 kg of H_2 which is well below the tolerable release limit (10 kg). Assuming an approximate average specific heat for the TBM of 0.33 J g^{-1} K^{-1} (950 kg of steel and 3955 kg of Pb-17Li) the reaction enthalpy would theoretically be sufficient to increase, the TBM temperature by approximately 500 K.

In case of a simultaneous rupture in vessel and in TBM the consequences the pressurisation of the vacuum vessel and the hydrogen produced by the reaction remain at the same order.

In addition a quantity of liquid Pb-17Li, depending of the location of the leak, will fall in the divertor region.

CONCLUSION

The safety analysis performed for the WCLL TBM has shown that the main potential hazards fulfil the ITER requirements.

Nevertheless this analysis has point out the fact that further R&D is required to have a better knowledge of the consequences of the steam- Pb-17Li reaction.

REFERENCES

[1] L. GIANCARLI, M. DALLE DONNE, W. DIETZ - « Status of the European Breeding Blanket Technology »Fusion Engineering and Design 36 (1997) 57-74

[2] L. GIANCARLI and all « Objectives Feasibility Assessment of the WCLL Mock-up testing in ITER. » Proc. of the 20th Symposium on Fusion Technology, MARSEILLE, 7-11 September, 1998

[3] P. SARDAIN, G. BENAMATI, I. RICAPITO, G. MARBACH « Consequences of Pb-17Li/water Interaction within a Blanket Module » Proc. of the 20th Symposium on Fusion Technology, MARSEILLE, 7-11 September, 1998

TASK LEADER

Gabriel MARBACH

DRN/DER/SERSI
CEA Cadarache
13108 St Paul Lez Durance Cedex

Tél. : 33 4 42 25 34 14
Fax : 33 4 42 25 48 68

E-mail : marbach@babaorum.cad.cea.fr

WP-A7-1.1
WP-A7-2.2
WP-B7-1.1
WP-B7-2.3

Task Title : DEMO-BLANKET : SEGMENT DESIGN & ANALYSIS

Data Base and ITM Reliability Assessment

INTRODUCTION

The aim of these sub tasks is to : 1/ collect, validated and process relevant failure data for fusion reactor design activities and 2/ assess the reliability/availability of the conceptual designs and test-items.

An European reliability file is set up and periodically revised in association with ENEA (Italy) and Fzk (Gemany). Data are issued from nuclear industry and analogue systems.

Reliability/Availability assessments either for the helium cooled pebble bed (HCPB) or the water cooled liquid lithium (WCLL) blanket and related test items are carried on in common with the European partners.

1998 ACTIVITIES

Two blanket concepts are under development in the European Blanket Project. The first concept uses liquid Pb17Li as breeder and neutron multiplier and water as coolant (WCLL). The second concept uses lithium ceramic as breeder, beryllium as neutron multiplier and helium as coolant (HCPB). The two concepts represent design alternatives for the DEMO blanket and will be tested independently in ITER.

An extended experimental program will be carried out in fusion environment in order to validate the conceptual design options and related technology. As the only step foreseen between the present tokamaks and DEMO is ITER, this experimental program must be carried out in ITER or ITER-like machines. Thus two mock-ups, [R1,R2], representative of the DEMO blankets will be placed in ITER ports and tests will be carried during the BPP (Basic Performance Phase).

The unavailability of the Test Blanket Modules (TBMs) including the Test Blanket Auxiliary Systems (TBAS) have been assessed and the influence on the availability of ITER is analysed, [P1]. Reference systems in ITER are the cooling systems for the first wall, the divertor, the limiter and the vacuum vessel.

These TBM's are new technology components and no operating experience feedback is available for them. Subsequently, evaluations must be estimated based on the available nuclear experience feedback. This extrapolation is, to large extend, dependent on the expert judgement. A data base has been set up, [R4] and contains the most common items present in the blanket concepts. As for auxiliary components a direct use of the existing conventional components data bases is satisfactory, [R5].

For the immediate use of this assessment, the auxiliary components are limited to the cooling circuits for the FW, limiters, divertors and vacuum vessel. A reasonable Failure Modes and Effects Analyses (FMEA) has already been performed in the past.

The assessment integrates also the previous assessments on the WCLL and the HCPB TM's.

As it has been already recalled in different occasion on the reliability of the blanket, one of the key figures is the mean down time (MDT). Past assessments, [R3,R6,R7], have proved that the resultant blanket availability is very sensitive to the value of the MDT. While, the value of the MDT is dependent on the blanket accessibility and the remote handling systems (RHS) and procedures. However, at this stage of the analysis no additional effort will be devoted to the treatment of this key issue. A reasonable assumption of 8 weeks of MDT has been used for this assessment.

The details of the assessment are given in [P1].

CONCLUSIONS

The contribution of the TM's (HCPB+WCLL) in ITER overall failure rate (without the modules cooling systems) is about $6.7\ 10^{-7}$ /h. If TM's cooling systems should be considered, the total contribution to ITER overall failure rate is about $1.4\ 10^{-4}$ /h, for details see [P1].

REFERENCES

[R1] M. Futterer et al. « Design Description Document (DDD) for the European Water-Cooled Pb-17Li Test (WCLL) Blanket Module » CEA technical note, SERMA/LCA/2125, DMT 97/549, Nov.1997

[R2] L. Boccaccini et al. « Design Description Document (DDD) for the European Helium-Cooled Pebble Bed (HCPB) Test Blanket Module, 7/1998.

[R3] H. Schnauder, C. Nardi, M. Eid « Comparative availability analysis of the four European DEMO blanket concepts in view of the selection exercise » Fus. Eng. & Des. 36 (1997) 343-365.

[R4] T. Pinna « Structure of a component failure rate data base for fusion applications » ENEA technical report, ENEA/FUS/TECN/S&F 32/96, Nov. 1996.

[R5] L. C. Cadwallader et al. « Failure rate screening data for fusion reliability and risk analysis »INEL-EGG-FSP-7922, Jan. 1988.

[R6] B. Bielak, M. Eid « Reliability/Availability Assessment of the water cooled lithium-lead ITER test module » CEA technical note, DMT 97/262, SERMA/LCA/2026, July 1997.

[R7] C. Nardi et al. « Evaluation on the influence of the Test Blanket Modules on the ITER cooling circuits availability » ENEA report, ENEA RTI-DEMO/WCLL/001/98, Feb. 1998.

REPORTS AND PUBLICATIONS

[P1] M. Eid « European Blanket : CEA contribution to the Reliability/Availability analysis and related activities » CEA report, SERMA/LCA/RT/2474/A, Dec. 1998.

TASKLEADER

Mohamed EID

DRN/DMT/SERMA
CEA Saclay
91191 Gif-sur-Yvette Cedex

Tél. : 33 1 69 08 31 75
Fax : 33 1 69 08 99 35

E-mail : meid@Cea.fr

WP-A8-3.1

Task Title : Pb17Li PHYSICO-CHEMISTRY
On-Line monitoring and stabilisation of the Li-Content

INTRODUCTION

The aims of this task are to solve some physico-chemical problems due to the extended use of the Pb17Li alloy in the liquid metal blanket. During operation, tritium generation and potential accidental ingress of air or water will result in Li depletion from the alloy, leading to modification of its physical and chemical properties. To ensure safe and efficient operation of the blanket, it is thus necessary to have a reliable and accurate method for the determination of the lithium content and for its adjustment.

The methods proposed for monitoring the composition of Pb17Li can be divided into two categories, batch methods and continuous methods. The former, which are attractive owing to their simplicity, rely on the removal of a sample of alloy for analysis. The latter, which are more complex, are favored due to their on-line application. Two candidates have been proposed for the continuous determination of the lithium content: (i) *an electrochemical lithium sensor* which compares the lithium activity in the liquid alloy and in a biphasic Li_3Bi/Li-Bi mixture using a sodium β-alumina electrolyte, (ii) *an electrical resistivity meter* which is based on the fact that the electrical resistivity of the Pb-Li alloy is dependent on composition and temperature. Besides, *a plugging indicator* based on plugging temperature measurements has also been proposed. Such a device could be considered as an intermediate candidate as it partly works in continuous mode. Its principle is derived from the Na technology and it needs to be tested with the Pb17Li alloy. With regard to the electrochemical lithium sensor and the electrical resistivity meter, those apparatus for the detection of composition changes in Pb-Li alloys were mainly tested on a laboratory scale. The present objective was to test them on a larger scale such as a liquid metal loop system. The Anapurna loop was used to carry out this work.

1998 ACTIVITIES

The three methods (electrochemical lithium sensor, electrical resistivity meter and plugging indicator) have been successively studied in the Anapurna loop (Fig. 1). In 1998, they have been compared.

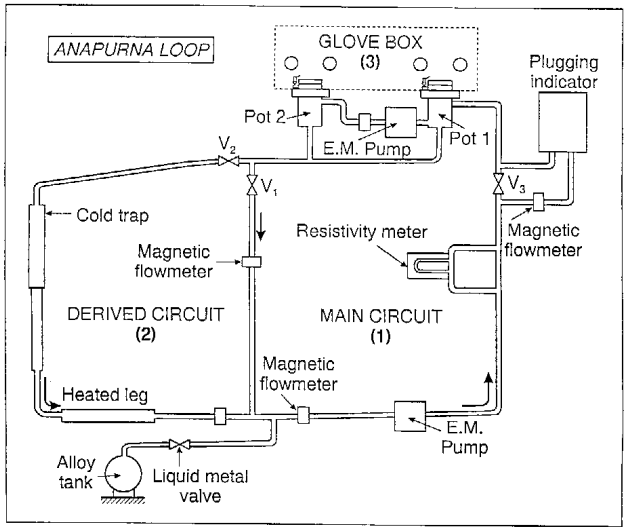

Figure 1 : Schematic diagram of the Anapurna loop

THE ELECTROCHEMICAL LITHIUM SENSOR

The sensor compares the Li activity in the liquid alloy and in a biphasic Li-Bi mixture (the reference system) using a sodium β-alumina electrolyte. At equilibrium, the measured electromotive force (emf) of such a cell follows the Nernst law. Its design comprises a solid β electrolyte thimble sealed in a cylindrical stainless steel housing by means of a ceramic cement. The central electrode, made of stainless steel, dips into the reference system and exits the thimble through a vacuum tight sealant situated at the top of the probe. The other electrical connection is made to the external surface of the steel housing which makes contact with the Pb-Li alloy to be monitored.

In a first step, it was decided to test them in a container with static Pb-Li alloy rather in a loop system. Tests were performed in a glove box under an Argon atmosphere. A fixed mass of Pb17Li was melted in a container at 400°C. The sensor preheated above the liquid alloy during 30 minutes was then immersed. Composition change of the alloy was obtained by small lead additions. It was observed that the sensor signal is relatively in good agreement with the expected composition change. This indicates that the concept is satisfying for Li measurements in Pb-Li alloys. A stable signal was observed 10 minutes after immersion of the sensor into Pb17Li, and a reproducibility of ± 1 mV was achieved. It was deduced by linear regression method that a variation of 1 mV corresponds to a composition change of 0.15 ± 0.05 at % Li.

We must say that for most of sensors which were tested at that time, the mean life time was very short because of cracks in the β-alumina electrolyte due to thermal shocks. Some of them were broken after their first immersion. After this period, no more tests were performed in Pb-Li alloys with these electrochemical sensors. However, recent improvement in the mechanical properties of the alumina ceramic has been obtained. For example, good performance of an electrochemical sodium sensor was achieved for determination of the sodium concentration in aluminium melts. The immersion conditions in such environment are more severe because the temperature is higher (close to 725°C). This new ceramic being less sensitive to thermal shock, it is expected that similar results would be also obtained in Pb-Li alloys where temperature is lower (less than 500 °C).

THE ELECTRICAL RESISTIVITY METER

The body of the cell in 316L stainless steel was connected to the main circuit of the loop (Fig. 1) and attached to a capillary section (o.d. 4.8 mm, i.d. 3.0 mm, length 450 mm) also made of 316L stainless steel. The liquid alloy was pumped around the capillary by means of a miniature electromagnetic pump.

Two plates were attached to the capillary section 150 mm apart and two silver leads were placed on each plate to supply a constant current and monitor the resistance of the cell. The capillary was inserted in a furnace and the temperature was controlled by four thermocouples.

Resistance data were determined by a version of the four terminal method. A constant current of 3 A generated by a stabilized power supply was passed through the capillary section and a standard 0.01 Ω resistance. The resistance of the capillary (R_t) was calculated from the potential difference across the standard (V_s) and the cell (V_t): $R_t = 0.01\ V_t/V_s$. The resistance of the Pb-Li alloy (R_m) was then obtained from the resistance of the monitor filled with alloy (R_t) and the resistance of the empty monitor (R_c) using the expression for parallel conductors. The resistivity of the alloy (ρ_m) can be obtained by the relationship $\rho_m = R_m A/I$ where A is the cross-sectional area and I the length of the capillary between the two plates. The geometrical constant A/I is specific to each monitor. Prior to use, the resistance of the empty capillary and the constant A/I were determined (A/l = 5.74 in the present case). The calibration of the resistivity meter was performed manually before connection to the loop. Data concerning resistances, temperatures and resistivities were collected for various alloy compositions.

For use on loop, the meter must be able to operate continuously. Therefore, a computer controlled system was developed to collect data and record fluctuations in composition. A multiplex device with six input channels was used: four of these were connected to the thermocouples on the capillary section, one carried the voltage across the plates, the final input was the voltage across the standard resistance.

Then, the output of the multiplex was carried out to a digital voltmeter. A microprocessor controlled the channel selection of the multiplex and read the voltage displayed on the digital voltmeter. A program was written for data acquisition and calculation so that, at regular time interval, data were collected and the lithium composition was determined. Information was transferred to a screen, a line printer and stored on disk.

The study of the resistivity meter was carried out with Pb-Li alloys of various compositions. At first, addition of oxygen and lead to Pb-Li alloys were made to decrease the Li content to a fixed value (close to 13.5 at.%). Then, the Li composition was increased by addition of a Li-Pb compound to the liquid alloy. Sufficient quantities of LiPb (equimolar composition) were prepared and dissolved in the liquid alloy to obtain a composition close to Pb17Li at the end of the experiment.

The reaction of oxygen with Pb-Li alloys was detected by the apparatus and the decrease in lithium content was in agreement with Li_2O formation. Then, the adjustment of the lithium concentration was performed by adding LiPb compounds. These compounds were easily prepared by mixing lead and lithium in equimolar proportions in the liquid state.

The ingots produced after solidification of the mixture and immersed into the alloy of the loop were entirely dissolved in a short time without any difficulty. The resistivity meter responded very well after each LiPb addition and a steady increase in lithium content was observed. The monitor was thus sensitive to composition change, the minimum unambiguously detectable limit being $\pm$ 0.15 at% Li which corresponds to an accuracy of $\pm$ 0.2 10^{-8} Ωm on the resistivity. Its response time was only limited by the rate sampling/mixing in the loop.

The potential of the electrical resistivity meter to monitor continuously the lithium concentration of Pb-Li alloys in a loop system has been demonstrated throughout this work. The apparatus is able to detect lithium depletion in case of oxygen ingress. Then, adjustment of the lithium content can be easily controlled by adding LiPb compounds to Pb-Li alloys. This compound is the easiest to handle to obtain the requested Li-concentration.

THE PLUGGING INDICATOR

The plugging indicator was initially developed for the determination of the oxygen concentration in liquid sodium. The principle consists in determining the temperature at which the crystallization of sodium oxide takes place. This is based on the measurement of the plugging temperature obtained by decreasing the temperature of the liquid metal until a drop in the flow rate (corresponding to the deposition of crystals) is observed. The oxygen content is thus approximately deduced from this plugging temperature. It was proposed to transfer this technology to Pb-Li alloys as the device could be sensitive to lithium concentration changes.

It had to be tested if the plugging temperature could be identified with the liquidus temperature of the Pb-Li alloy.

The plugging indicator was connected to the Anapurna loop as shown in Fig. 1. It was set up vertically in a derived part of the main circuit (part 1). It is made of a 316 L stainless steel cylinder (≈ 0.9 litre). The alloy flows into a narrowed section equipped with a pellet where the alloy temperature is lowered by an air cooling system. In the present experiments, the circulation of air and Pb-Li alloy is in opposite direction so that the air turbine is placed at the top of the plugging indicator. The temperature is measured very close to the pellet by a thermocouple introduced in a thimble.

The plugging indicator tests were performed with Pb-Li alloys initially at 400°C. Experiments were carried out with various flow rates. For each test, the air cooling system was set in operation so that the temperature of the Pb-Li alloy entering in the plugging indicator started to decrease. Simultaneously, the pellet temperature and the flow rate in the apparatus were both recorded as a function of time (t). When the flow rate was stabilized to zero, the cooling system was stopped and the reheating phase took place.

Besides plugging measurements, a thermal analysis study was also carried out to measure the liquidus temperature of the alloy. A small amount (100 g) of the Pb-Li alloy used for the plugging indicator tests was taken from the loop for the analysis. In this simple experiment performed out of the loop, a thermocouple was dipped into the liquid alloy contained in a crucible and the temperature was recorded as a function of time during cooling of the alloy. The liquidus temperature of the Pb-Li alloy was thus determined from the thermal curve.

With regard to the flow rate effect, the plugging time is increased with faster alloy circulation. Moreover, the flow drop is not so abrupt for high rates. It results that the plugging temperature determination is not so accurate. Nevertheless, the tests show that the plugging temperature is not affected by the flow rate of the alloy. The small variations which could be detected are not significant because of the experimental errors on the temperature measurements (± 2°C).

The results indicate that the plugging temperature can be easily measured. However, the plugging indicator can detect Li composition change, assuming the Li variation is sufficiently large and higher than 1 at %. It seems that the plugging temperature and the liquidus temperature of the alloy can be identified.

The liquidus temperature being determined from the plugging measurements, the Li concentration can be deduced using the Li-Pb phase diagram. It is obvious that the liquidus line of the phase diagram must be known unambiguously to determine accurate Li concentrations from the plugging measurements. This could be a disadvantage of the method.

CONCLUSION

Various methods of monitoring the Li composition of Pb17Li alloy have been examined in a loop system. The work has been mainly focused on continuous methods which are more attractive even if more complex. Nevertheless, batch methods based on chemical analyses have also been tested in the frame of this work. They are very simple and a deviation of 0.3 at % Li can be detected but their disadvantage is the fact that samples have to be taken from the loop.

Three concepts have been tested for the on-line determination of the Li content of the liquid alloy. The concepts based on the *Li electrochemical sensor* and on the electrical resistivity meter require calibration prior to insertion in the loop. Although the tested electrochemical sensors were susceptible to thermal shock and to fracture, our results show that the concept is very attractive. The sensor is specific to lithium, simple to use and it can detect a composition change of ± 0.15 at% Li. The improvement of the mechanical properties of the solid electrolyte (β-alumina) which is the key element of the sensor should not make difficulties since new sensors have been produced with success in 1995 for more severe immersion conditions. The good performance obtained in such environments is also expected in presence of Pb17Li alloy.

The *resistivity meter* is robust and very sensitive to composition change, the minimum unambiguously detectable limit being ± 0.15 at% Li. Although nominally sensitive to any solute, this will not influence its operation because potential impurities have small solubilities in Pb17Li. The resistivity meter is easy to handle but its replacement in the loop could be slightly more complicated than the electrochemical sensor. The *plugging indicator* does not need calibration and it is very robust. However, changes in the composition of the liquid alloy must be higher than 1 at % Li to be detected. The plugging temperature is well related to the liquidus temperature but it is necessary to have a good knowledge of the Li-Pb phase diagram to deduce the Li concentration of the alloy. Therefore, it is thought that the monitors with greatest potential for the continuous monitoring of the Li content in Pb-Li alloys are the electrochemical sensor and the resistivity meter.

Throughout this work, methods to replace the lost lithium and to adjust the Li content of Pb-Li alloys have also been examined. It is shown that for additions to liquid alloy, the LiPb compound (equimolar composition) was the easiest to handle to obtain the requested Li-concentration because its dissolution process is well controlled and rapid.

PUBLICATIONS

[1] F. BARBIER, F. HERBERT, "Monitoring of the Li content with a plugging indicator", RT SCECF 467 (June 1998)

[2] F. BARBIER, F. HERBERT, "Continuous monitoring of the Li content in liquid Pb17Li alloy", RT SCECF 475 (November 1998)

TASK LEADER

F. BARBIER

DTA/CEREM/DECM/SCECF/LECNA
CEA Saclay
91191 Gif-sur-Yvette Cedex

Tél. : 33 1 69 08 16 13
Fax : 33 1 69 08 15 86

E-mail: barbier@ortolan.cea.fr

WP-A9-2.2

Task Title : Pb17Li WATER INTERACTION : WATER LARGE LEAKS

INTRODUCTION

In the frame of the liquid breeder blanket programme, several activities are devoted to the interaction between the coolant (water) and the lithium lead alloy. They concern experiments and modelling with software as well. This programme is subject to a collaboration between ENEA and CEA.

1998 ACTIVITIES

Two main phenomena are considered for Pb17Li/water interaction, the effects of which on safety must be significantly different: small leakage (microcracks,...) and large leakage (cooling tube rupture). The main concerns are as follows :

- for the small leakage, hydrogen production, thermal spots coming from solid reaction products aggregation, corrosion coming from lithium hydroxide,...

- for the large leakage, pressure peak due to water vaporisation and hydrogen production, hydrogen evolution, history of solid reaction products,...

Several experiments are devoted to the study of these phenomena:

- RELA II for the small leakage

- BLAST,(the results of which are known) and LIFUS 5 (planned for 1999) for the large leakage (see figures below).

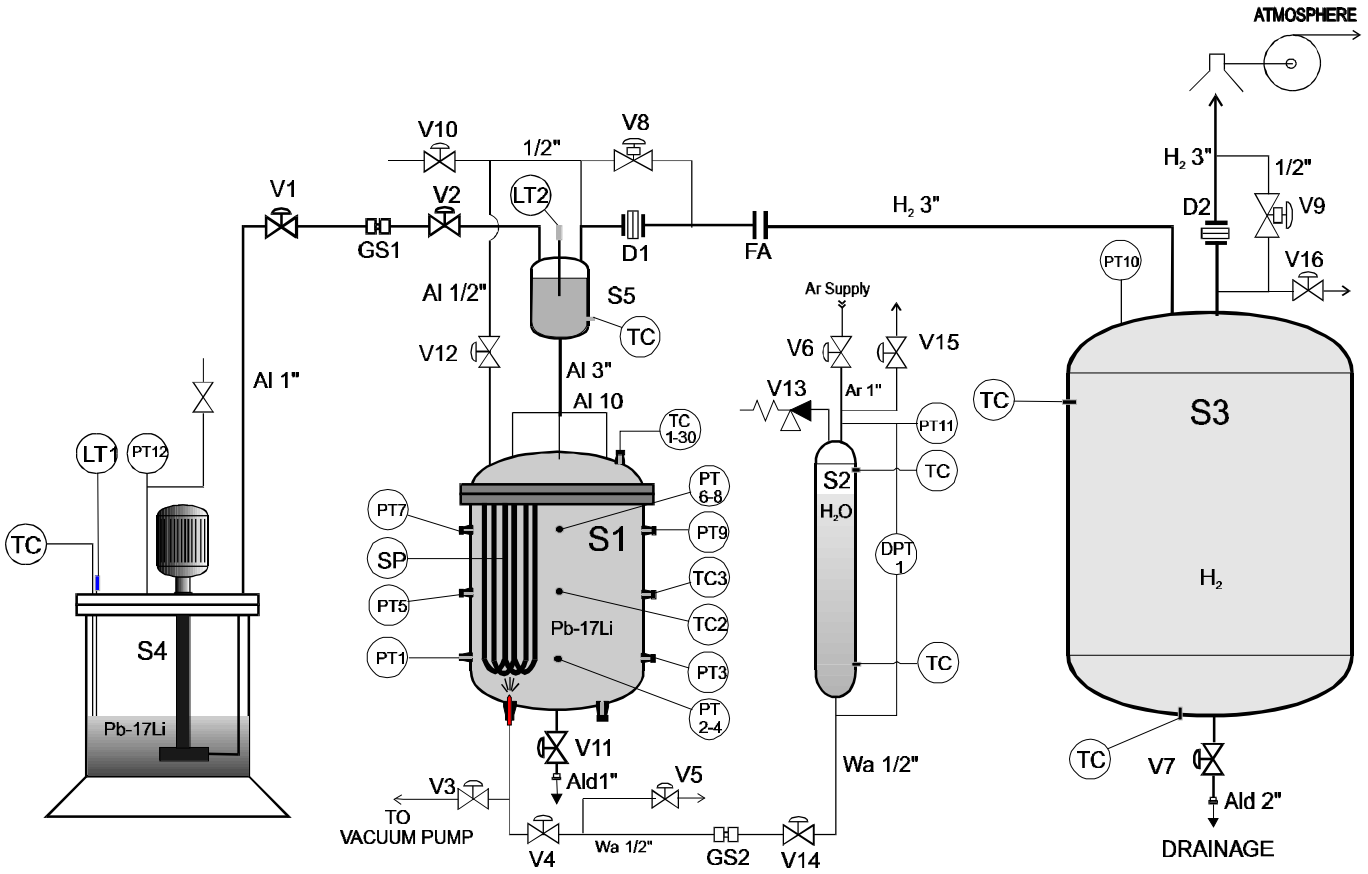

FIG. 1

LIFUS 5 facility

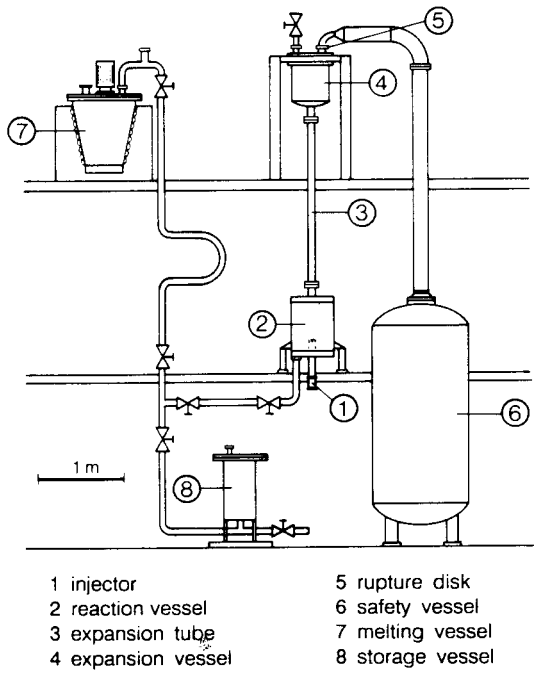

BLAST facility

The study which is presented here is related to the assessment of the consequences of the large leakage.

The main phenomena which are involved in macro-leaks (tube rupture within a blanket module) are as follows:

- possible water-hammer effect due to high pressure water impact,

- thermal reaction due to water vaporisation
  first pressure peak (see figure below)

- chemical reaction leading to hydrogen production
  second pressure peak (see figure below)

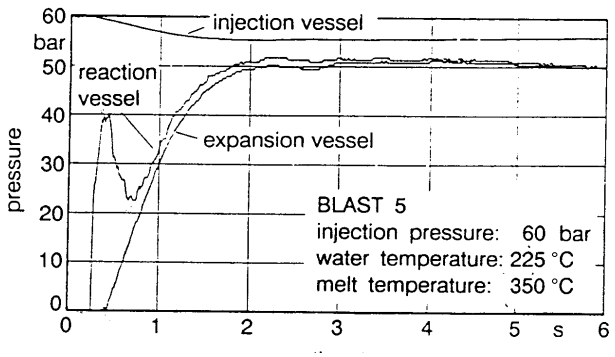

BLAST experimental results

The assessment strategy includes the following steps:

- the evaluation of interaction models is made through available experimental results (BLAST),

- pre calculations of LIFUS 5 are done,

- the current models are to be improved for a better simulation of the reaction course (kinetics, reaction products),

- the improved models will be validated on available experimental results,

- the influence of sensitive parameters (stoichiometric ratio, water injection,...) will be studied,

- post calculations of LIFUS 5 will be done.

The main difficulties are related to the simulation of the chemical reaction. The great influence of the initial conditions on the reaction course and thus on pressure peaks, can affect the accuracy of the results in so far they are not precisely known. Moreover, the simulation of specific phenomena (limitation of the mixing between the reactants due to a shield made by solid reaction products) is difficult.

The chemical effect is calculated with the PLEXUS code, using a sodium/water reaction model. In this model, only the following chemical reaction is considered:

$$2\ Na + 2\ H_2O \rightarrow H_2 + 2\ NaOH$$

The results are shown on the following figures

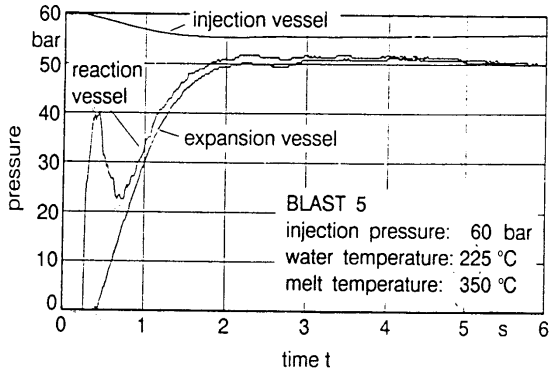

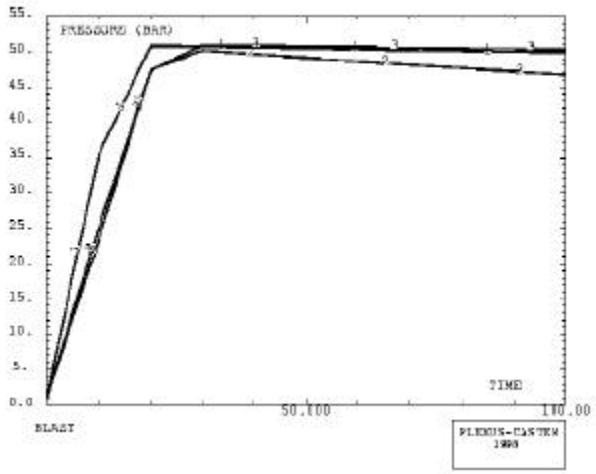

BLAST: PLEXUS calculation

Since the model assumes an instantaneous and total reaction, it does not represent the reaction kinetics. The injected mass of water has to be adjusted in order to fit the model on the BLAST results.

The thermal effect is calculated with the SIMMER code which has been developed in the frame of the assessment of severe accidents within fast breeder reactors. This code can notably be used to simulate interaction phenomena.

The results are shown on the following figures. A good agreement with the experimental results is found without any parameter adjustment.

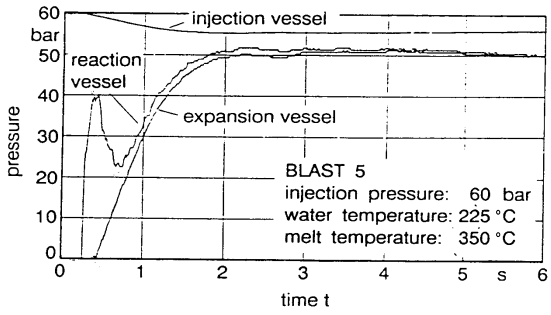

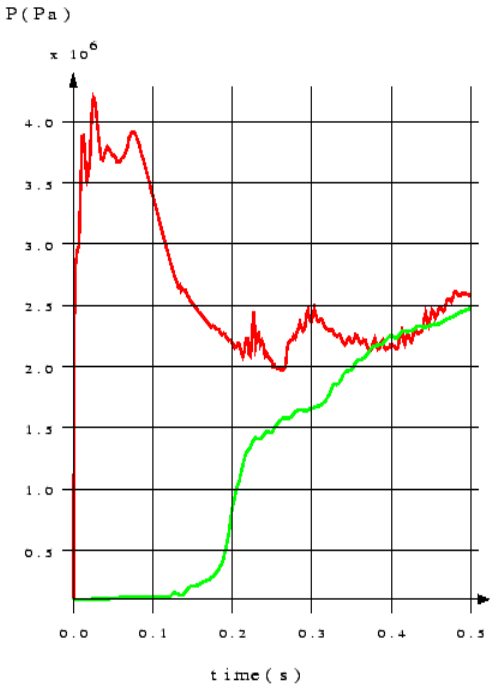

CONCLUSION

Concerning Pb17Li/water interaction due to water macro-leaks some experiments have already been done (BLAST). They have shown two main processes: a "thermal" effect (short time) and a "chemical" effect (long time). Others experiments will be carried out in the next future (LIFUS), which will be representative of the ITER Test Modules.

They will notably bring further informations on the pressure evolution and the hydrogen production. The experimental results allow us to validate the models for the assessment of the consequences of large leakage. Pre calculations of future experiments can be done. The models are to be improved in order to get a better simulation of the reaction course

REFERENCES

[1] P. Sardain, Assessment of the pressure peak in the LIFUS experiment, International workshop on Liquid Metal Blanket Activities, Paris, 1997

[2] Kottowski et al., Studies with respect to the estimation of liquid metal blanket safety, Fusion Engineering and design, 445-448, 1991

[3] Benamati et al.,LIFUS 5 experimental facility on Pb17Li/water interaction to be built up at ENEA Brasimone center. Technical specifications, Brasimone 01/03/1997

[4] Kondo et al., Status and achievment of assessment programme for SIMMER III, a multiphase, multicomponent code for LMFBR safety analysis, NURETH 8 Kyoto 1997

[5] P. Sardain, G.L. Benamati, I Ricapito, G. Marbach
Consequences of Pb17Li/water Interaction within a Blanket Module
Symposium On Fusion Technology, Marseille France September 1998

REPORTS

[1] P. SARDAIN
Consequences of Pb17Li/water Interaction within a Blanket Module
Report DER/SERA/LETh 98/5030

TASK LEADER

Pierre SARDAIN

DRN/DER/SERSI/LECC
CEA Cadarache
13108 St Paul Lez Durance Cedex

Tél. : 33 4 42 25 37 59
Fax : 33 4 42 25 71 87

E-mail: sard@buffet.cad.cea.fr

WP-A9-3.1

Task Title: Pb17Li/WATER INTERACTIONS, DEFINITION OF COUNTERMEASURES

Required countermeasures

INTRODUCTION

In the frame of the safety studies for the water-cooled test blanket module (WCLL-TBM), three types of events were identified which would lead to an interaction between Pb17Li and water. These are:

1. a small leak, the most probable places are the bends of the double-walled tubes and the welds with the tube plate,

2. an In-TBM LOCA with rupture of a cooling pipe or sudden failure of a weld between tube and tube plate, subsequent pressurization of the TBM with and without failure of the TBM as a confinement,

3. an ex-vessel LOCA in the ancillary systems where e.g. a failure of a cooling system component would damage the Pb17Li circuit.

1998 ACTIVITIES

Because case 1 is quite easily detectable (gas production in the Pb17Li circuit, quick Li depletion, pressure drop increase in the Pb17Li circuit) and because only little hydrogen and heat is released, no safety problems are expected to arise from such an event. The analysis therefore focused on cases 2 and 3. The hydrogen production entailed by Pb17Li-water interaction was identified as the major safety criterion. The expected pressurization of the pit vaults was equally investigated. Other LOCA related safety issues (e.g. hydrogen production due to interaction between overheated beryllium and steam) were treated in WP A6.

IN-TBM LOCA

This event is classified as Class IV. A LOCA inside the TBM causes the interaction of the cooling water with the Pb17Li. The determination of the subsequent generation of heat and hydrogen is being investigated within the ongoing EU R&D program. Previous experiments seem to indicate a self-limiting reaction. Nevertheless, due to the remaining uncertainties, the maximum values for reaction enthalpy and hydrogen production are calculated. The hydrogen is assumed to remain confined in the TBM (no release into the vacuum vessel).

With the reduced size WCLL-TBM the theoretically possible hydrogen production is just above 5 kg and thus just over the tolerance limit given by ITER. A small reduction of the TBM size would eliminate the problem.

IN-VESSEL AND IN-TBM LOCA WITH RUPTURE OF FIRST WALL

This event is classified as Class V. The water ingress into the vaccum vessel extinguishes the plasma immediately, but no disruption is assumed. Additionally, Pb17Li is spilled and flows down in the divertor region. The amount of spilled Pb17Li depends on the location of the leak. The hydrogen produced during the Pb17Li/water interaction enters the VV. The surface and nuclear heating disappear instantaneously, only decay heat remains.

EX-VESSEL LOCA

This event is classified as Class IV for the failure of one out of two cooling circuits. No safety credit is given for the fact that two independant cooling systems are available. Here, two large ex-vessel breaks in the cooling circuits are assumed so that no active cooling is available at all.

The pit volume is assumed to be pressurized with the released steam, and, conservatively, no condensation on cold surfaces is considered. The blow-down is assumed to damage the Pb17Li circuit thus enabling a reaction between Pb17Li and the released steam/water.

Postulating a blow-down of the complete water inventory of both cooling circuits (1 m^3 at 300°C, 15.5 MPa) into the pit vault (2156 m^3), would lead to the release of a two-phase mixture with x = 0.43 at 84°C and 0.056 MPa.

At the same time the air (initially at 0.1 MPa, 40°C) heats up thus causing an additional pressure increase of 0.014 MPa so that the final pressure will reach 0.17 MPa. These values disregard space occupation by ancillary equipment and do not include the additional heat take-up from hot structural material. This pressure rise in the pit seems to raise only little concern for the structural integrity of the pit vaults. If required, actively cooled condensation surfaces or other countermeasures could be envisaged.

The behavior of the TBM during these accidents were investigated in the safety related taks of WP A6:

CONCLUSIONS

From the different events involving Pb17Li/water interaction, only large leaks either in the TBM itself or in the pit where the ancillary circuits are deployed are safety relevant, in particular because the production and release of several kilograms of hydrogen cannot be fully excluded. Only when counting the Pb17Li inventory in the TBM itself and in the ancillary circuits, the potential hydrogen production would exceed the allowable maximum of 5 kg. To reach an inherently safe condition, a small reduction of the total Pb17Li volume in the system would be required.

Means of prevention consist in the use of double confinement between Pb17Li and water (except in the header area), leak detection and the spatial separation of the ancillary circuits for water and Pb17Li. Should a failure occur nevertheless, an active accident management as proposed in 1997 could be applied.

PUBLICATIONS

[1] M. A. Fütterer, Pb17Li-water interaction in the WCLL-TBM: Consequences and countermeasures, CEA report DRN/DMT SERMA/LCA/98-2370/A, December 1998.

TASK LEADER

Michael A. FÜTTERER

DRN/DMT/SERMA/LCA
CEA Saclay
91191 Gif-sur-Yvette Cedex

Tél. : 33 1 69 08 36 36
Fax : 33 1 69 08 99 35

E-mail : michael.futterer@cea.fr

WP-A10-2.2

Task Title : EXPERIMENTAL DEMONSTRATION OF MHD PHENOMENA TURBULENCE IN MHD FLOW SHEAR LAYERS

INTRODUCTION

The objective is to give a contibution to the understanding of the Pb17Li flow behaviour in the WCLL blanket and in particular to assess the presence of two-dimensionnal turbulences in MHD flow shear layers and to characterize them under representative magnetic field. Relevant parameters and scaling laws have to be obtained in order to evaluate the impact of MHD effects on Pb17Li velocity and temperature distribution and consequently on the T-permation towards the water coolant in WCLL blankets.

1998 ACTIVITIES

Theoretical, numerical and experimental results were obtained in 1998 within the framework of the studies on the turbulence of MHD flows in the water-cooled lithium lead blankets of fusion reactors.

The activity this year has been marked :

- on the experimental level, by the construction of a new MATUR-5 cell and by a first series of experimental results obtained under intense magnetic fields which can reach 6 Tesla,
- on the theoretical level, by a thorough re-examination of the Hartmann layer present in the vicinity of the perpendicular walls of the magnetic field,
- on the numerical level, by a simulation of the MATUR-5 flow modeled by the quasi-2D equation of Sommèria-Moreau [1] using the FLUENT code.

EXPERIMENTAL STUDIES

MATUR-5 experimental device

The configuration of the experimental device MATUR-5 is identical to that of the preceding versions. The circular cell with a radius of 11 cm contains a mercury layer with a thickness set at 1 cm, in which the electric current is injected by electrodes located in a circle of 9.3 mm in radius and closes by the external cylindrical wall maintained at constant temperature, thus starting a rotational movement of the external fluid cylinder. A central heating plot allows the injection of several watts in power in order to observe the turbulent transport of a scalar order of magnitude as for the heat through the shear layer.

Compared to the former versions, the modified parameters are essentially the magnetic field and the value of the source current.

Whereas the magnetic field was up to now limited to 0.2 Tesla, the MATUR-5 cell has been placed in a LCMI coil (Laboratoire des Champs Magnetiques Intenses) in Grenoble thus making the magnetic field continuously vary between 0 and 6 Teslas, and consequently allowing conditions representative of fusion reactor blankets to be reached.

The electrical current, characterizing the maximum speed of the fluid cylinder was up to then limited to 50A. The technology used in MATUR-5 allows an intensity of 150A to be reached, in other terms rates of roughly 1.5 m/s.

Experimental results

As under a moderate magnetic field, the thickness of the shear layer is much greater (by a factor of 10) than that predicted in laminar regime. It appears that the latter is independent from the electrical current but it significantly depends on the magnetic field.

The maximum speed measured under moderate magnetic field was reduced by half compared to the theoretical predictions because of the centrifugal re-circulation movement. The results obtained under intense magnetic field show the progressive disappearance of this re-circulation and of the transport of the associated kinetic momentum, thus leading to values measured in perfect agreement with the predictions as soon as the magnetic filed exceeds 2 Tesla.

The efficient values of the fluctuations of the two speed components remain roughly 12 % of the maximum speed, which is clearly greater than in classic turbulence.

The spectra measured all have the same shape, whatever the acquisition location and the parameters of the magnetic field and of the current, which can be considered as a signature of this MHD turbulence. This original shape, which is clearly different from the classic turbulence spectra, is characterized by :

- a shift towards the low frequencies, typically of roughly a hertz, or 100 to 1000 times less than in a classic turbulence, that is to say towards greater vortex sizes,

- the presence of 3 to 4 peaks easy to identify, associated to larger vortex structures, rather coherent and fed by an inverse cascade of energy specific to the two-dimensional turbulence,

- an inertial zone which is less spread out and marked by a law in power of type k^{-n}, with a value of n very close to 4 as soon as the magnetic field is rather high.

Whereas the mechanical inertia of the system is low (a few seconds), its thermal inertia is rather great (of about one hour). This is due to the fact that the turbulence poorly penetrates the central region where the transport of heat is controlled by conduction. The temperature measurements made in stabilized regime show that the heat flux transported constantly increases with the current, that is to say with the speed and the number of Reynolds. This is obvious on the average temperature profiles which follow a radius where the difference in the measured temperature between the central plot and the external wall decreases monotonously with the speed for a set flux.

We can also note that, in transient regime, the temperature gradient is much lower in the shear layer (where the turbulence is intense) than in the poorly mixed central region.

These temperature measurements must however be considered with care as the heating conditions are complex. Apart from the heat flux from the central plot, a thermal power is supplied by Joule effect in the Hartmann layers in which the currents circulate. This source of power increases with the square of the product of the magnetic field and of the current and can exceed the power delivered by the central spot with the high values of these two parameters. The results obtained will be re-examined by attempting to separate the effects of the two heat sources.

THEORETICAL RESULTS

The theoretical studies concerned a more accurate analysis of the Hartmann layer aiming at introducing the inertial effects and evaluating the three-dimensional effects in the core region located between the Hartmann layers.

These studies came from the comparison of numerical results and the experimental results obtained under moderate magnetic field which showed a good agreement as long as the electrical current, of which the inertial effects, was moderate and degraded at high intensities. The integration of the inertia forces in the Hartmann layer thus appear as a fundamental necessity of which the consequences could be of a very general interest for all the high speed flows.

This problem was addressed using a specific perturbation method based on two parameters : the inverse of the Hartmann number which measures the thickness of the Hartmann layer, and the inverse of the number of Reynolds which characterizes the ratio of inertia forces to the viscous friction.

The different orders of magnitude are developed according to these two parameters, on the one hand in the Hartmann layer and on the other hand, in the core. In the first order, we find the Sommeria-Moreau equation [1], and at the higher orders, the expected effects appear and the strictly 2 D flow progressively becomes 3D under the effect of inertia.

A new equation model integrating the terms of inertia introduced in the Hartmann layer into the braking force was thus developed.

NUMERICAL STUDIES

The numerical studies concern the direct simulation of the turbulent MHD flow using the FLUENT code including the simulation of the transport of a scalar such as temperature by coupling the Navier-Stokes equation with a source term modeling the friction forces in the Hartmann layer and an enthalpy equation.

The first numerical results have been compared in a satisfactory way to the experimental results obtained on the former version of MATUR under moderate field [2] [3] [4].

These have particularly shown in a satisfactory way, the evolution of the speed field towards an established regime of large vortex structures originating from the instability of the shear layer towards the large scales via an inverse energy cascade.

The numerical results corresponding to the new version of MATUR-5 under intense magnetic field present a level of accuracy close to that obtained under moderate field [5].

The present balance on the numerical simulation is as follows :

- the accuracy on the average speed distribution is very satisfactory, but that on the temperature presents a difference with the experiment which would suggest some improvements such as a better integration of the effective diffusivity in the parietal layer,

- the model deserves to be improved by introducing, in the equation, the corrections allowing the representation of the low 3 D of the flow and its contribution to the total dissipation of energy,

- the present level of development of the numerical tool is validated enough to already be able to apply it to the more representative flows of the fusion reactor blankets.

CONCLUSION AND PERSPECTIVES

The experimental results on the turbulent speed field which are now of great accuracy thanks to the high values of the magnetic field make up a data base likely to serve as a reference to any attempt at modeling. They show both the distributions of the most important average values (average speed, average temperature, tension of Reynolds) and the specific characteristics of this turbulence marked by a high two dimensionality (spatial distributions with low frequency peaks corresponding to large coherent vortex structures and with an inertial zone in power law of which the characteristic power goes from -5/3 at a low energy level to-3, then -4 when the kinetic energy increases.

The study of the Hartmann layer leads to a modeling of the three-dimensionality which persists in this flow. The new model takes form in the Somméria-Moreau equation [1] which allows the integration of an additional inertial term in the braking force of the flow.

The numerical results acquired which are based on the non-modified Somméria-Moreau equation show that this model is very satisfactory (accuracy level close to 5 %) to describe a turbulent shear flow under intense magnetic field. The comparison with the experimental results confirm, as for under moderate magnetic field, a slightly inferior accuracy on the temperature field.

The convergence of the theoretical , numerical and experimental studies is now clear :

- the theory allows the improvement in accuracy of the model-equation with a view to extending its validity to high speed regimes,

- the numerical model is already satisfactory at moderate speeds and will be applied to more representative flows of fusion reactor blankets,

- the experiment has provided a first set of important data which will be used as references for the scientific community concerned.

The experiments under intense magnetic field will be continued by modifying some parameters and by taking greater care with the heat transport. The theoretical study will be continued by an analysis of the internal structure of the large vortexes then completed by a study of the boundary layer located near the wall to characterize a detachment effect of the boundary layer. Finally, the numerical study will be continued by the modification of the model-equation to integrate the three-dimensional effects.

REFERENCES and REPORTS

[1] "Why, when and how MHD turbulence becomes two-dimensional"
Somméria, R. Moreau, J. Fluid Mech.(1982), vol. 118 pp 507-518.

[2] "1997 Progress report : Turbulence in MHD Flow Shear Layers"
NT DER/STML/LCFI 97/049. G. Laffont, R. Moreau.

[3] "Two dimensionnal numerical simulation of a MHD turbulent shear flow"
Y. Delannoy - R. Moreau . 3rd Pamir Conf., Aussois, France, Sept.22-26, 1997.

[4] "Quasi 2D turbulence MHD in MHD shear flows : The MATUR experiment and simulations"
Y. Delannoy and al. Transfer Phenomena in MHD and Electroconducting Flows, 1998, Kluwer Acad. Pub., Dordrecht, The Netherlands.

[5] "MHD turbulent shear layers : experiment and modelisation at hight Hartmann number"
Y. Delannoy and al.To be presented et the TMS Annual Meeting on Fluid Flow Phenomena in metal processing, San Diego, Feb28-March4, 1999.

TASK LEADER

Guy LAFFONT & R. MOREAU

DRN/DER/STML/LCFI
CEA Cadarache
13108 St Paul Lez Durance Cedex

Tél. : 33 4 42 25 73 14
Fax : 33 4 42 25 77 88

E-mail : guy.laffont@cea.fr

Task Title : DEMO-HCPB BLANKET : SEGMENT DESIGN & ANALYSIS

Design optimisation for alternative ceramics Li_2ZrO_3/Li_2TiO_3

INTRODUCTION

In order to reduce the risks associated to the R&D activities in the design of a Helium Cooled Pebble (HCPB) blanket for DEMO fusion power reactor, CEA has proposed to the EU to examine the use of the meta-zirconate/meta-titanate as breeding cermaics, [R1,R2]. The EU-HCPB blanket reference conceptual design makes use of the ortho-silicate as reference ceramic breeder. The replacement of the reference ceramic by any of these two candidates would certainly necessitate to re-optimise the design.

During the FY97, CEA has proposed an optimum conceptual design for the HCPB blanket using indifferently the meta-zirconate or the meta-titanate. The main features of the CEA proposed HCPB was the use of a breeder bed of 16-18 mm thickness for a Li6 enrichment of 25-28%. The resultant maximum operating temperatures mounted to some 1215 °C. Some uncertainties about the thermal stability of the pebbles [R3,R4] have advocated in the favour of a significant reduction of the maximum operating temperature in the breeder bed.

Meanwhile, the EU-fusion program has decided to switch from the use of the MANET to the use of the EUROFER97 as structural material.

Subsequently, CEA has devoted the FY98 activities to the revision of its previous proposal.

1998 ACTIVITIES

As already mentioned above, CEA has revised the HCPB blanket proposal, it presented in the FY97. With the two main objectives : 1/ to reduce the breeder bed thickness to reduce the observed maximum operating temperature and 2/ to take into account the use of the EUROFER97 as structural materials.

The whole neutronic optimisation calculations have to be re-carried out [R5]. A full detailed count is given in the task UT-N-Blk, of the same report. These calculations have resulted a set of optimum options in terms of TBR values. After some iterations between neutronic and thermal evaluations, the option Zr50%_08.09.80 has been selected based on the requirement of lowering the maximum operating temperature in the breeder bed.

The Zr50%_08.09.80 refers to a HCPB blanket based on the meta-zirconate ceramic breeder at 50% enrichment, with a cooling plate thickness of 8mm, a breeder bed thickness of 9mm and a Be-bed thickness of 80mm. Past experience ,[R1], has proved the that use of the titanate rather than the zirconate would not significantly alter the neutronic behaviour of the blanket.

Based on the resultant heating radial distributions, the thermal calculation had followed in order to evaluate the maximum operating temperature in the breeder bed. One of the critical issues, is the choice of the relevant pebble thermal conductivity model.

PEBBLE BED EFFECTIVE THERMAL CONDUCTIVITY

The pebble bed thermal conductivity relations for the zirconate and the titanate are those developed by P. Gierszewski et al. in reference [8] ;

$K_{bed} = 0.66 + 1.17 \times 10^{-7} T^{2.2}$, T in °C and Kbed in W/m/°K

zirconate pebbles of 1.2 mm (~ 82% DT, 63% pf), and

$K_{bed} = 0.62 + 5.5 \times 10^{-4} T$, T in °C and Kbed in W/m/°K

titanate pebbles of 1.2 mm (~ 82% DT, 63% pf)
Both relations are valid up to 1.3 Mpa.

P. Gierszewski estimates in reference [7], that for pebbles with 90% TD and 65% pf, the preceding relations would be corrected by 12%.

MAXIMUM OPERATING TEMPERATURE

In the precise case of the breeder bed option of Zr50%-08.09.80 the maximum heating rate issued from the neutronic calculation was estimated to be about 67 W/cm3 (BoL). Using the above relations describing the effective bed conductivity would produce a maximum operating temperature in the OB-breeder bed equal to 1085 °C (for CP and FW at 450 °C), [P1].

Although, this temperature is still higher than the 900 °C that has been recommended by the EU-HCPB project leader as indicative limiting figure, many of the material experts show no particular concerns about this value based on the present available experience. However, efforts are being employed to propose solutions that may lead to approaching the indicative limit of 900 °C.

Certainly one way to decrease the maximum operating temperature in the breeder bed is to improve the global thermal conductivity of the zirconate bed. Thermal conductivity improvement may result from using a specific type of coatings.

Another way to relief thermal limitations is to improve the pebble thermal stability. As it will be stated in the following section thermal stability is one of the strongest reasons to limit the maximum operating temperatures.

HCBP BLANKET SPECIFICATIONS

The revised proposal of the CEA for a HCPB using the meta-zirconate/meta-titanate would have the following specifications :

- the use of the EUROFER97 as structural material,
- the ceramic breeder (zirconate/titanate) bed is of 9mm thickness at 50% enrichment in Li6. The breeder bed packing factor is 56%. The pebbles are of 1-1.5mm size with a 15% porosity. The total number of the breeder bed is a 206/segment,
- the Be-bed is with a thickness of 80mm with a packing factor of 75%. The Be-bed is a binary bed with 63% packing factor for the large pebbles (1.5-2.3mm) and 18% for the finer pebbles (0.1-0.2mm). The total number of Be-beds is 206/segment,
- the cooling plates are made of EUROFER97 with a thickness of 8mm and a voide fraction of 40%. The number of cooling plates is 412 /segment,
- the global TBR is 1.14 if the ports are not considered and 1.08 at BoL (considering the ports),
- the maximum heating rate is about 67 W/cm3 (BoL) in the breeder bed resulting in a maximum operating temperature in the OB-breeder bed equal to 1085 °C (for CP and FW at 450 °C),
- the blanket contains 32 IB-segments and 48 OB-segments. The energy production is 22 MW/IB-segment and 44 MW/OB-segment with a total energy production rate of 2785 MW from the blanket,
- 40% of the blanket energy is produced in the breeder materials, 30-35% in the Be-bed (IB/OB) and 11% in the FW's.

CONCLUSIONS

CEA is proposing to examine the use of the meta-zirconate and the meta-titanate as breeder materials for the EU-HCPB blanket which uses the ortho-silicate as a reference ceramic breeder amterial, [P1].

CEA has assessed the impact of the use of any of these ceramic candidates and addressed the specification of the HCPB blanket optimised for this use.

REFERENCES

[R1] M. Eid, J. F. Salavy, 'Contribution to the HCPB blanket design optimisation in the case of the use of the zirconate/titanate as breeder material' technical report, DMT 97/551, SERMA/LCA 2154, CEA, 01/1998.

[R2] J. F. Salavy, M. Eid 'Neutronic & thermal characteristics of the HCPB blanket in the case of the use of the zirconate/titanate as breeder material' technical report, DMT 97/552, SERMA/LCA 2155, CEA, 01/1998.

[R3] D. Lulewicz - N. Roux, « Development of Li2ZrO3 and Li2TiO3 pebbles. Report Jannuary-December1997 » technical report - DT97/064 JDL/NR/FL, CEA.

[R4] J D. Lulewicz - N. Roux, « Examination at CEA of Li4SiO4, Li2ZrO3 and LI2TiO3 pebbles specimens before and after the long time annealing test at FzK » technical report - DT98/081 JDL/NR/FL, CEA.

[R5] M. Eid et al. « Neutronic Optimisation of the HCPB Blanket using the zirconate/titanate as breeder materials » CEA technical note, SERMA/LCA/RT/98-2384/A, Sept.1998.

[R6] M. Eid et al. « Status report on the HCPB Blanket using the zirconate/titanate as breeder materials » CEA technical note, SERMA/LCA/RT/98-2462/A, Dec.1998.

[R7] P. Gierszewski « Canadian ceramic breeder technology : recent results » Fusion Engineering & Design, 27 (1995) 297-306.

[R8] Private Communication, from P. Gierszewski to N. Roux « Comments on N. Roux paper in the SOFT19, Lisbon », Fax on 4 November 97.

REPORT AND PUBLICATION

[P1] M. Eid et al. « European Blanket ; CEA contribution to the HCPB Design, impact of the use of the zirconate/titanate as breeder materials » CEA technical note, SERMA/LCA/RT/98-2475/A, Dec.1998.

TASK LEADER

Mohamed EID

DRN/DMT/SERMA
CEA Saclay
91191 Gif-sur-Yvette Cedex

Tél. : 33 1 69 08 3175
Fax : 33 1 69 08 9935

E-mail : meid@Cea.fr

WP-B2-1

Task Title : ITER TEST MODULE BLANKET FEASIBILITY & DESIGN
Adaptation to HIP fabrication technology

INTRODUCTION

This subtask is performed in the framework of the Helium-cooled (HCPB) Test Blanket Module (TBM) Feasibility & Design studies which have the aim of defining the TBM reference design and identifying the possible manufacturing sequence and techniques. This subtask is focused on the evaluation of the advantages of using the HIP technique for the FW manufacture compared to the initially proposed diffusion bonding technique.

In this initially proposed technique, cooling channels are obtained by assembly by diffusion bonding of structural plates with milled grooves, while the HIP technique proposes to HIP a tube inside such structural plates. Therefore, the main difference between the two techniques is that, in case of diffusion bonding, initial defects at the joining zone may occur due to partial failure of the bonding process. In order to evaluate the interest of the HIP technique compared to diffusion bonding, the impact of such a possible initial defect between two coolant channels has been assessed.

1998 ACTIVITIES

In 1997, a mechanical analysis of the first wall submitted only to internal channel pressure loading has been performed [1]. This year studies have consisted in the second part of these analyses which included thermal loading.

A two-dimensional FE model of the outboard first wall has been produced (***Figure 1***) to evaluate the thermal stresses in the stainless steel with the help of the FE code CASTEM 2000 [2]. An evaluation with regard to the RCC-MR mechanical criteria has then been performed.

Transient calculations have been performed assuming a nuclear heating cycle simulating a normal operating cycle in ITER [3]. Transient thermal results on two operating cycles are reported in ***Figure 2,*** showing the evolution of the maximum stainless steel temperature (point P1) and the temperature evolution of a point (P2) in the corner of the cooling channel. At steady-state, the temperature range of the Be/stainless steel interface is about [494 - 512] °C.

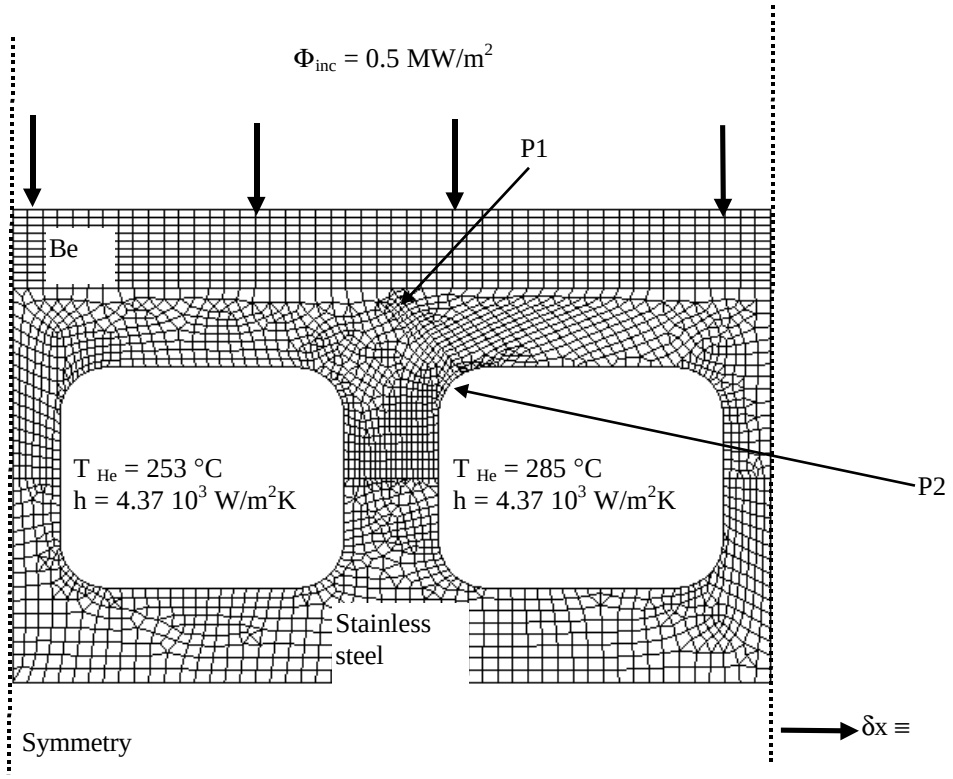

Figure 1 : Thermo-mechanical model of the TBM-I First Wall

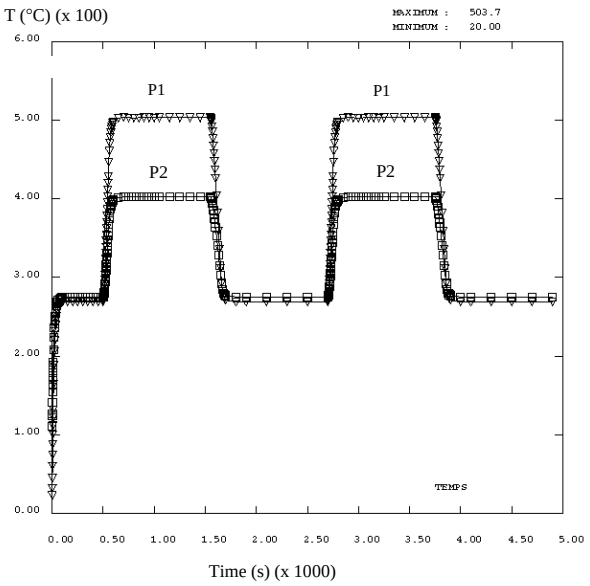

Figure 2 : Temperature (°C) evolution in the stainless steel First Wall

The corresponding maximal thermal stress level is reported in ***Figure 3*** and indicates a transient maximum thermal stress of 311 MPa occurring 200 s after the end of the power ramp-up. At steady-state, the maximum von Mises stress is a little bit lower at about 308 MPa. This effect is explained by the fact that the back of the first wall has a slightly higher thermal response coefficient than the front part. The maximum stress state is obtained when the front region has almost reached its maximum temperature as the back part is still much colder. The range of the von Mises thermal stress level in the stainless steel at steady-state under full power heating is [37-308] MPa.

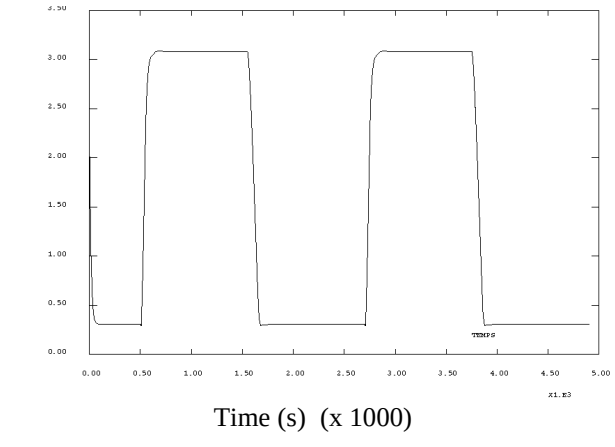

Figure 3 : Max. von Mises stress (MPa) in the stainless steel First Wall

The thermo-mechanical results have been analysed with the help of the RCC-MR criteria [4] against the risk of progressive deformation. Table 1 summarises the maximum primary and secondary stress levels obtained in the stainless steel during the cycle transient.

Table 1 : Maximum primary and secondary stress levels in the stainless steel first wall at steady-state under full power heating. Comparison with the RCC-MR criteria [4] against the risk of progressive deformation of the structure

Max von Mises primary stress [1] (MPa)	Max von Mises secondary stress (MPa)	Max von Mises primary + secondary stress (MPa)	Allowable limit for primary + secondary stress (3Sm rule) (MPa)	Margin
35	311	346	438	1.27

From Table 1, it can be seen that the maximum stress state is dominated by thermal stresses and that there is no risk of progressive deformation of the structure under normal operating cycle with a good safety margin of 1.27.

Similar evaluation has been done in the case of a debonding of a diffusion weld between coolant channels using primary stress results from [1]: 140 MPa instead of 35 MPa. As shown in Table 2, the limit imposed by the RCC-MR are overreached.

Table 2 : Maximum primary and secondary stress levels in the stainless steel first wall at steady-state under full power heating with a debonding of a diffusion weld between coolant channels [1]. Comparison with the RCC-MR criteria against the risk of progressive deformation of the structure

Max von Mises primary stress [1] (MPa)	Max von Mises secondary stress (MPa)	Max von Mises primary + secondary stress (MPa)	Allowable limit for primary + secondary stress (3Sm rule) (MPa)	Margin
140	311	451	438	0.97

It should be however noted that the maximum primary stress of 140 MPa obtained in the case of a diffusion weld debonding has been evaluated with a 2D model, which assumes that the debonding occurs on the all length of the weld. In reality, the defect may occur on a limited portion of the weld. The present evaluation is therefore very conservative.

CONCLUSION

Thermo-mechanical results have permitted to complete the stress analysis performed in the case of a potential debonding of a diffusion weld between two adjacent coolant channels in the First Wall.

[1] evaluated in [1] for 8 MPa internal pressure loading in the coolant channel

They have shown that the safety margin evaluated in the DDD [5] may be significantly reduced in the case of a debonding of one diffusion weld. A conservative 2D approach has lead to the conclusion that in case of severe debonding (large initial defect of a weld), the limit criteria may even be overreached. Local 3D calculation may constitute a good way to assess the impact of a more limited and realistic defect in a weld.

REFERENCES

[1] Y. Poitevin, L. Giancarli, « Contribution of the CEA to the HCPB ITER Test Blanket Feasibility & Design Studies, Part 1 », CEA report SERMA/LCA/2141 (November 1997).

[2] CASTEM 2000 Manual, CEA/DMT/Saclay (1998).

[3] ITER Design Description Document, WBS1.6A Blanket System (1997).

[4] RCC-MR, AFCEN, June 1985 Edition.

[5] Design Description Document of the HCPB Test Blanket (Status of the 26.9.1997).

PUBLICATION

[1] Y. Poitevin, L. Giancarli
Contribution to the HCPB ITER Test Blanket Feasibility & Design Studies, Part 2, CEA report, SERMA/LCA/RT/98-2469/A, Dec. 1998.

TASK LEADER

Yves POITEVIN

DRN/DMT/SERMA
CEA Saclay
91191 Gif-sur-Yvette Cedex

Tél. : 33 1 69 08 31 86
Fax : 33 1 69 08 99 35

E-mail : ypoitevin@cea.fr

WP-B6-1.3

Task Title : CONTRIBUTION TO THE SAFETY APPROACH OF THE DEMO HCPB BLANKET CONCEPT

INTRODUCTION

Technological analyses relative to the blankets of a DEMOnstration reactor based on the principle of a Tokamak associated with the DT reaction have been performed in Europe for several years now.

Of the two concepts retained after selection in 1995, one option uses a lithium-ceramic as breeder material and helium as the coolant ; beryllium in form of pebbles bed is used as neutron multiplier (HCPB : Helium Cooled Pebble Bed) [1].

An assessment of the safety of such a concept was analysed last year in the frame of the ITER Test Module studies. For this year the purpose of our work is to propose a qualitative analysis of the hydrogen hazard in the case of the DEMO-HCPB Power Plant concept.

The hydrogen hazard is apparently very limited in a reactor of DEMO-HCPB type: contact between steam and beryllium could only occur if there are two simultaneous failures:

- A failure at steam generator level,
- A failure in the blanket permitting a leak in the helium cooling circuit (previously polluted with water) towards the bed of beryllium pebbles.

In the case of HCPB ITM (ITER Test Module), contact between water and beryllium could be caused by a LOCA in the vacuum chamber of a standard module associated simultaneously with a failure of the ITM. This situation could occur for example in the event of an undetected LOFA in the ITM (without automatic plasma shutdown). The plasma shuts down on a disruption during the failure of the module and this disruption leads to a water leak in the vacuum chamber from a standard module.

This type of sequence will not be examined below : the analysis will be only focused on the cases of accidental sequences presenting a generic interest for the HCPB concept.

The analysis of the hydrogen hazard can be divided under two sub-headings:

- Identification of one or several sequence(s) permitting contact between water and beryllium,
- Analysis of hydrogen generation in the module (which supposes, among other things, not only a good understanding of the beryllium-water reaction, but also an accurate estimation of the associated thermal conditions).

1998 ACTIVITIES

IDENTIFICATION OF THE SEQUENCES PERMITTING CONTACT BETWEEN STEAM AND BERYLLIUM

As the confinement strategy and the definition of the safety and protection systems are not yet defined for the future DEMO facility, a realistic analysis of the accidental sequences liable to result in this situation cannot be made.

We shall therefore restrict ourselves to the discussion of a few generic sequences.

One of them could be a steam generator break without plasma shutdown with the following steps :

- Large break in the steam generator (or heat exchanger in the case of the ITM).

  The consequence of such a break is the ingress of steam into the circuit concerned, pressurization of this circuit (with pressure valve opening), and disrupted cooling of the associated blankets.

- Absence of plasma shutdown (or late plasma shutdown).

- A rise in the temperature of the blanket leads to its failure.

  It should be noted that even if a cooling circuit no longer assures its cooling function, the increase in the temperature of the blanket would be progressive, as the blankets are cooled by two independent parallel circuits and the second circuit would remain operational (the heat calculations show that when a single cooling circuit is in service, the temperature of the first wall rises from 500° C to 730° C in three minutes and then stabilises :If the shutdown of the plasma occurs within a reasonable lapse of time no failure will occur).

It is obviously impossible to quantify such a sequence from a probabilistic standpoint; it can only be assessed qualitatively.

The initiating event is a low-probability event: it can be compared to a strong line of defence (occurrence about 10^{-3} to 10^{-4} a year). The absence of plasma shutdown within a reasonable lapse of time can also be considered as a strong line of defence.

A double failure is therefore likely to lie beyond the scope of usual design, although with a margin that cannot be considered as particularly large.

An other sequence may be a break in the Steam Generator associated with a loss of power with the following steps :

- Break in the steam generator identical as in the first case.

- Loss of power.
  This situation is usually considered deterministically in all the sequences studied in the safety analysis. In this case it can be considered that plasma shutdown would also be the result.

- Inner failure of the blanket module, resulting either from a strong disruption following plasma shutdown, or a temperature rise due to residual heat (which supposes a simultaneous failure of the residual heat removal system).

The probability of this second sequence is even more difficult to estimate due to lack of data; it is liable to lie beyond the usual design scope.

In conclusion, we can say that we have identified certain plausible situations in which a double failure could occur. Their probability is likely very low although it cannot be discarded as a residual risk.

HYDROGEN GENERATION IN THE EVENT OF MODULE FAILURE

Let us now consider the assumption of an inner or module failure with contact between steam and the beryllium pebbles.

This event is very similar to the cases of accidents that have been analysed in the framework of studies on breeding blankets in the second phase of ITER [2]. These studies showed the particular importance of two parameters:

- The temperature of the beryllium bed at the time of the accident,

- The possibilities of power removal after the beginning of the reaction.

In all cases, it can be considered that there exist two distinct domains of behaviour that depend on the initial temperature of the bed of beryllium.

In the cases in which the temperature is lower than this transition value when contact between the steam and the beryllium occurs, the reaction is slight enough at the beginning to enable the generated heat to be removed: the reaction rapidly dies out and the quantity of hydrogen produced is small.

In the case in which the temperature is higher than this transition value, there is, on the contrary, runaway of the reaction, and the generation of hydrogen only stops when a reaction is no longer possible through lack of one of the constituents.

In the configuration studied for accidents in ITER, this transition temperature was about 750° C [2]. This value can be considered as indicative only, as it depends considerably on various parameters:

- The possibility of removing heat by conduction to structures at lower temperatures,

- The possibility of heat removal linked to the circulation of gas and steam fluxes passing through the bed of beryllium.

Finally, a last parameter concerns the kinetics of the reaction itself. Numerous experiments have been performed with several types of beryllium including pebbles. The effect of kinetic is significant (and it is sure that further experiments are needed in representative conditions to decrease the uncertainties), but likely not as determining as knowledge of the temperature itself in view of the complexity of the assumptions concerning the conservative heat calculation during the circulation of gas and steam in the bed of pebbles.

In conclusion, the determination of the maximal quantity of hydrogen generated supposes that heat conditions in the bed of pebbles is calculated conservatively taking into account the possibilities of conduction and heat removal by circulation of gas and steam.

CONCLUSION

In the case of the DEMO-HCPB concept, in which the secondary system intended to produce electric energy is a water circuit, the possibility of contact between water and the beryllium present in the blankets cannot be totally excluded.

Management of the hydrogen hazard requires first of all defining safety systems able to maintain the bed of beryllium at temperatures that permit preventing reaction runaway.

In view of the presence of two cooling systems per blanket, correct control of heat conditions should be possible provided suitable plasma shutdown and residual heat removal systems are provided for.

REFERENCES

[1] L. GIANCARLI, M. DALLE DONNE, W. DIET, "Status of the European Breeding Blanket Technology" - Fusion Engineering and Design 36 (1997) 57-74

[2] W. GULDEN , X. MASSON, H. JAHN, M. FERRARI, G. MAZZONE, A. BIANCHI, G. MARBACH, "ITER Breeding Blanket Safety Analysis" Proc. Of the 20th Symposium on Fusion Technology, MARSEILLE, 7-11 September, 1998

[3] R.A. ANDERL, R.J. PAWELKO, M.A. OATES, G.R. SMOLIK and K.A. McCARTHY - "Steam-chemical Reactivity Studies for Irradiated Beryllium" J. FUS. Energy 16 (1997)101-108.

[4] F. DRUYTS, "Determination of Be/Air and Be/Steam Reactivities with TG/DTA", Proc. Of the 20th Symposium on Fusion Technology, MARSEILLE, 7-11 September, 1998.

TASK LEADER

Gabriel MARBACH

DRN/DER/SERSI
CEA Cadarache
13108 St Paul Lez Durance Cedex

Tél. : 33 4 42 25 34 14
Fax : 33 4 42 25 48 68

E-mail : marbach@babaorum.cad.cea.fr

WP-B8-2

Task Title : DEVELOPMENT OF Li_2ZrO_3 AND Li_2TiO_3 PEBBLES

Development of Li_2ZrO_3 and Li_2TiO_3 pebbles made by sintering

INTRODUCTION

Li_2ZrO_3 and Li_2TiO_3 pebbles are investigated at CEA as candidate alternative ceramic breeder materials for the HCPB blanket concept. Among the objectives of the European ceramic breeder program are first the selection of one alternative ceramic between Li_2ZrO_3 and Li_2TiO_3, and, next, the selection of one ceramic between the alternative ceramic and the reference one (Li_4SiO_4)

1998 ACTIVITIES

During 1998, the work was focused on two items :

- The fabrication, characterization, and optimization of the Li_2ZrO_3 and Li_2TiO_3 pebbles.

- The performance testing of the Li_2ZrO_3 and Li_2TiO_3 pebbles and pebble beds.

FABRICATION, CHARACTERIZATION, AND OPTIMIZATION OF Li_2ZrO_3 AND Li_2TiO_3 PEBBLES

Fabrication of the pebbles

Following the evaluation of two fabrication processes, i.e., agglomeration-sintering, and extrusion-spheronization-sintering, which are liable to provide pebbles fulfilling the requirements for utilization in the HCPB blanket, the latter process was chosen in 1998 for further development. Among the advantages of this process are its applicability to the fabrication of both Li_2ZrO_3 and Li_2TiO_3 pebbles, and the capability to produce pebbles with a shape close to spherical and with a narrow pebble size distribution. Moreover, the specifications fixed by CEA on pebbles microstructure could be met after few trials.

All steps of the extrusion-spheronization-sintering process make use of conventional techniques of powder technology and, therefore, industrial production is not expected to raise any significant problem. In order to early address the scalability of fabrication to larger quantities, the pebble shaping step, which is one major step in the fabrication process, is already being made with the collaboration and facilities of an industrial firm.

The work on the fabrication of Li_2ZrO_3 and Li_2TiO_3 pebbles is reported in[1] and is summarized here.

It is recalled that pebbles specifications were initially fixed as follows :

a) spherical shape,
b) ~ 1 mm diameter,
c) high density (provided tritium release is not unduly affected),
d) small grain size (to favour both tritium release and mechanical strength),
e) high purity level.

In order to meet this set of specifications a parametric study was performed at each step of the fabrication. Fabrication steps, and corresponding main parameters are briefly recalled hereafter.

- Preparation of the Li_2ZrO_3 and Li_2TiO_3 powders using the reaction of Li_2CO_3 powder and ZrO_2 and TiO_2 powder : purity, particle size, and specific surface area of the starting powders, proportions of the starting powders, temperature and time of the synthesis reaction.

- Preparation of the paste to be extruded : nature and proportion of binder and plasticizer, mixing conditions.

- Extrusion : extrusion conditions (pressure, nozzle diameter...).

- Cutting of granules : design of cutting device, length of the granules.

- Spheronization of the granules : design of spheronization plate, spheronization time and speed.

- Sintering : time and temperature of sintering.

Characteristics of the pebbles

The parametric study enabled to identify suitable conditions to fulfill the specifications.

Thus, shape was improved after a few trials, and can be now considered to be as spherical as practicable when starting from cylindrical granules. Size distribution is narrow, ranging from 1 to 1.2 mm. Densities of ~ 86% T.D., and grain sizes of ~ 1 µm can be obtained for Li_2ZrO_3 pebbles, and densities of ~ 93% T.D., and grain sizes of ~ 1-2 µm can be obtained for Li_2TiO_3 pebbles. The purity level, as evaluated from Spark Source Mass Spectrometry analysis, indicates the presence of very small amounts of impurity elements which, further, raise very little activation concern [1].

Initial goals being met, the subsequent objective was to check the performance of these pebbles as regards the HCPB blanket requirements, and, if needed, to adjust fabrication parameters in order to tailor pebbles properties.

Optimization of the pebbles

Following the testing campaign (see next section), the characteristics of the Li_2ZrO_3 pebbles were found quite satisfactory to meet the present HCPB requirements. The characteristics of the Li_2TiO_3 pebbles were found adequate too. However, in view of the better tritium release behaviour observed in the EXOTIC-8 experiment, under identical conditions, of specimens of pebbles and pellets with a slightly lower density, an attempt is being made to slightly lower the Li_2TiO_3 pebbles density so as to improve the tritium release behaviour, provided such density change does not result in an unacceptable degradation of any key property. A new testing campaign will be required to check the performance of the new pebbles so as to either adopt the revised characteristics or make the best compromise on properties.

PERFORMANCE TESTING OF Li_2ZrO_3 AND Li_2TiO_3 PEBBLES

The most promising specimens of pebbles obtained in the optimization work were subjected to several relevant tests being available at CEA, and in the European and worldwide organizations. In this respect, it has to be stressed that it is very important that candidate ceramic pebbles and pebble beds be tested using the same facilities and experimental conditions so as to obtain a reliable comparison of ceramics candidates performance.

Tests performed at CEA

a) Crush tests of single pebbles.

b) Long-term (up to 4 months) annealing tests, in air, in the range 900°C to 1200°C.

c) Thermal cycling tests at 17°C/s heating and cooling rate, between 170°C and 600°C, and between 350°C and 800°C.

d) Out-of-pile tritium release annealing tests (both isochronal and isothermal) of pebbles specimens subjected to a short time irradiation in the OSIRIS reactor.

Tests performed at FZK

a) Annealing tests at 970°Cduring 96 days, in flowing He + 0.1% H_2.

b) Uniaxial compressive tests of the pebble beds up to 6 MPa, and up to 700°C.

c) Thermal shock and thermal cycling tests.

Tests performed at JAERI-Naka

Measurement of thermal conductivity of pebble bed of Li_2TiO_3, using the hot-wire method.

Tests performed at RNG

In-situ tritium release tests of Li_2TiO_3 and Li_2ZrO_3 pebbles are conducted in the EXOTIC-8 experiment, as well as a test of irradiation behaviour of Li_2TiO_3 pebbles up to DEMO end-of-life conditions.

Results of the above mentioned tests were reported in [2-6] and can be summarized as follows :

- As could be expected, changes on thermal annealing are the larger, the higher the annealing temperature. However, no significant changes, except a little grain growth, and a little lithium vaporization were observed for Li_2ZrO_3 pebbles on annealing at ~ 1000°C in air and in He + 0.1% H_2. A larger grain growth was observed for Li_2TiO_3 pebbles, with no apparent effect on crush load, on annealing at ~ 1000°C in air, and He + 0.1% H_2. Blackening of the Li_2TiO_3 pebbles was observed which disappears on heating in air, and can be attributed to a substoichiometry in O_2.

- A good behaviour was observed in the uniaxial compression test of pebble beds with no fracture of Li_2ZrO_3 pebbles and very little fracture of Li_2TiO_3 pebbles (0.3% fracture at 4 MPa and at 400°C). No plastic deformation was observed for any of the ceramics at 400°C. Some agglomeration of pebbles was observed at 700°C, small for Li_2TiO_3, even smaller for Li_2ZrO_3, which in both cases disappears under application of modest mechanical forces.

- The first measurement ever obtained of thermal conductivity of Li_2TiO_3 pebble bed was made at JAERI-Naka. Comparison with the other candidate ceramics will be made with the same facility, and under identical conditions.

- No change in microstructure, and no fragmentation was observed for both Li_2ZrO_3 and Li_2TiO_3 pebbles on thermal cycling at CEA at ~ 15°C/s during 300 cycles in the ranges 170°C-600°C, and 350°C-800°C, and no change in crush load was observed for Li_2TiO_3 pebbles after the test.

- Results of in-pile tritium release in EXOTIC-8 confirmed once again the excellent behaviour of Li_2ZrO_3 pebbles. Results showed once more the effect of the ceramic material density on its tritium release performance. The behaviour of 90% T.D. Li_2TiO_3 pebbles was found to be intermediate between that of the current Li_2ZrO_3 pebbles and of the Li_4SiO_4 pebbles.

CONCLUSION

The extrusion-spheronization-sintering process was chosen at CEA for the lab-scale fabrication of Li_2ZrO_3 and Li_2TiO_3 pebbles. The as-optimized pebbles characteristics allow a satisfactory pebbles performance as shown in the relevant tests performed so far.

Additional tests are necessary to complete the data bases of properties of Li_2ZrO_3 and Li_2TiO_3 pebbles and pebble beds, as only with equivalent data bases of properties will a sound selection of one ceramic for the HCPB blanket be able to be made.

Most of the future tests require quantities of pebbles larger than those available with the current laboratory fabrication means. Therefore, one of the next objectives is the scaling-up of the production of the Li_2TiO_3 (Li_2ZrO_3) pebbles, which will involve the use of pre-industrial means at all fabrication steps.

REFERENCES

[1] J.D.Lulewicz, N.Roux, Characteristics of Li_2ZrO_3 and Li_2TiO_3 pebbles fabricated by the extrusion-spheronization-sintering process. International workshop on ceramic breeder blanket interactions Petten (1998)

[2] J.D.Lulewicz, N.Roux, Examination at CEA of Li_4SiO_4, Li_2ZrO_3 and Li_2TiO_3 pebbles specimens before and after the long annealing test at FZK. CEA/DTA/CE2M/LECMA DT 98/81 (1998)

[3] G.Piazza, M.Dalle Donne, H.Werle, E.Günther, R.Knitter, N.Roux, J.D.Lulewicz, Long-term annealing of ceramic breeder pebbles for the HCPB DEMO blanket. International workshop on ceramic breeder blanket interactions Petten (1998)

[4] J.Reimann, E.Arbogast, S.Muller, K.Thomauske, Thermomechanical behaviour of ceramic breeder pebble beds. International workshop on ceramic breeder blanket interactions Petten (1998)

[5] J.G.van der Laan, R.Conrad, K.Bakker, N.Roux, M.P.Stijkel, In-pile behaviour of some lithium titanates to medium lithium burn-ups. 20th Symposium on Fusion Technology, Marseille (1998)

[6] N.Roux, Summary of the results of 1998 performance testing of Li_2ZrO_3 and Li_2TiO_3 pebbles, internal document. CEA/DTA/CEREM/CE2M/LECMA DT 99/103 (1999)

TASK LEADER

Nicole ROUX

DTA/CEREM/CE2M/LECMA
CEA Saclay
91191 Gif-sur-Yvette Cedex

Tél. : 33 1 69 08 25 86
Fax : 33 1 69 08 91 75

E-mail : françoise.lefèvre@cea.fr

UT-SM&C-BLK

Task Title : HELIUM COOLED PEBBLE BED BLANKET

INTRODUCTION

The CEA has proposed, within the EU-Fusion Program, to examine the use of the lithium meta-zirconate/meta-titanate as breeder materials for DEMO-HCPB blanket and to assess the impact of the use of these candidates on the general design features. The reference breeder material for the EU-HCPB blanket of DEMO is the lithium ortho-silicate, proposed and studied by FzK.

Accordingly, the CEA has presented a 1st proposal in 1997 [R1,R1] and assessed the impact of using these potential candidates on the DEMO-Blanket general features. The main characteristics of that proposal was the use of a breeder beds as thick as 16-18 mm with ceramic breeder materials as rich as 25-28% in Li6. The resultant maximum operating temperatures was evaluated to be as high as 1215 °C. Some recent experimental work on pebble thermal stability have increased the uncertainty in the thermal stability of the Li-zirconat/-titanante at such high temperatures. Although the full interpretation of these results has not yet been completed, the HCPB-blanket project leader joined by materials experts have recommended to revise the CEA proposed design to result in lower operating temperatures. Due to the absence of all experimental figures, the project leader advised to keep the maximum operating temperature around the indicative value of 900 °C for both meta-zirconate and the meta-titanate ceramics.

In additions, the EU-Fusion Program has decided to use the EUROFER97 rather than the Martensitic (MANET) as structure material. A change that would alter significantly the TBR and the neutron induced activation characteristics of the HCPB blanket .

Subsequently, it appeared necessary to revise the CEA proposal in order to integrate the materials experts' recommendations and the DEMO new specifications.

1998 ACTIVITIES

In 1998, a wide set of optimum configurations, in the TBR sense, has been determined for DEMO-HCPB. A given configuration will be fully defined by the cooling plate thickness (t1), the breeder bed thickness (t2) and the Be-bed thickness (t3) for a given breeder ceramic at a given Li-6 enrichment. Thus the option Zr50%-08.09.80 will assign a 8mm for the cooling plate thickness, a 9mm of breeder bed thickness and a 80mm of Beryllium bed thickness in the case of the lithium meta-zirconate ceramic with 50% enrichment in Li-6.

The BoL Li6 enrichment will be fixed at 50% for all studied configurations. This resulted from the investigations done in 1997, [R1], where thermal calculations showed that approaching values near to 900-1000°C of maximum operating temperatures should necessitate decreasing the breeder thickness to values less than 12mm. At such small thickness of the breeder bed, only Li6 enrichment equal or higher than 45% will guarantee the TBR value of 1.07 at BoL (considering the ports).

GEOMETRICAL MODEL

The HCPB blanket geometry has been described by a 3D local model in the equatorial plan region. It allows to calculate the maximum neutron heating rates in the beds and optimise the TBR as well. The 3D-local model used in the neutronic optimisation is fully described in [R1, P1]. Three ceramic bed thickness have been considered 9, 10 and 12 mm. At each ceramic bed thickness, the Be-bed thickness has been varied from 30 to 80 mm and the optimum Be-bed thickness is determined.

TBR OPTIMISATION

TBR optimisation calculations were carried on using TRIPOLI4, the CEA Monte Carlo neutron transport code. The details of this parametric evaluations are given in [P1]. The local TBR values are calculated with statistical uncertainty less than 0.1% in the worst case. The choice between different possible breeder bed thickness will be decided in function of the maximum nominal temperature observed in the equatorial breeder bed. Among different examined options, the series of Zr50%_08.12.80, Zr50%_08.10.80 and Zr50%_08.09.80 have resulted in a local TBR of 1.43, 1.42 and 1.41, respectively. At Be-bed thickness of 80mm, the optimum TBR change slightly with the breeder bed thickness between 12 and 8mm. The final choice will be done in function of the maximum operating temperature.

BREEDER DEPLETION

The 2nd needed quantity is the Li-depletion in the time. Starting from the depletion rate of Li6 and li7 per neutron emitted in the plasma at 14.1 Mev calculated by TRIPOLI4, the li6-enrichment as function of the operating time at full power could be determined, [P1,P2]. The variation of the Li6-enrichment against the operating time in the case of the Zr-08.09.80 option shows that the Li6-enrichment lower limit of 47% would be attainable around 28 000 hours of full power operation. An enrichment of 47% is corresponding to a local TBR of 1.39 (corresponding to a 1.05 global 3D TBR with the ports, at the EoL).

NEUTRON FW LOAD

The resultant FW_{OB} maximum neutron loading was evaluated to be equal to 2.87 MW/m^2 while the mean neutron loading is equal to 2.50 MW/m^2 with an offset factor of 1.15 due to the neutron source poloidal distribution.

HEAT RATE RADIAL DISTRIBUTION

The heating rate radial distribution in the OB-breeder bed in the vicinity of the equatorial plan, for the Zr50%-08.09.80 option, is evaluated to 67 W/cm^3 within the 20mm behind the FW and decreases to 8 W/cm^3, 50 cm further.

MAXIMUM OPERATING TEMPERATURE

All examined options have been evaluated and the maximum operating temperature in each option was determined. In the precise case of the breeder bed option of Zr50%-08.09.80 the maximum heating rate issued from the neutronic calculation was estimated to be about 67 W/cm^3 (BoL). Using the relations describing the effective bed conductivity as mentioned in [P1] would produce a maximum operating temperature in the OB-breeder bed equal to 1085 °C (for CP and FW at 450 °C).

The option Zr50%-08.09.80 results in the lowest maximum operating temperature.

PEBBLE THERMAL STABILITY

The main restriction on the maximal allowable operating temperature is due to the existing uncertainty on the thermal stability of the lithium meta-zirconate and the lithium meta-titanate at temperatures as high as 1000 °C and slightly beyond.

Long annealing behaviour in air for temperatures between 800 and 900 has been tested for the meta-zirconate and meta-titanate in pebbles form and results are reported in [R4]. It concludes that, for lithium zirconate, produced by extrusion and sintered at 1050°C for 2 hours, grain size shows almost no-significant change between 800 °C - 900 °C, up to 75. Results were confirmed in the tests effectuated at Fzk in He+0.1%H_2 at 970 C during 96 days. In this campaign, X-ray diffraction pattern tests indicated no additional phase within the detection limits (~ 1%). However, a slight densification was observed from porosity measurements from 89% TD at the beginning-of-test to 90.5% at the end-of-test. It has also been observed that the annealing effect decreases significantly for the pebbles having been sintered at higher temperatures (~1200 °C) for zirconate and titanate. Thus, It seems that potential improvements in the pebble thermal long term behaviour would be possible by developing fabrication procedures using higher sintered temperatures. However, the tritium release behaviour of the pebbles sintered at higher temperatures should be re-examined.

As for crash load time evolution, only zirconate and titanate pebbles were tested in the CEA testing progrogram. For titanate pebbles sintered at 1050 °C, crush load seems tend to a limit of 1.7 daN after 90 days of continuous annealing at 900 C. For the zirconate pebbles sintered and annealed in the same conditions, the crush load limit tends towards a constant value of 1.9 daN. In all three ceramics one may conclude that crush load decreases by almost 50%. However, the crush load limit of the silicate pebbles presents specific concerns for HCPB regarding the fact that it has the lesser crash load limit. While, the crush load limits for the zirconate/titanate should not en principal rise any specific concerns.

The effect of thermal cycling has also been examined in two configurations ; 1/ cycling at temperatures between 80 and 600 °C for some 600 cycles, and. 2/ cycling at a range between 1100 °C and 1200 °C for some 30 cycles. It seems as if the crush load after cycling tends to the crush load corresponding to the upper temperature of the cycle.

THERMAL POWER BALANCE

The total plasma energy is transferred to the blanket and the in-vessel surrounding structure through neutrons at 14.1 MeV (1800 MW_{th}) and alpha-particles (400 MWth). Neutronic calculations estimated the global quantity of useful thermal energy deposed and amplified by the neutron transportation in different blanket structure by 2875 MWth, [R5].

It showed also that the major part of the thermal energy comes from the breeder bed zone with the same share of 41% of the total energy production, in the IB- and the OB-breeders, in the IB- and OB-segments, respectively.

The 2^{nd} important contribution is that of the multiplier with almost 35.5% in the case of the OB-segments and 30% in the IB-segments.

The rest of the contributions comes from the metallic structures principally made of the Eurofer (FW, cooling plates, side-walls, and back-walls). The contribution of the metallic parts rises to about 25% of the total production of the thermal energy in the blanket.

ACTIVATION CALCULATION

The activation of the structure components such as the FW and the CP in the HCPB blanket has been assessed. For all structure components, neutron irradiation time was taken equal to 20000 h of full power irradiation regime.

The specific activity of the Eurofer structures attain some 10^{+12} Bq/kg and 2 10^{+11} Bq/kg, just after 20000h of full irradiation time, for the FW and the other blanket structures, respectively. Calculations shows that the main contribution comes from radioactive elements such as F55 (~25%) and W187 (20%), just after shutdown. After 200 years, the specific activity becomes lower than 10^{+6} Bq/kg.

Roughly estimations show that an OB-segment will emit some 3.5 10^{+15} Bq just after shutdown. This maximum activity is shared between the FW (2.3 10^{+15} Bq) and the other components (1.2 10^{+15} Bq).

The dose rate is relatively higher for the FW components compared to the CP ones. For all structures, dose rate is of the order of 10^{+5} Sv/h just after shutdown. It decreases by factor of 2 after one cooling year and by 3 decades after 10 years. Just after shut down, the main contributions in the dose rate come from the W187 and the V52. The situation changes after one year and lasts for few tens of years with major contributions coming from F55 and Co60.

As for the specific decay heating rate, we observe the same tendency of having the FW relatively hotter than the other structures, [P2]. The heating rates of 10^{-4} kW/kg and 4 10^{-5} kW/kg are observed just after shut down for the FW and the CP, respectively. Then, they decrease by some 2 decades in one year. After 10 years, the heating rates are already lower than 10^{-7} kW/kg, whatever the structure is.

CONCLUSIONS

CEA has to revised its concept proposed in 1997, [R1, R2]. The revised concept make use of a breeder bed of 9mm thickness, a Be-bed of 80mm thickness and a cooling plates with 8mm thickness, [P1,P2]. The zirconate enrichment in Li6 is increased up to 50%. The maximum heating rate in the breeder bed of this concept (Zr50%-08.09.80) is about 67 W/cm^3 resulting in a maximum operating temperature equal to 1085°C.

The corresponding overall 3D TBR (considering the ports) is equal to 1.09 at BoL. Breeder depletion calculations showed that this blanket (Zr50%-08.09.80) may operate continuously at full power for some 28 000-29 000 hours before attending the EoL TBR limit of 1.05 (3D with ports).

Limitations on the maximum operating temperature in the ceramic breeder comes from uncertainty in the thermal stability of the pebbles and Li transport at high temperatures. However, experimentally confirmed figures are lacking.

REFERENCES

[R1] M. Eid, J. F. Salavy, 'Contribution to the HCPB blanket design optimisation in the case of the use of the zirconate/titanate as breeder material' technical report, DMT 97/551, SERMA/LCA 2154, CEA, 01/1998.

[R2] J. F. Salavy, M. Eid 'Neutronic & thermal characteristics of the HCPB blanket in the case of the use of the zirconate/titanate as breeder material' technical report, DMT 97/552, SERMA/LCA 2155, CEA, 01/1998.

[R3] D. Lulewicz - N. Roux, « Development of Li2ZrO3 and Li2TiO3 pebbles. Report Jannuary-December1997 » technical report - DT97/064 JDL/NR/FL, CEA.

[R4] J D. Lulewicz - N. Roux, « Examination at CEA of Li4SiO4, Li2ZrO3 and LI2TiO3 pebbles specimens before and after the long time annealing test at FzK » technical report - DT98/081 JDL/NR/FL, CEA.

[R5] M. Eid et al. « European Blanket ; CEA contribution to the HCPB Design, impact of the use of the zirconate/titanate as breeder materials » CEA technical note, SERMA/LCA/RT/98-2475/A, Dec.1998.

REPORTS AND PUBLICATIONS

[P1] M. Eid et al. « Neutronic Optimisation of the HCPB Blanket using the zirconate/titanate as breeder materials » CEA technical note, SERMA/LCA/RT/98-2384/A, Sept.1998.

[P2] M. Eid et al. « Status report on the HCPB Blanket using the zirconate/titanate as breeder materials » CEA technical note, SERMA/LCA/RT/98-2462/A, Dec.1998.

TASKLEADER

Mohamed EID

DRN/DMT/SERMA
CEA Saclay
91191 Gif-sur-Yvette Cedex

Tél. : 33 1 69 08 3175
Fax : 33 1 69 08 9935

E-mail : meid@Cea.fr

Task Title : PURIFICATION OF LIQUID METALS

INTRODUCTION

During operation of the water-cooled liquid metal blanket, the steel box which acts as the liquid metal container can be corroded by the Pb17Li alloy flowing at low velocity. The corrosion products dissolved in the alloy are then transported with the flow. In some regions, characterized for example by low temperatures, these corrosion products can crystallize and form aggregates which can be deposited on the walls. The processes of corrosion, formation of aggregates and deposition depend on several factors such as temperature, hydrodynamics, solubility, kinetics of exchange at the solid/liquid interface, roughness of the wall... Another significant factor is the high external magnetic field used to confine the plasma.

The deposition in uncontrolled zones can lead to plugging and the accumulation of activated products is a problem for the maintenance. Therefore, it is necessary to remove the metallic impurities present in the liquid alloy and purification methods have to be developped. One way is to promote the preferential deposition of the products in controlled areas either by cold trapping or by magnetic trapping. It results that the deposition process has to be understood from a basic point of view.

1998 ACTIVITIES

In 1998, the effect of a magnetic field on the formation of deposits in Pb17Li liquid alloy has been examined. More specifically, the deposition of metallic elements resulting from the corrosion of steels by the liquid alloy under thermal gradient and magnetic field has been studied. The case of martensitic steel exposed to Pb17Li has been considered and the deposits formed in such conditions have been identified.

EXPERIMENTAL PROCEDURE

Martensitic steel (type 56T5: 86.7Fe-10.5Cr-0.66Ni-0.65Mo-0.61Mn-0.48Nb-0.18V-0.22Si) has been used as material. It was prepared in tubes which were closed at one end by welding and filled with liquid Pb17Li under an argon atmosphere. The open ends of the tubes were then sealed under vacuum. Two steel tubes were exposed to Pb17Li: one was placed under thermal gradient without magnetic field (test 1), the second one was placed under thermal gradient with magnetic field (test 2). The tubes were vertically located in a furnace where a temperature gradient was established for the test duration.

In test 1 without magnetic field, the temperature gradient was 510-250 °C. In test 2 with magnetic field, a temperature gradient 510-250 °C was arranged and a permanent magnet (0.25 T) was placed around a region of the tube where deposition was thought likely to occur in the hope of trapping out any ferromagnetic materials. In the present experiment, the magnet was placed in a temperature region ranging from 390 to 320 °C.

On completion of tests (3300 h), the crystals formed on the walls of tubes or in the bulk of the lithium-lead alloy were characterized and the composition of the solidified Pb17Li was analyzed.

CHARACTERIZATION OF DEPOSITS FORMED WITHOUT MAGNETIC FIELD

In test 1, no corrosion layer was observed on the surface of 56T5 steel. The only evidence for corrosion was the direct observation of crystals on the walls of tubes after the removal of Pb17Li, indicating that mass transfer occurred. Therefore, the main constituents of this steel seem to corrode at a similar rate when it is in contact with molten Pb17Li. Dissolved metallic elements were found in Pb17Li (in wppm): 13 for Fe, 3.5 for Mn, < 1.5 for Cr and < 0.7 for Ni.

The characterization of crystals deposited on the steel surface was complex because they were distributed all over the tube and exhibited varying compositions. Nevertheless, some results may be drawn.

The hottest part of the tube (480-510 °C) was mainly composed of iron-rich crystals having the composition 97.5Fe-2.5Cr. In the temperature range 400-480 °C, other types of crystals were observed in small quantities: Fe-Cr crystals (38Fe-59Cr-3Mo), Ni-Fe-Mn-Sn crystals (29.2Ni-27.2Fe-14Mn-28.3Sn-1.1Cr-0.3Mo) and Fe-Nb crystals (28.2Fe-65.7Nb-2.5Cr-3Mo). For lower temperature (T<400 °C), the Ni-Fe-Mn-Sn crystals were found associated with higher chromium content (32Ni-10.5Fe-16Mn-33.5Sn-8Cr).

It was deduced that the Fe/Cr ratio of these crystals decreases with temperature. However, at temperature less than 350°C, the Fe and Cr concentrations were both lowered and the crystals reach the composition 33.5Ni-7Fe-18Mn-39Sn-2.5Cr which corresponds to the ternary compound $(Ni,Fe,Cr)_2MnSn$.

Although the concentrations of Ni and Mn in steel, and Sn in Pb17Li are very low, these three elements are easily associated to form crystals.

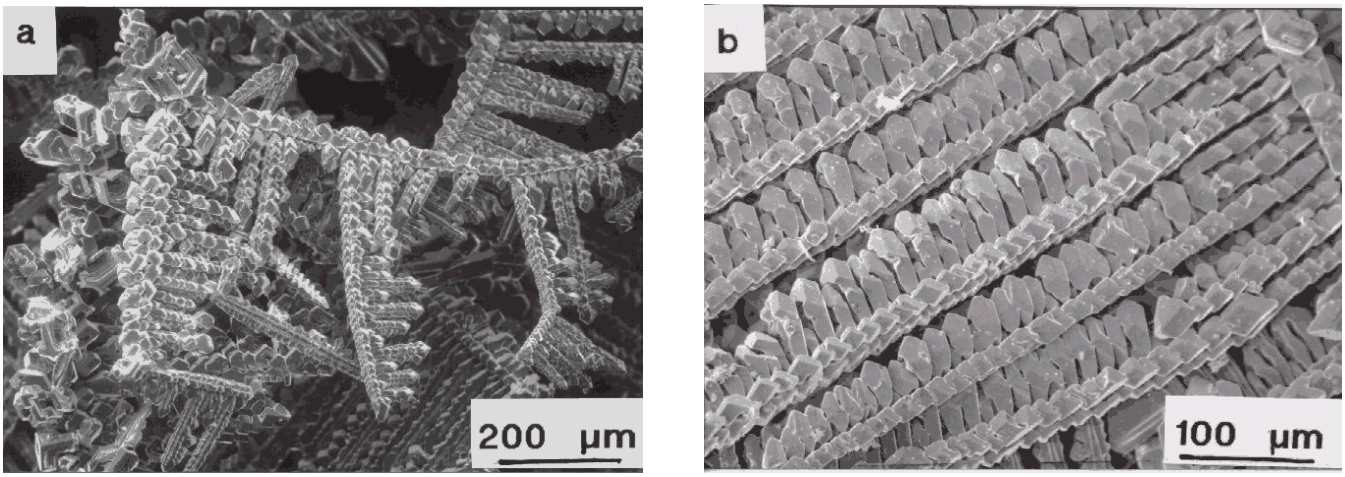

(a) General view *(b) Orientated 92Fe-8Cr crystals*

Figure 1 : Deposits in Pb17Li under magnetic field

CHARACTERIZATION OF DEPOSITS FORMED IN THE PRESENCE OF A MAGNETIC FIELD

In test 2, the corrosion behavior of 56T5 steel seems similar to that observed in test 1. Corrosion is detected because crystals are found but the experimental procedure does not permit to say if there is a quantitative effect of the magnetic field on the corrosion process. Furthermore, the magnetic field is placed in a low temperature region so its effect on corrosion is probably limited. The concentration of metallic elements present in Pb17Li alloy at the end of this test has been determined. It was found (in wppm): 6.5 for Fe and 1.9 for Cr. The Fe concentration is thus divided by a factor of 2 compared to test 1.

A completely different situation was observed with regard to the distribution of crystals in test 2. In fact, the region which had been at a temperature ranging from 510 to 390 °C during the test was nearly free from deposition. Most of the crystals were found in the region which was directly in the magnetic field (temperature range 390-320 °C). Figure 1 shows abundant crystals which were detected in this area after removal of Pb17Li. Another evidence for the effect of the magnetic field is the fact that the crystals are not randomly distributed but orientated along directions (Fig. 1b). The EDS analysis indicates they are composed of iron and chromium: 92Fe-8Cr. A large quantity of these crystals was suspended in the frozen alloy (about 75 mg) but some of this material were also found adhering to the surface of the tube. For temperatures less than 300 °C (corresponding to the part of the tube below the magnetic field), some crystals were sparsely detected. The analysis showed their composition to be a mixture of Ni, Mn and Sn corresponding to the ternary compound $(Ni,Fe,Cr)_2MnSn$. The deposition of this material seems unaffected by the presence of the magnetic field because it was also found in this range of temperature in test 1.

Therefore, the presence of the magnetic field alters the distribution of corrosion products formed under thermal gradient.

Preferential deposition of ferromagnetic Fe-Cr crystals in the region affected by the field has been observed. The decrease of the Fe content remaining in the Pb17Li alloy at the end of the test is consistent with magnetic trapping effect.

CONCLUSION

A series of simple deposition tests has been carried out in Pb17Li contained in martensitic tubes under a thermal gradient. Different types of crystals have been identified, composed of Fe and Cr or a mixture of Fe, Cr, Ni, Mn and Sn. They were found in various quantities and distributed all over the steel surface.

The deposits with Ni, Mn and Sn were detected in very small quantities at low temperature below 300 °C. In presence of a magnetic field, there was a marked difference in behavior.

There was nearly an absence of crystals in the high temperature region out of the magnet. The majority of deposits was observed in the region placed in the magnetic field, some adhering to the steel walls and some in the bulk of the Pb17Li. Only one type of this ferromagnetic deposit composed of Fe and Cr was found. The magnetic field has no effect on the small amount of deposits composed of Ni, Mn and Sn.

There is evidence for the magnetic field effect on the trapping of ferromagnetic material. Deposition is observed in the region directly affected by the field and the concentration of iron in solution in Pb17Li is lowered. Therefore, magnetic trapping would be an effective method to remove Fe and Cr from the liquid alloy.

PUBLICATIONS

[1] F. BARBIER, "Deposition of corrosion products in liquid Pb17Li under a magnetic field: case of a martensitic steel", RT SCECF 476 (December 1998).

TASK LEADER

F. BARBIER

DTA/CEREM/DECM/SCECF/LECNA
CEA Saclay
91191 Gif-sur-Yvette Cedex

Tél. : 33 1 69 08 16 13
Fax : 33 1 69 08 15 86

E-mail: barbier@ortolan.cea.fr

Task Title : LIQUID METAL EMBRITTLEMENT

INTRODUCTION

In the frame of the future fusion reactors, liquid metals might be used as coolants in parts submitted to high heat peaks (for example, divertor), or as tritium breeding materials (for example, lithium-lead alloy). This implies that the properties of the structural materials must not be affected by the presence of the liquid metal. Thus, for a safe operation of the reactor, one must be aware of the problems which can arise during the solid-liquid contact.

It has long been known that ductile solid metals exposed to specific liquid metal environments may exhibit a significant reduction in elongation to failure and fracture strength when they are tested in tension. Under certain experimental conditions, the liquid metal embrittlement (LME) can be quite dramatic and one of the peculiarities of this phenomenon is the crack propagation rate which is reported to be very high (up to 50-500 $cm.s^{-1}$). The fact that a liquid metal can drastically affect the material resistance to fracture has serious technological significance.

Embrittlement in liquid metal environments has been the subject of many reviews describing the phenomenological features of the LME, the prerequisites for its occurrence, the effects of variables including grain size, strain rate, temperature, metallurgical state... However, despite decades of research, a qualitative explanation of LME has not yet emerged and its prediction is still missing. It is therefore appropriate that LME should be reviewed in the light of more recent work to provide a current assessment of this phenomenon.

1998 ACTIVITIES

In 1998, the literature survey has been pursued. The various mechanisms and models which have been advanced so far to describe the LME have been examined in details.

There are different models of LME mechanism:

- the dissolution - diffusion models of Robertson and Glickman,
- the brittle fracture theory based model, denominated SJWK, proposed by Stoloff, Johnson, Westwood and Kamdar,
- the ductile failure based models of Lynch and Popovich,
- the liquid metal atoms penetration based model of Gordon.

This list is not complete, but the main purpose is to present the most outstanding models. A diagram which summarizes the elementary mechanisms involved in each model has been proposed (Fig. 1). This diagram describes, for each model, the sequence of the elementary mechanisms leading to the propagation of cracks in presence of stress and liquid metal.

They are represented by arrows, which are numbered in order to link the following description of the models to the diagram. It allows to make a quick comparison between the different models and to see whether they use common elementary mechanisms or not. Furthermore, if we make this hypothesis that several mechanisms can occur at the same time to produce LME, as it has yet been proposed, this diagram gives a general overview of all the mechanisms that could be involved.

The concept of the adsorption-induced surface energy lowering is the central point of all these models, excepted for Robertson who does not mention the occurrence of adsorption. The adsorption-induced surface energy lowering has first been introduced by Rebinder, as the origin of the Rebinder effect (RE) which is one of the effects exerted by a liquid or a gaseous medium on the mechanical properties of solids. RE appears as a plastic flow increase and a strength reduction. The main problem in using the Rebinder effect to describe LME is that it has a pure thermodynamic character. That is the reason why many authors have improved his work by adding molecular mechanisms and/or by adding kinetic modelization of the phenomenon.

Robertson has presented his dissolution-diffusion based model in 1966. The main purpose of his theory is to give an expression for the crack propagation rate. There is no reference to a crack initiation stage, consequently the final expression concerns only the propagation rate. This model uses only macroscopic, thermodynamic and elastic concepts.

According to *Glickman*, LME is a clear manifestation of the Rebinder Effect (RE). He adds to this approach a mechanism based on dissolution and diffusion of solid metal atoms. Glickman worked mainly with solid copper and lead-bismuth melt. His model of the phenomenon is mainly kinetic, but also thermodynamic because it is based on Rebinder’s effect.

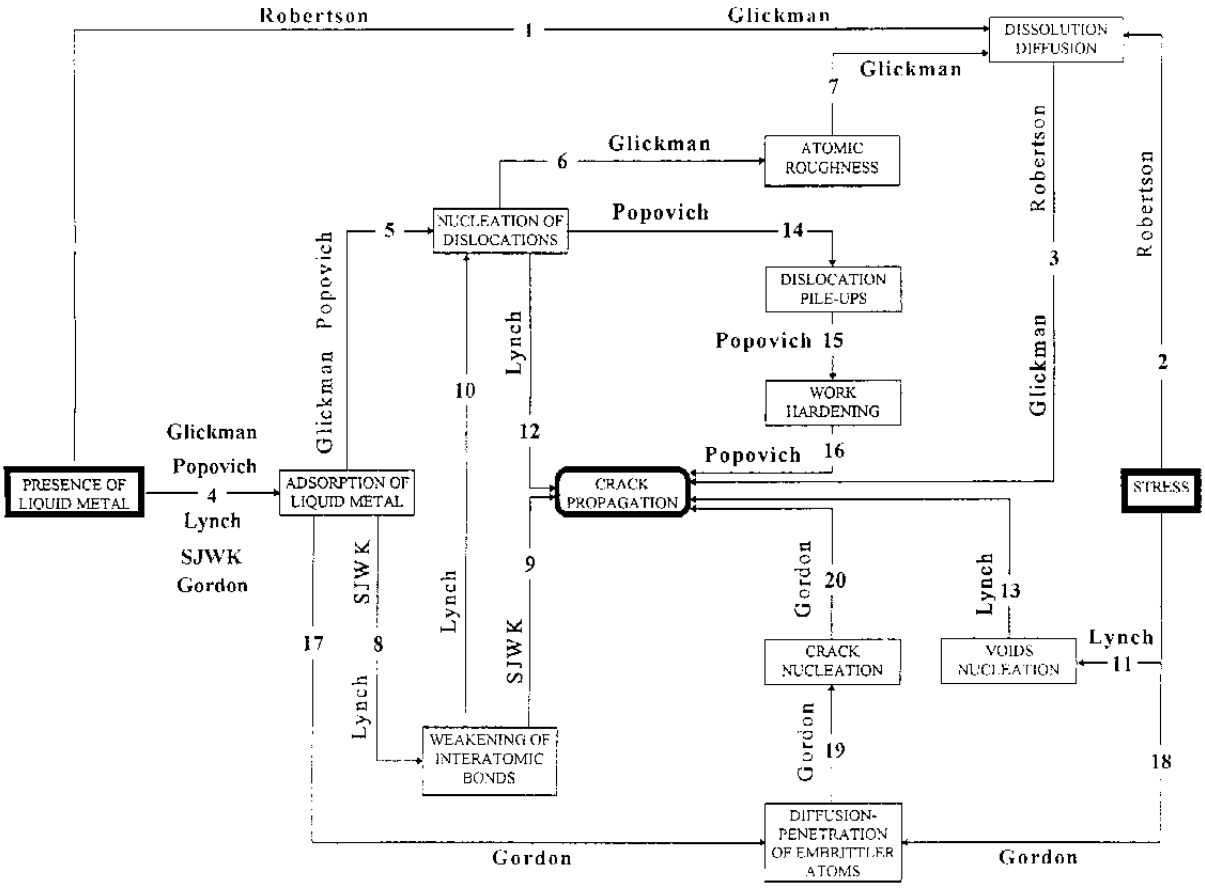

Figure 1 : Diagram illustrating all the elementary steps involved in the different LME models

The *SJWK* model is based on the « weakening of interatomic bond » mechanism, which is a particular case of the brittle fracture theory. It manages to rationalize the effects of many experimental variables: temperature, strain rate, grain size, slip character, but it was not capable of predicting susceptibility of a new substrate-environment system.

The *Lynch* model , which is also based on « the decrease of the strength of the interatomic bonds », differs from *SJWK* model, because it assumes that crack propagation does not occur by atom-by-atom rupture of the bonds. This model gives an explanation for the presence of ductility at a microlevel. It is mainly based on metallographic investigations on many different systems.

Popovich presents a mechanism for LME, based on the Rebinder effect and on enhanced plastic flow. At the thermodynamic aspect developed by Rebinder, he adds an atomistic approach. His model is only qualitative and give no quantitative expression for the time to rupture or for the crack propagation rate.

The *Gordon* model is based on the penetration of liquid metal atoms along the grain boundaries. This concept is that the actual crack nucleation event is not the rate-controlling step in the crack initiation, but rather than during an incubation period there is a preparation process which is rate-controlling.

For Gordon, the present approach must allow to explain the delayed fracture, often observed in experimental studies.

CONCLUSION

The survey has been concerned with the most outstanding models that have been proposed so far in the literature to describe liquid metal embrittlement. Unfortunately, the review does not allow an easy comparison between them. In fact, we cannot conclude that one model is more appropriate than another one for a specific solid metal - liquid metal couple. Attempts to apply these models in a system have often been carried out taking into account experimental results obtained in specific conditions. Therefore, we think it is difficult to draw general conclusions via such limited data.

Some models have been developed to be in agreement with the behavior of large number of systems. In spite of some advances, the difficulty still remains to understand and to predict why a particular embrittling species attacks a particular metal and how the embrittled metal will crack. As a consequence, the approach which consists in comparing the results obtained in two different systems is not relevant, since the elementary mechanisms which simultaneously work in one system may not be the same as those involved in the other.

For example, diffusion-penetration mechanism should not be eliminated because it is not involved in some systems. In fact, it takes place in the embrittlement of copper-bismuth system, like other elementary mechanisms such as adsorption. For this reason, studying the elementary processes that occur in the embrittlement of a specific solid-liquid couple may lead to improved understanding.

The chemisorption process, which is assumed in most of the models, should be studied. Liquid penetration at sites of high stress concentrations (e.g., grain boundaries) and its effect on embrittlement should be also more investigated in the future. For example, in a recent paper, a mechanism of grain boundary penetration via the development of a macroscopic amorphous layer has been proposed to explain the loss of ductility in the aluminum-gallium system. Such a mechanism could be expanded to other systems. It is necessary therefore to investigate new experimental work in that field including microstructural and mechanical studies.

PUBLICATIONS

[1] B. JOSEPH, M. PICAT and F. BARBIER, "Liquid metal embrittlement: a state-of-the-art appraisal", RT SCECF 474 (October 1998)

[2] B. JOSEPH, M. PICAT and F. BARBIER, "Liquid metal embrittlement: a state-of-the-art appraisal", The European Physical Journal - Applied Physics **5**, 19-31 (1999).

TASK LEADER

F. BARBIER

DTA/CEREM/DECM/SCECF/LECNA
CEA Saclay
91191 Gif-sur-Yvette Cedex

Tél. : 33 1 69 08 16 13
Fax : 33 1 69 08 15 86

E-mail : barbier@ortolan.cea.fr

Task Title : FABRICATION OF PERMEATION BARRIERS USING CVD PROCESSES

INTRODUCTION

The R&D programme devoted to the fabrication of the tritium permeation barrier (TPB) in the Water Cooled Lithium-Lead (WCLL) blanket concept is focused on the development of Fe-Al coatings by different techniques (hot dipping , CVD, plasma spraying).

The purpose of the study is to show the interest of the CVD techniques to propose alternative materials for the TPB.

TiAlN deposition by Plasma Assisted CVD (PACVD) and vapour aluminization have been checked in a first part. The chromizing and siliconizing feasability has been studied in 1998 on T91 martensitic steel substrates.

1998 ACTIVITIES

CHROMIZING FEASABILITY

Chromizing has been performed using a pack cementation method. The piece to be treated is put in a box in contact with a cement which powder is composed of Cr as donor, NH_4Cl as activator and Al_2O_3 as inert filler which role is to avoid the sintering of the cement. The activator decomposes under temperature and reacts with the donor to produce gaseous compounds of the element to deposit.

The cement has been specifically prepared using a spray-drying process which produces an homogeneous powder with an average particle size of 50 µm for a composition of 25 % of Cr, 4 % of NH_4Cl and 71 % of Al_2O_3.

The chromizing has been optimized in a furnace equiped with a pumping system in order to work under low pressure if necessary. Treatments have been performed at 750°C not to exceed the tempering temperature of the steel. Times of 16 hours have been tested.

Coatings of about 1.5 µm thick have been obtained as illustrated on Fig. 1. The layer is rather dense and uniform. There is no defect such as inclusions, cracks, porosities.... The adhesion is ensured by diffusion between the film and the substrate. A control by Energy Dispersive Spectroscopy (EDS) analysis performed on the surface gives a composition of about 92 % of Cr and 8 % of Fe. The X Ray Diffraction analysis (XRD) reveals the formation of $Cr_{23}C_6$ compounds. The formation of chromium carbides during chromization has been already observed and it strongly depends on the steel carbon content which participates to the coating formation by diffusion. Surface analysis by Glow Optical Discharge Spectroscopy (GDOS) confirms this carbon enrichment.

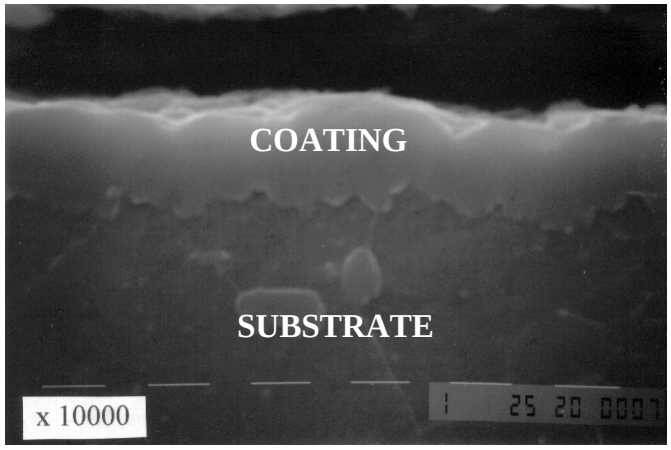

Figure 1 : SEM metallography of the chromized layer (cross-section)

SILICONIZING FEASABILITY

CVD methods such as processes using $SiCl_4$ or pack cementation are currently used for siliconizing of steels according to the literature. So the effort has been focused on the realization of a oxide top layer to check a similar coating structure as in the case of the Fe-Al/Al_2O_3 bi-layer performed in the frame of the WPA4 programme devoted to the barrier fabrication.

In effect, in other fields, amorphous silica coatings have shown remarkable long-term corrosion protection in oxidizing and sulphidizing environments up to 1000°C and this seems to be due to its amorphous structure which provides a more effective diffusion barrier than the polycristalline oxide scales formed on iron- or chromium-based alloys exposed to these environments. Silica coatings are also considered for diffusion barriers in high temperature hydrocarbon conversion reactors.

Silica deposition has been optimized in order to perform the coating on the siliconized steel. A Plasma Assisted CVD (PACVD) method starting from an organosilicon precursor (hexamethyldisiloxane : HMDS-O) has been tested because it presents the advantage to be easily transferable to an industrial scale. The coatings have been performed in a pilote-scale reactor. The decomposition of the gaseous phase is activated by the electrical discharge and no additional heating is necessary. So, the deposition temperature does not exceed 300°C which does not modify neither the substrate properties nor the siliconized layer.

An ion cleaning is carried out before the deposition step (in the same device) in order to ensure a good adhesion of the coating.

Uniform and covering coatings are obtained with thicknesses of a few micrometers. The layers are very dense and present a glassy morphology (Fig. 2) which illustrates the formation of an amorphous structure according to the X Ray Diffraction analysis. There is no crack or pinholes and the film presents a good adhesion during test of rupture in liquid nitrogen. Rutherford Backscattering Spectroscopy (RBS) and Nuclear Reaction Analysis (NRA) reveal the obtention of different Si/O stoechiometries according to the ratio between the oxygen and the HMDS-O flow rates : films of plasma-polymers are formed for low oxygen concentration in the vapour phase whereas silica coatings are deposited for high O_2/HMDS-O ratio.

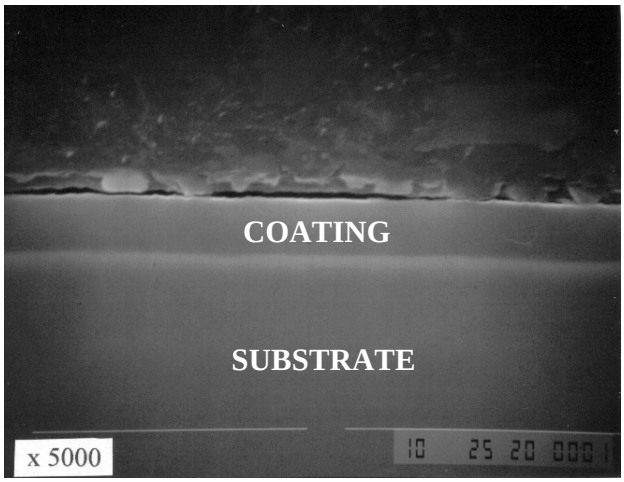

Figure 2 : SEM metallography of a silica coating (cross-section)

CONCLUSIONS

This study shows the interest of the CVD methods to form various coatings with metallurgical characteristics interesting with regards to the barrier function (high uniformity, compacity, adhesion....). A large panel of techniques can be used with a choice relevant with the specifications required by the application. In particular, specific developments can be performed to produce coatings at temperatures compatible with the substrate properties.

The feasability of TiAlN and silica deposition has been tested and the possibility of aluminizing and chromizing has been shown with different operating condition ranges. It must be noticed that SiC coatings which seem promising barriers and resistant to corrosion by liquid metals could be easily performed by the PACVD method used for the silica deposition.

PUBLICATIONS

[1] C. CHABROL, F. SCHUSTER "Fabrication of permeation barriers using CVD processes" NT DEM n° 98/81.

TASK LEADER

Claude CHABROL

DTA/DEM/SGM
CEA Grenoble
17, rue des Martyrs
38054 Grenoble Cedex 9

Tél. : 33 4 76 88 99 77
Fax : 33 4 76 88 99 85

E-mail : chabrol@chartreuse.cea.fr

UT-SM&C-PBM

Task Title : PEBBLE BED THERMO-MECHANICAL MODELLING

INTRODUCTION

There is evidently an increasing interest in the use of the pebble-beds as a blanket component in the future fusion reactors. In ITER Breeding Blanket (ITER-BB) and in DEMO-Helium Cooled Pebble Bed (DEMO-HCPB) concept both beryllium and breeding ceramics are proposed in the form of pebble beds for the blanket.

However, the behaviour of different pebble bed types under fusion-like load conditions is far from being modelled with satisfaction. CEA has thus initiated, since 1995, a R&D programme aiming at the modelling and experimental validation of the pebble-bed mechanical behaviour. Within a fusion like environment, the pebbles are subjected to irradiation-induced swelling, thermal (gradient, cyclic) stress and bed wall-induced stress.

After the FY96-FY97 experimental campaigns to validate a model based on the soil mechanics approach, [R1-R6], precisely on the Hujeux model derived from Cam-Clay model. After validation, the model has been implemented in CASTEM2000, the CEA qualified code in mechanics (CEA/DRN/DMT), [R1-R5].

1998 ACTIVITIES

During the FY98, R&D effort has been oriented towards the better understanding of the pebble bed behaviour under given thermal loading and swelling conditions, and comparing between different models. Two possible approaches have been compared ; 1/ the finite elements model (FEM) and 2/ the discrete elements method (DEM).

The FEM approach is that of the CEA developed model new implemented in CASTEM, as described above. While, the DEM approach is that developed at MIT (Boston) and implemented in the 2D DEM code, MIMES.

Both approaches have thus been applied in one specific case and compared. The studied case is described in the following sections.

GEOMETRY & MATERIALS

ITER-BB configuration has served as base of the study-case. Interest has been drawn principally towards the Be-pebble bed of ITER blanket. Be-pebble bed is a binary bed of relatively high packing factor 63%/18% (large pebbles/small pebbles) and pebbles are with 1.5-2.3/0.1-0.2mm diameters.

The pebbles are confined in an elementary basic cell of 316L-N stainless steel with typical dimensions of 800x60x250 (mm), [P1].

THERMAL LOADING

Be-pebbles (at 310 °C) are subjected to a cyclic loading and will tend to expand more than the structure itself (at 200 °C). Relative thermal strain of each material are given in details in [P1].

IRRADIATION-INDUCED SWELLING

Be-pebbles swelling is mainly due to He-particles production as a result of the neutron-Be interaction. The effective volumetric irradiation swelling of the Be-bed is evaluated to be less than 1% at the EoL (3 Mwy/m^3). This value is extrapolated from the experimental measurements obtained from the mixed bed $Be+Li_2SiO_3$ irradiation experiments, [P1].

GRAVITY LOADING

An order of magnitude equal to 0.8 m of a Be-column static head has been considered to represent the gravity effect. This equivalent to some 15 kg.

CONCLUSIONS

The most significant conclusions out of the methods comparative analyses are described in the following.

The DEM approach seems interesting in the sense that it allows a step-by-step (in the time) to follow up the local void fraction and the pebbles-contact forces evolution. The thermal loading and the irradiation-induced swelling can easily be modelled using the DEM. Besides, it should be underlined that the dynamic aspect of the approach constitutes its main attractiveness. One the other hand, the pebble-deformation should also be taken into account, but a DEM/FEM coupled approach seems to be too costly at high number of pebbles. The DEM has thus appeared limited to the modelling of large pebbles.

The FEM approach based Cam-Clay type of modelling gives good evaluations when dealing with round-shape pebbles at very high number. It allows the determination of ranges for the setting parameters. It predicts with satisfaction the overall stress level in the surrounding structures and determine the criteria for the evaluation of the structure failure.

However, attention should be paid to the fact that the model has been validated upon non-rigid compression tests. The blanket pebble bed appears to be relatively too rigid to be directly applied in the blanket configuration with no-additional corrections.

Additional efforts are still needed to improve pebble-bed mechanical response understanding. A model which is adequate to the fusion blanket operational conditions may come out of the coupling of the two approaches : the FEM and the DEM. The adequate model should be able to take into account the cyclic nature of the mechanical and thermal loads in the future fusion machines, as well.

REFERENCES

[R1] A. Duchesne, X. Raepsaet « Compte-rendu de la campagne d'essais triaxiaux sur matériaux granulaires à grains arrondis » Rapport DMT 96/353, SERMA LCA/ 1929.

[R2] Fusion Technology, 1996 Annual Report of the Association CEA/Euratom, Task UT-PBM, compiled by Ph. Magaud, CEA/DRFC, (5/1997).

[R3] A. Duchesne et X. Raepsaet, « Un modèle élasto-plastique de CASTEM-2000 utilisable pour la modélisation du comportement mécanique d'un lit de particules » DMT 97/237, SERMA/LCA 2054.

[R4] M. Eid, « Status of Thermal and Thermo-mechanical Behaviour of Pebble Beds» DMT 97/558, SERMA/LCA 2158

[R5] Fusion Technology, 1997 Annual Report of the Association CEA/Euratom, Task UT-PBM, compiled by Ph. Magaud, CEA/DRFC, (5/1998).

REPORTS AND PUBLICATIONS

[P1] Y. Poitevin et al. « Evaluation of the numerical approaches to modelise the mechanical behaviour of fusion blanket pebble beds » CEA technical report, SERMA/LCA/RT/98-2431/A, Oct.1998.

[P2] Y. poitevin et al., « Modelisation of the mechanical behaviour of breeding blanket pebble bed » 20th SOFT, Marseille September 1998.

TASKLEADER

Mohamed EID

DRN/DMT/SERMA
CEA Saclay
91191 Gif-sur-Yvette Cedex

Tél. : 33 1 69 08 3175
Fax : 33 1 69 08 9935

E-mail : meid@Cea.fr

Task Title : CVD/PVD COATINGS RESISTANT TO LIQUID METALS

INTRODUCTION

The choice of liquid metals as breeder and coolant for fusion reactor blankets, requires to use specific materials which present a good chemical stability in liquid metals. Another solution lies in the protection of more classical structural materials against liquid metals corrosion by using coatings. Chemical and Physical Vapour Deposition (CVD, PVD) are proposed to produce corrosion barriers in media such as liquid Li or LiPb.

1998 ACTIVITIES

MATERIALS RESISTANT TO LIQUID METALS : LITERATURE ANALYSIS

Barrier coatings may be interesting solutions to test for corrosion applications with regards to bulk materials from economical and technical point of view. CVD and PVD techniques are candidates in other fields such as Al casting, galvanizing... where corrosion protection against liquid metals is currently met with operating conditions more drastic than in the case of the Li or LiPb breeders (temperature level, thermal shocks...).

Corrosion by liquid metals is governed by different mechanisms which depend on the physico-chemistry of the liquid-solid system, the material structure, the thermal and mechanical conditions.... and can be illustrated by different attack features. Some data about the behaviour of different materials in lithium, in lead and even in the liquid Pb17Li alloy are partially available in handbooks and literature but they strongly depend on the tested conditions.

In liquid lithium, depending on the conditions, Ni and Co are not stable whereas Nb and Ta base alloys exhibit very good corrosion resistance as well as W and W alloys, pure Ti, V and Zr. Different carbides such as SiC, TiC, ZrC and NbC show promising results.

In lead, refractory metals such as Nb, Mo, Ta and W have a good behaviour at different temperatures whereas Ti and Zr are attacked at 815°C. A wide range of ceramics resists after 100 hour exposure at 815°C : B_4C, SiC, TiC, ZrC, Cr_3C_2, BN, TiN, Si_3N_4, MgO, Al_2O_3, ZrO_2, $MgAl_2O_4$.

More recent works carried out in conditions closer to the breeder blanket specifications complete these data. Al_2O_3 must be avoided in lithium whereas its corrosion resistance is very good in LiPb. Nitrides such as TiN, AlN and BN seem to be resistant in both media. Oxides such as MgO and Al_2O_3-MgO could be used in LiPb as well as Y_2O_3 if its density is correct.

CVD AND PVD DEPOSITION : EXPERIMENTAL RESULTS

The use of coatings as corrosion barriers introduces other factors to guaranty their efficiency such as : covering capability of the deposition technique, adhesion of the coating to the substrate, compacity and absence of defects such as cracks or pinholes.

CVD and PVD respect these specifications. In addition, they allow «moderate » deposition temperatures which can be compatible with the structural material properties. Finally, they offer a large variety of materials (metals, ceramics...) with various compositions.

The CVD and PVD feasibility of different coatings among nitrides, carbides, oxides and refractory metals has been tested in this work. The tested materials have been selected on the basis of the literature analysis, e.g. (Ti,Al)N, SiC, Y_2O_3 and Al_2O_3 by CVD and W by PVD, for their interest they should present for protection against LiPb. In this study, the deposition of the different materials has been performed on specimens in pilote-scale deposition reactors. A physico-chemical and metallurgical characterization has been mainly carried out to check the homogeneity and the compacity of the layers deposited on martensitic steels (8-10 % Cr).

CVD deposition

CVD deposition includes different static and dynamic processes which can be selected for the final applications according to their own specificities. So, different CVD methods have been used to deposit the selected materials.

(Ti,Al)N films either Al-rich or Ti-rich have been deposited at 550°C by Plasma-Assisted CVD (PACVD) starting from a method of in situ chlorination of a TiAl metallic charge.

SiC coatings have been performed at 500°C, also by PACVD, but starting from a metalorganic precursor of Si such as tetramethysilane (Fig . 1).

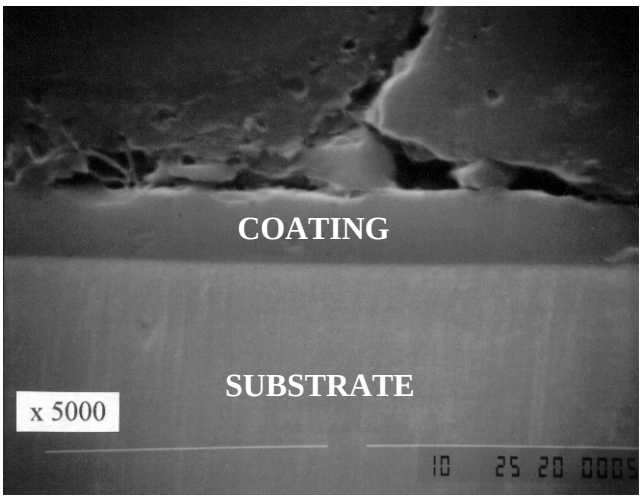

Figure 1 : SiC CVD coating
(SEM metallography on cross-section)

For both oxides, yttria and alumina, the deposition has been carried out using a Pyrosol® method starting from metalorganic precursors (MOCVD) such as yttrium (III) acetylacetonate trihydrate and aluminum-i-propoxide respectively in the ranges of 520-530°C and 450-500°C. For the alumina, the coating has been deposited on the martensitic steel previously treated by a pack cementation CVD process in order to form a Fe-Al sub-layer.

PVD deposition

The W deposition has been carried out by a magnetron sputtering process. A parametric study of the deposition conditions has been carried out to achieve good layer characteristics (Fig. 2). The temperature does not exeed 350°C during deposition.

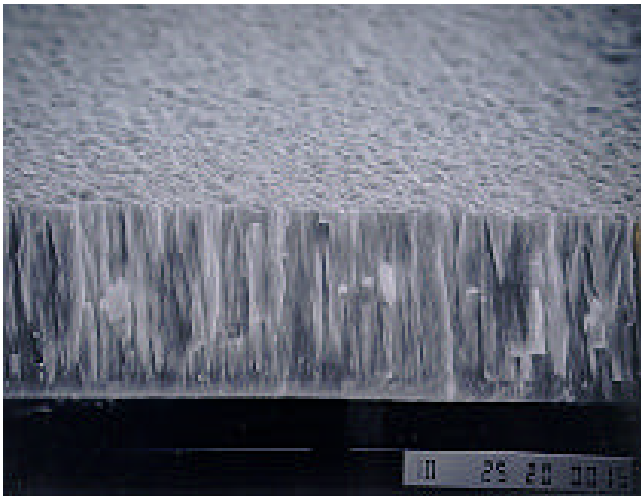

Figure 2 : W PVD coating (SEM fractography)

Film characterization

With some optimizations, both CVD and PVD techniques provide dense coatings with fine morphologies, good uniformity and adhesion.

Films of a few micrometers thick can be typically deposited without redhibitory defects for the corrosion barrier function such as cracks, porosities....

CONCLUSIONS

A literature analysis on materials resistant to molten metals has enabled to select some candidates which should resist to exposure in Li or LiPb among ceramics (nitrides, carbides, oxides) and refractory metals.

The deposition of titanium-aluminum nitride, silicon carbide, yttria, alumina and tungsten has been studied because of the interest they should present as corrosion barrier for the protection of the structural materials such as martensitic steels in liquid LiPb.

This study shows the interest of CVD and PVD for the deposition of various materials thanks to a large panel of existing techniques. They provide thin coatings with good quality and without redhibitory defects with regards to the corrosion barrier function. The deposition of multi-layered coatings could also be considered.

The behaviour of the different coatings could be checked thanks to exposure in LiPb in specific equipments such as the Melodie loop of CEA/CEREM.

PUBLICATIONS

[1] C. CHABROL, P. JULIET, F. SCHUSTER "CVD / PVD coatings resistant to liquid metals" NT DEM n° 98/77.

TASK LEADER

Claude CHABROL

DTA/DEM/SGM
CEA Grenoble
17, rue des Martyrs
38054 Grenoble Cedex 9

Tél. : 33 4 76 88 99 77
Fax : 33 4 76 88 99 85

E-mail : chabrol@chartreuse.cea.fr